

# Black hole at the Galactic Center

- **A.Ф. Захаров (Alexander F. Zakharov)**

- **E-mail: [zakharov@itep.ru](mailto:zakharov@itep.ru)**

- *Institute of Theoretical and Experimental Physics,*
- *B. Cheremushkinskaya, 25, 117218 Moscow;*

- **Bamberg, Germany**

- **20 June, 2012**



- **Black Holes (Amanda Lear)**
- I'm trying to understand why  
Like a black hole in the sky....
- A door opening on a new dimension...  
It's another time  
And it's another space  
It's something that science can't describe  
No one has ever seen (???)  
No one has ever been  
A black hole in the sky, why?

# Outline of my talk

- Introduction
- Crafoord prize and its winners
- Shadows for Kerr as a tool to evaluate BH characteristics
- Shadows around Reissner-Nordstrom BHs
- Observations of BH at Sgr A and a tidal Reissner-Nordstrom BH
- Bright star trajectories around BH at GC as a tool to evaluate BH parameters and DM cluster
- Conclusions

# References

- AFZ, F. De Paolis, G. Ingrosso, and A. A. Nucita, *New Astronomy Review*, **56**, 64 (2012).
- D. Borka, P. Jovanovic, V. Borka Jovanovic and AFZ, *PRD*, **85**, 124004 (2012).





Contents lists available at SciVerse ScienceDirect

## New Astronomy Reviews

journal homepage: [www.elsevier.com/locate/newastrev](http://www.elsevier.com/locate/newastrev)

## Shadows as a tool to evaluate black hole parameters and a dimension of spacetime

Alexander F. Zakharov<sup>a,b,\*</sup>, Francesco De Paolis<sup>c</sup>, Gabriele Ingresso<sup>c</sup>, Achille A. Nucita<sup>c</sup><sup>a</sup> Institute of Theoretical and Experimental Physics, 25, B. Chermushkinskaya St., Moscow 117259, Russia<sup>b</sup> Bogoliubov Laboratory of Theoretical Physics, Joint Institute for Nuclear Research, Dubna, Russia<sup>c</sup> Dipartimento di Fisica Università di Salento and INFN, Sezione di Lecce, Italy

## ARTICLE INFO

## Article history:

Available online xxxxx

## ABSTRACT

Shadow formation around supermassive black holes were simulated. Due to enormous progress in observational facilities and techniques of data analysis researchers approach to opportunity to measure shapes and sizes of the shadows at least for the closest supermassive black hole at the Galactic Center. Measurements of the shadow sizes around the black holes can help to evaluate parameters of black hole metric. Theories with extra dimensions (Randall–Sundrum II braneworld approach, for instance) admit astrophysical objects (supermassive black holes, in particular) which are rather different from standard ones. Different tests were proposed to discover signatures of extra dimensions in supermassive black holes since the gravitational field may be different from the standard one in the general relativity (GR) approach. In particular, gravitational lensing features are different for alternative gravity theories with extra dimensions and general relativity. Therefore, there is an opportunity to find signatures of extra dimensions in supermassive black holes. We show how measurements of the shadow sizes can put constraints on parameters of black hole in spacetime with extra dimensions.

© 2011 Elsevier B.V. All rights reserved.

## Contents

1. Introduction	00
2. Shadows for Kerr black holes	00
2.1. Mirage shapes	00
2.2. Equatorial plane observer case	00
2.3. Polar axis observer case	00
2.4. General case for the angular position of the observer	00
3. Shadows for Reissner–Nordström black holes	00
3.1. Basic definitions and equations	00
3.2. Capture cross section of photons by a Reissner–Nordström black hole	00
3.3. Shadows for a Reissner–Nordström black holes with a tidal charge	00
4. The space RadioAstron interferometer	00
5. Searches for mirages near Sgr A* with RadioAstron	00
6. Discussion	00
7. Conclusions	00
Acknowledgements	00
References	00

[Home](#)

[News](#)

[Features](#)

[Columns & blogs](#)

Archive

[Specials](#)

[In focus](#)

- X chromosome
- Future computing
- Stem cells
- Bird flu
- Mars
- GM crops

[Stories by subject](#)

NEWS CHANNELS

- [My news](#)
- [Biotechnology](#)
- [Careers](#)
- [Drug discovery](#)
- [Earth and environment](#)
- [Medical Research](#)
- [Physical Sciences](#)

[Feedback](#)

[About this site](#)

[About us](#)

[For librarians](#)

TOP STORIES

[Air pollution influences crop disease](#)  
04 April 2005

[Hunters win hike in polar bear quota](#)  
04 April 2005

[Genetic patch treats 'bubble-boy' disease](#)  
03 April 2005

[Transgenic cows have](#)

## NEWS

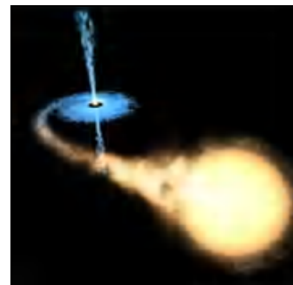
Published online: 31 March 2005; | doi:10.1038/news050328-8

### Black holes 'do not exist'

[Philip Ball](#)

#### These mysterious objects are dark-energy stars, physicist claims.

Black holes are staples of science fiction and many think astronomers have observed them indirectly. But according to a physicist at the Lawrence Livermore National Laboratory in California, these awesome breaches in space-time do not and indeed cannot exist.



Black holes, such as the one pictured in this artist's impression, may in fact be pockets of 'dark energy'.

© ESA/NASA

Over the past few years, observations of the motions of galaxies have shown that some 70% the Universe seems to be composed of a strange 'dark energy' that is driving the Universe's accelerating expansion.

George Chapline thinks that the collapse of the massive stars, which was long believed to generate black holes, actually leads to the formation of stars that contain dark energy. "It's a near certainty that black holes don't exist," he claims.

Black holes are one of the most celebrated predictions of Einstein's general theory of relativity, which explains gravity as the warping of space-time caused by massive objects. The theory suggests that

a sufficiently massive star, when it dies, will collapse under its own gravity to a single point.

But Einstein didn't believe in black holes, Chapline argues. "Unfortunately", he adds, "he couldn't articulate why." At the root of the problem is the other revolutionary theory of twentieth-century physics, which Einstein also helped to formulate: quantum mechanics.

**“ It's a near certainty that black holes don't exist. ”**

George Chapline  
Lawrence Livermore National  
Laboratory

In general relativity, there is no such thing as a 'universal time' that makes clocks tick at the same rate everywhere.

Instead, gravity makes clocks run at different rates in

different places. But quantum mechanics, which describes physical phenomena at infinitesimally small scales, is meaningful only if time is universal; if not, its equations make no sense.

This problem is particularly pressing at the boundary, or event horizon, of a black hole. To a far-off observer, time seems to stand still here. A spacecraft falling into a black hole would seem, to someone watching it from afar, to be stuck forever at the event horizon, although the astronauts in the spacecraft would feel as if they were continuing to fall. "General relativity predicts that nothing happens at the event horizon," says Chapline.

## Quantum transitions

However, as long ago as 1975 quantum physicists argued that strange things do happen at an event horizon: matter governed by quantum laws becomes hypersensitive to slight disturbances. "The result was quickly forgotten," says Chapline, "because it didn't agree with the prediction of general relativity. But actually, it was absolutely correct."

This strange behaviour, he says, is the signature of a 'quantum phase transition' of space-time. Chapline argues that a star doesn't simply collapse to form a black hole; instead, the space-time inside it becomes filled with dark energy and this has some intriguing gravitational effects.

Outside the  
'surface' of a

ADVERTISEMENT

dark-energy star, it behaves much like a black hole, producing a strong gravitational tug. But inside, the 'negative' gravity of dark energy may cause matter to bounce back out again.

**HGM2005**  
**Kyoto, Japan**  
**18th – 21st April 2005**



**Register now for HUGO's 10th  
annual human genome meeting**  
**Deadline for abstracts**  
**January 21st 2005**



**[Click here for information on HGM2005](#)**

If the dark-energy star is big enough, Chapline predicts, any electrons bounced out will have been converted to positrons, which then annihilate other electrons in a burst of high-energy radiation. Chapline says that this could explain the radiation observed from the centre of our galaxy, previously interpreted as the signature of a huge black hole.

He also thinks that the Universe could be filled with 'primordial' dark-energy stars. These are formed not by stellar collapse but by fluctuations of space-time itself, like blobs of liquid condensing spontaneously out of a cooling gas. These, he suggests, could be stuff that has the same gravitational effect as normal matter, but cannot be seen: the elusive substance known as dark matter.

[▲ Top](#)

---

## References

1. Chapline G. *Arxiv*,  
<http://xxx.arxiv.org/abs/astro-ph/0503200>  
(2005).

[▲ Top](#)

# Mirages around Kerr black holes and retro-gravitational lenses

- Let us consider an illumination of black holes. Then retro-photons form caustics around black holes or mirages around black holes or boundaries around shadows.
- (Zakharov, Nucita, DePaolis, Ingrosso,
- *New Astronomy* 10 (2005) (479-489);  
astro-ph/0411511)

# RETRO-MACHOS: $\pi$ IN THE SKY?

DANIEL E. HOLZ

Institute for Theoretical Physics, University of California, Santa Barbara, CA 93106

AND

JOHN A. WHEELER

Department of Physics, Princeton University, Princeton, NJ 08544

*Draft version September 20, 2004*

## ABSTRACT

Shine a flashlight on a black hole, and one is greeted with the return of a series of concentric rings of light. For a point source of light, and for perfect alignment of the lens, source, and observer, the rings are of infinite brightness (in the limit of geometric optics). In this manner, distant black holes can be revealed through their reflection of light from the Sun. Such retro-MACHO events involve photons leaving the Sun, making a  $\pi$  rotation about the black hole, and then returning to be detected at the Earth. Our calculations show that, although the light return is quite small, it may nonetheless be detectable for stellar-mass black holes at the edge of our solar system. For example, all (unobscured) black holes of mass  $M$  or greater will be observable to a limiting magnitude  $\bar{m}$ , at a distance given by:  $0.02 \text{ pc} \times \sqrt[3]{10^{(\bar{m}-30)/2.5}} (M/10 M_{\odot})^2$ . Discovery of a Retro-MACHO offers a way to *directly* image the presence of a black hole, and would be a stunning confirmation of strong-field general relativity.

*Subject headings:* gravitational lensing—black hole physics—relativity

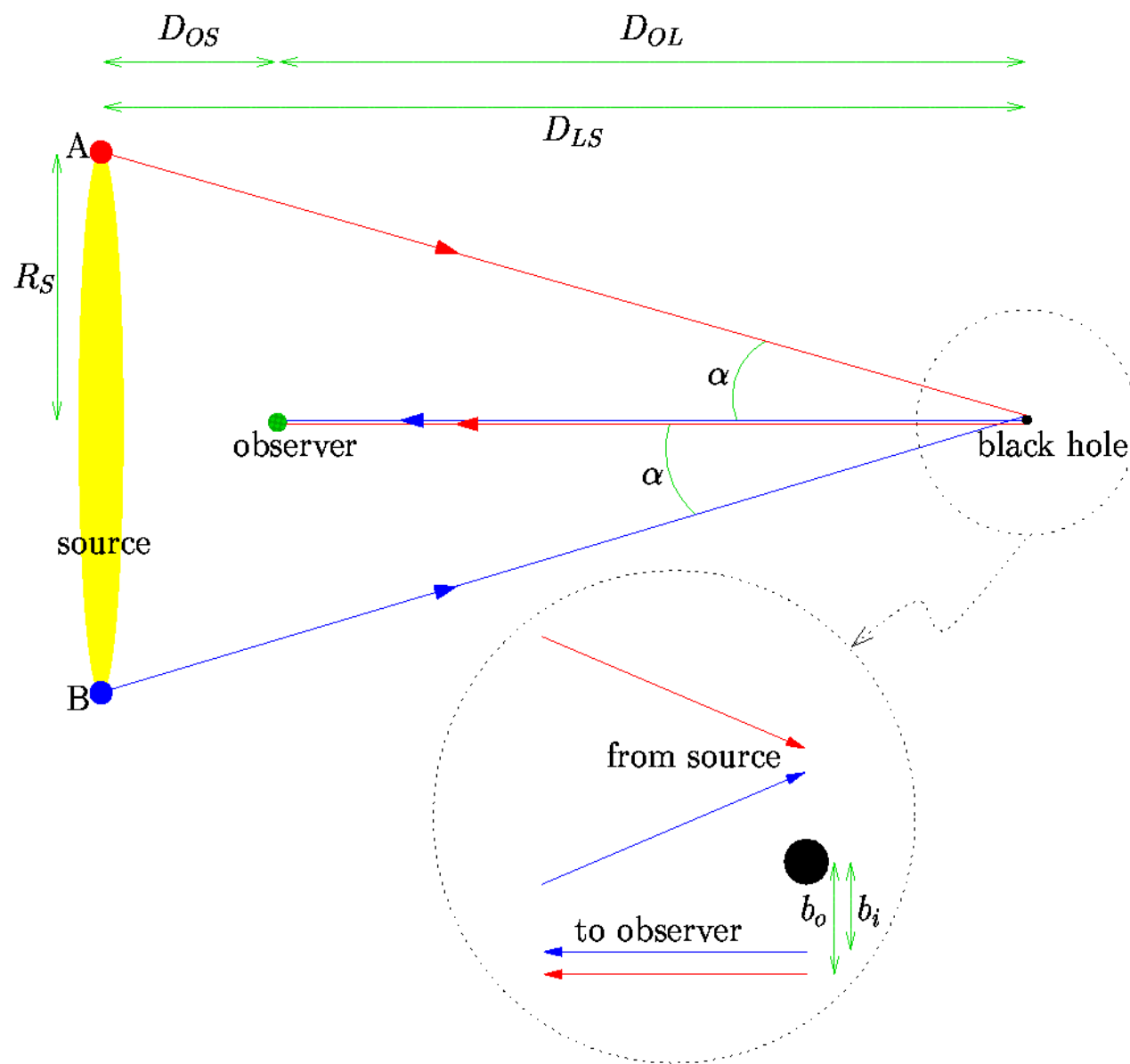


FIG. 1.— Perfect alignment: the (extended) source, observer, and lens are colinear. The resulting image of the source, as lensed by the black hole, is a ring. (The angles in this figure are greatly exaggerated.)

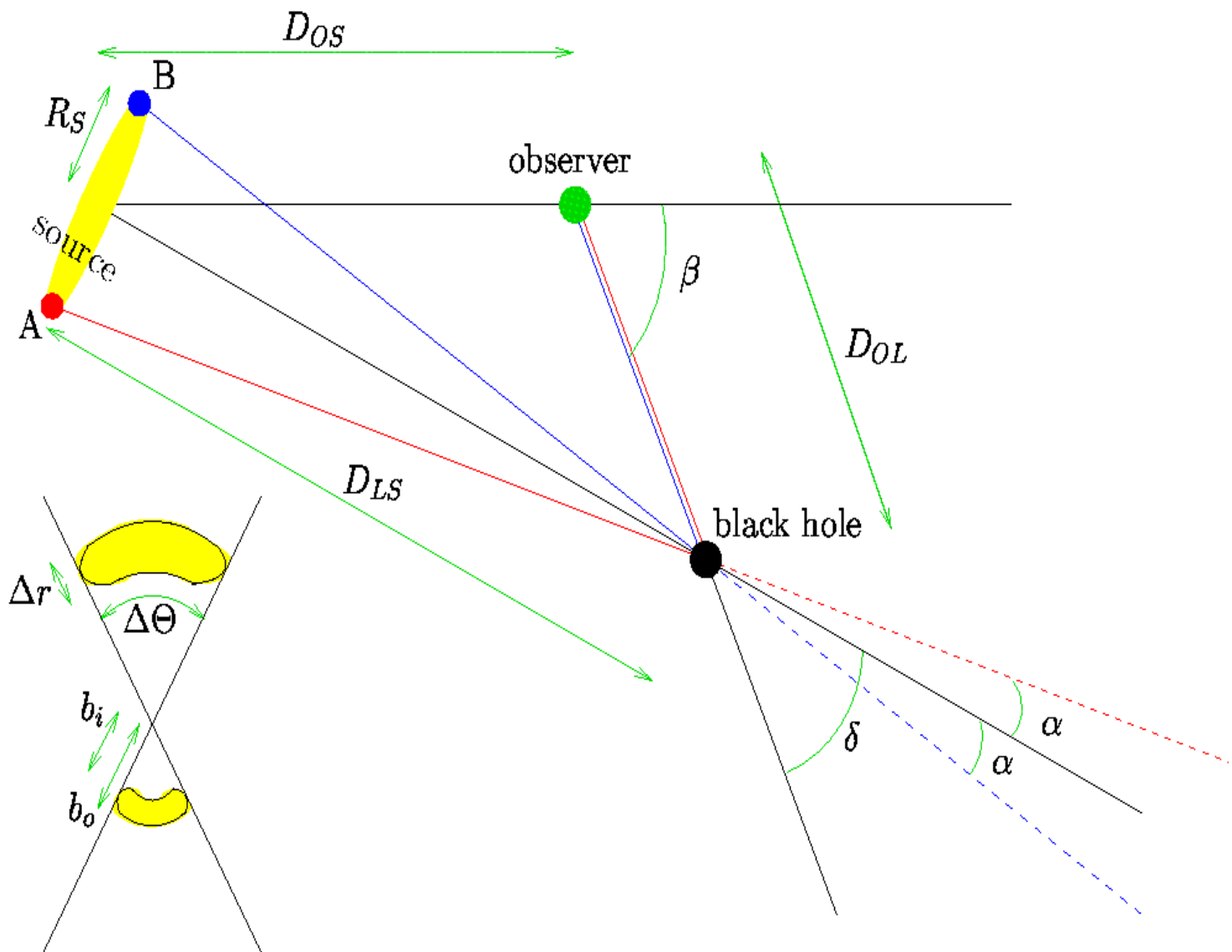


FIG. 2.— Imperfect alignment: the source, observer, and lens are not colinear. Pairs of images are produced, centered on the source–observer–lens plane, on opposite sides of the lens (see inset).





INTERNATIONAL SERIES OF  
MONOGRAPHS ON PHYSICS 69

The  
Mathematical Theory  
of Black Holes

S. Chandrasekhar

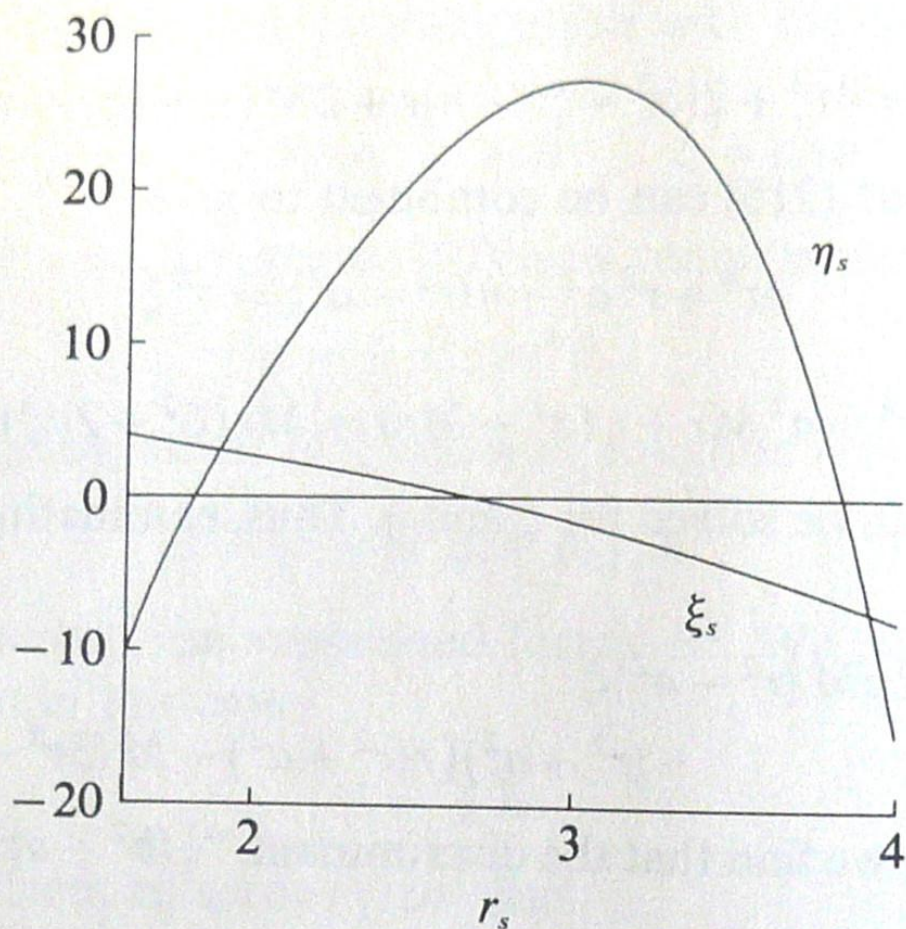


FIG. 34. The locus  $(\xi_s, \eta_s)$  determining the constants of the motion for three-dimensional orbits of constant radius described around a Kerr black-hole with  $a = 0.8$ . The unit of length along the abscissa is  $M$ .



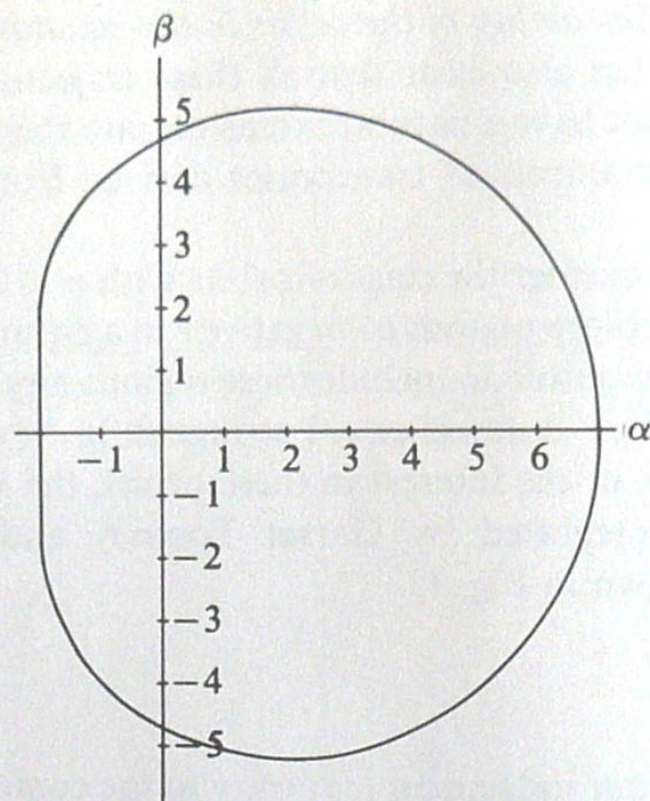


FIG. 38. The apparent shape of an extreme ( $a = M$ ) Kerr black-hole as seen by a distant observer in the equatorial plane, if the black hole is in front of a source of illumination with an angular size larger than that of the black hole. The unit of length along the coordinate axes  $\alpha$  and  $\beta$  (defined in equation (241)) is  $M$ .

black hole from infinity, the apparent shape will be determined by

$$(\alpha, \beta) = [\xi, \sqrt{\eta(\xi)}]. \quad (242)$$

The full classification of geodesic types for Kerr metric is given by Zakharov (1986). As it was shown in this paper, there are three photon geodesic types: capture, scattering and critical curve which separates the first two sets. This classification fully depends only on two parameters  $\xi = L_z/E$  and  $\eta = Q/E^2$ , which are known as Chandrasekhar's constants (Chandrasekhar 1983). Here the Carter constant  $Q$  is given by Carter (1968)

$$Q = p_\theta^2 + \cos^2 \theta [a^2 (m^2 - E^2) + L_z^2/\sin^2 \theta], \quad (1)$$

where  $E = p_t$  is the particle energy at infinity,  $L_z = p_\phi$  is  $z$ -component of its angular momentum,  $m = p_i p^i$  is the particle mass. Therefore, since photons have  $m = 0$

$$\eta = p_\theta^2/E^2 + \cos^2 \theta [-a^2 + \xi^2/\sin^2 \theta]. \quad (2)$$

The first integral for the equation of photon motion (isotropic geodesics) for a radial coordinate in the Kerr metric is described by the following equation (Carter 1968; Chandrasekhar 1983; Zakharov 1986, 1991a)

$$\rho^4 (dr/d\lambda)^2 = R(r),$$

where

$$R(r) = r^4 + (a^2 - \xi^2 - \eta)r^2 + 2[\eta + (\xi - a)^2]r - a^2\eta, \quad (3)$$

and  $\rho^2 = r^2 + a^2 \cos^2 \theta$ ,  $\Delta = r^2 - 2r + a^2$ ,  $a = S/M^2$ . The constants  $M$  and  $S$  are the black hole mass and angular momentum, respectively. Eq. (3) is written in dimensionless variables (all lengths are expressed in black hole mass units  $M$ ).

If we fix a black hole spin parameter  $a$  and consider a plane  $(\xi, \eta)$  and different types of photon trajectories corresponding to  $(\xi, \eta)$ , namely, a capture region, a scatter region and the critical curve  $\eta_{\text{crit}}(\xi)$  separating the scatter and capture regions. The critical curve is a set of  $(\xi, \eta)$  where the polynomial  $R(r)$  has a multiple root (a double root for this case). Thus, the critical curve  $\eta_{\text{crit}}(\xi)$  could be determined from the system (Zakharov 1986, 1991a)

$$\begin{aligned} R(r) &= 0, \\ \frac{\partial R}{\partial r}(r) &= 0, \end{aligned} \tag{4}$$

for  $\eta \geq 0, r \geq r_+ = 1 + \sqrt{1 - a^2}$ , because by analysing of trajectories along the  $\theta$  coordinate we know that for  $\eta < 0$  we have  $M = \{(\xi, \eta) | \eta \geq -a^2 + 2a|\xi| - \xi^2, -a \leq \xi \leq a\}$  and for each point  $(\xi, \eta) \in M$  photons will be captured. If instead  $\eta < 0$  and  $(\xi, \eta) \notin M$ , photons cannot have such constants of motion, corresponding to the forbidden region (see, (Chandrasekhar 1983; Zakharov 1986) for details).

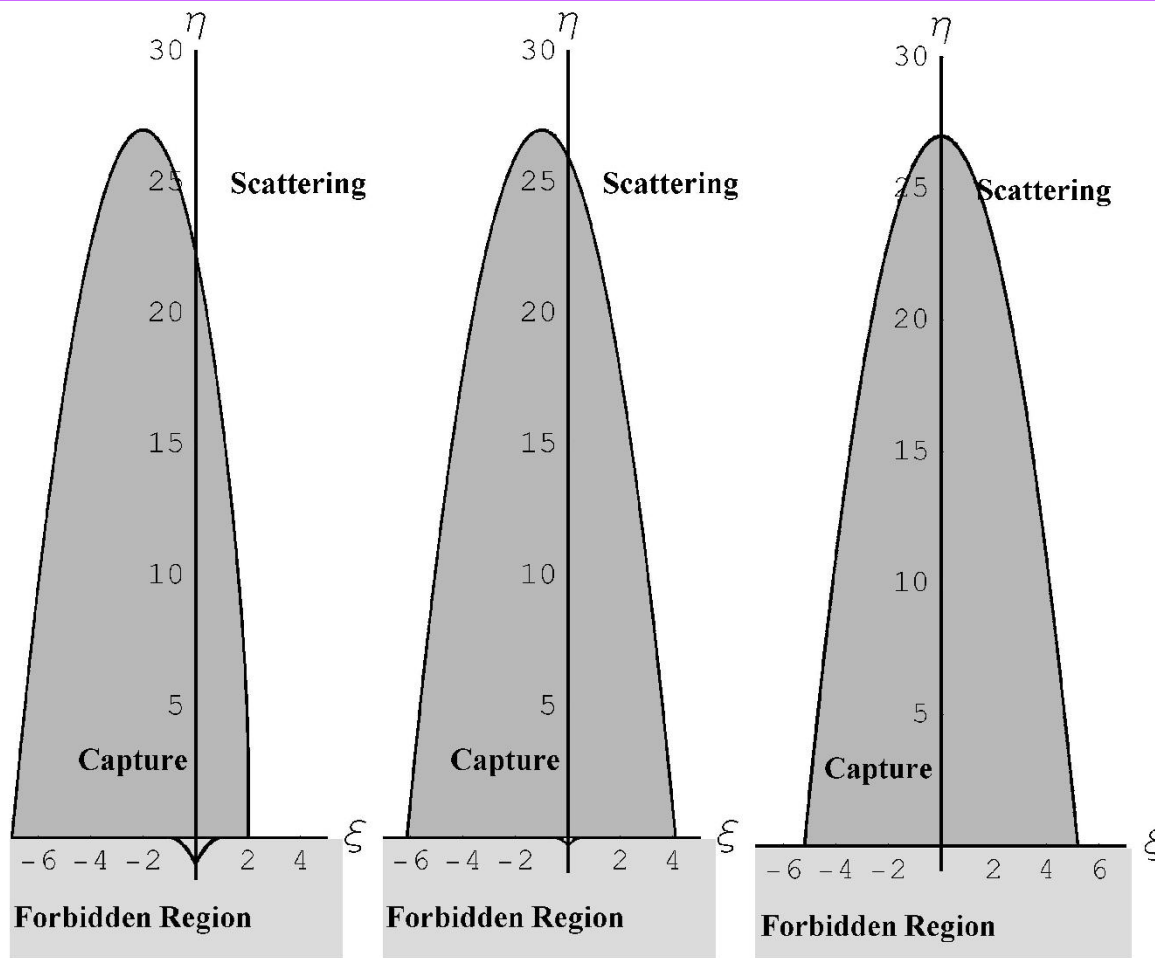


**Fig. 1.** Different types for photon trajectories and spin parameters ( $a = 1., a = 0.5, a = 0.$ ). Critical curves separate capture and scatter regions. Here we show also the forbidden region corresponding to constants of motion  $\eta < 0$  and  $(\xi, \eta) \in M$  as it was discussed in the text.

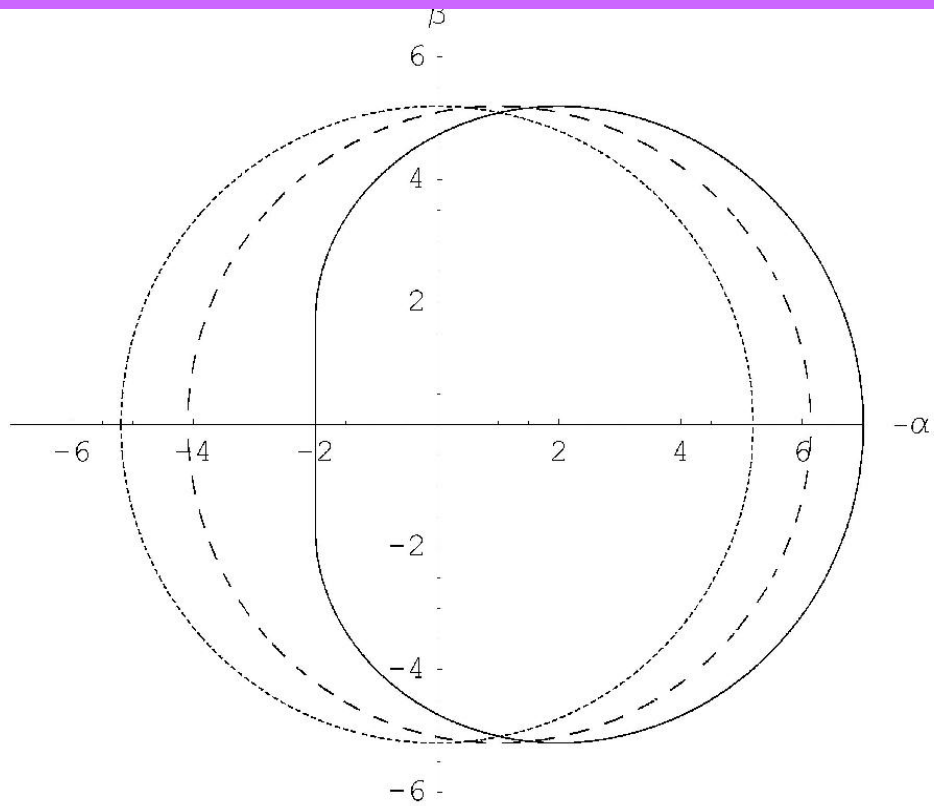


**Fig. 2.** Mirages around black hole for equatorial position of distant observer and different spin parameters. The solid line, the dashed line and the dotted line correspond to  $a = 1$ ,  $a = 0.5$ ,  $a = 0$  correspondingly



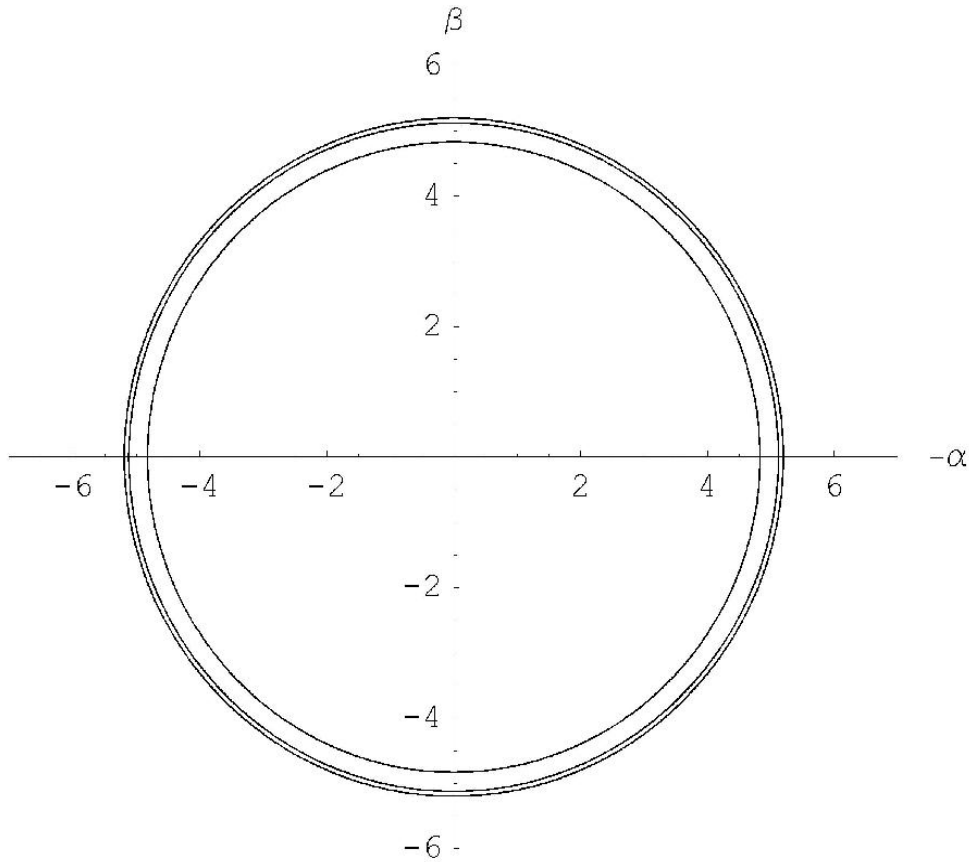


**Fig. 3.** Mirages around a black hole for the polar axis position of distant observer and different spin parameters ( $a = 0, a = 0.5, a = 1$ ). Smaller radii correspond to greater spin parameters.



**Table 1.** Dependence of  $\eta(0)$  and mirage radii  $R_{\text{circ}} = (\eta(0) + a^2)^{1/2}$  on spins.

$a$	0	0.2	0.4	0.5	0.6	0.8	1.
$\eta(0)$	27	26.839	26.348	25.970	25.495	24.210	22.314
$R_{\text{circ}}$	5.196	5.185	5.149	5.121	5.085	4.985	4.828

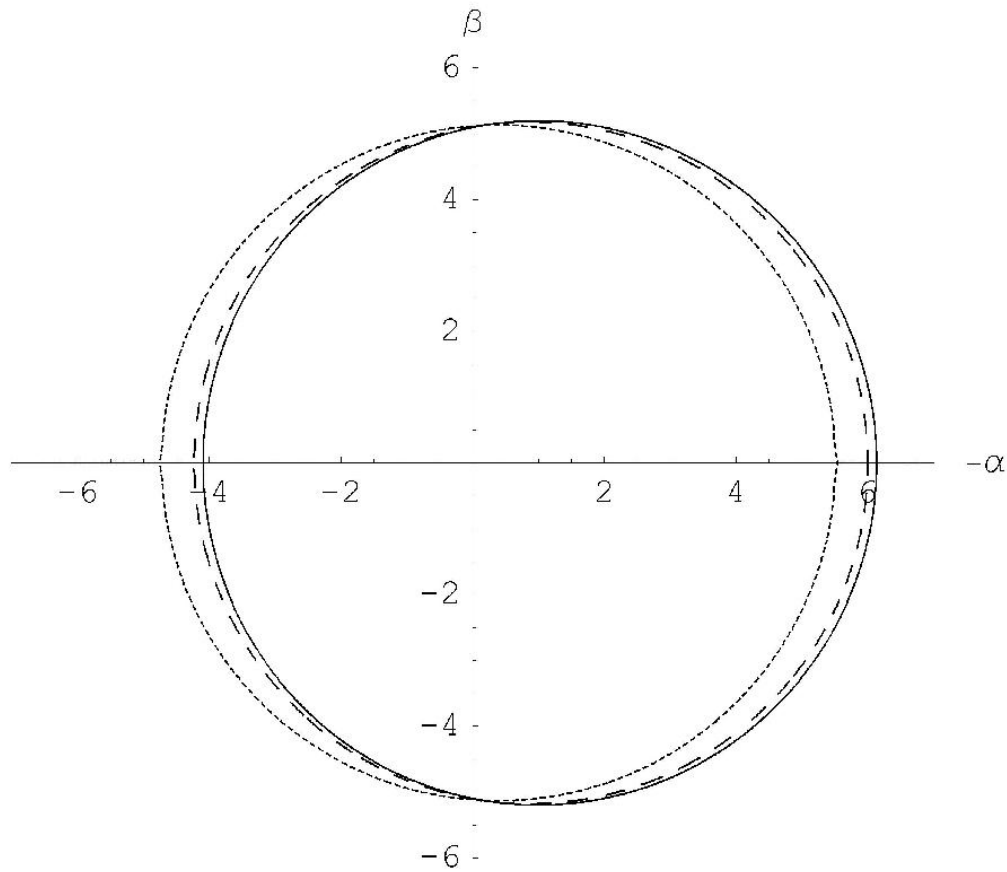


**Fig. 4.** Mirages around black hole for different angular positions of a distant observer and the spin  $a = 0.5$ . Solid, dashed and dotted lines correspond to  $\theta_0 = \pi/2, \pi/3$  and  $\pi/8$ , respectively.

- **gr-qc/0604093, April 21, 2006**
  - Title: **Kerr black hole lensing for generic observers in the strong deflection limit**
  - Authors: V. Bozza, F. De Luca, G. Scarpetta

found by Carter [9]

$$\pm \int \frac{dx}{\sqrt{R}} = \pm \int \frac{d\vartheta}{\sqrt{\Theta}} \quad (4)$$

$$\begin{aligned} \phi_f - \phi_i &= a \int \frac{x^2 + a^2 - aJ}{\Delta\sqrt{R}} dx - a \int \frac{dx}{\sqrt{R}} \\ &+ J \int \frac{\csc^2 \vartheta}{\sqrt{\Theta}} d\vartheta, \end{aligned} \quad (5)$$

where

$$\Theta = Q + a^2 \cos^2 \vartheta - J^2 \cot^2 \vartheta \quad (6)$$

$$\begin{aligned} R &= x^4 + (a^2 - J^2 - Q)x^2 + (Q + (J - a)^2)x \\ &- a^2 Q, \end{aligned} \quad (7)$$

and  $\phi_i$  is the initial value of the azimuthal coordinate of the photon.

The roots of  $R$  represent inversion points in the radial motion. In gravitational lensing we consider photons coming from infinity, grazing the black hole and going back to infinity. For such trajectories there is only one inversion point  $x_0$ , representing the closest approach distance. The minimum allowed value of  $x_0$  can be found solving the equations  $R(x) = 0$  and  $R'(x) = 0$  simultaneously. However, in Kerr black hole, we do not have a unique minimum closest approach  $x_m$ , but rather a continuous family of values which depend on the approach trajectory followed by the photon. In particular, it is possible to establish a relation among the minimum closest approach  $x_m$  and the corresponding values of the constants of motion  $J$  and  $Q$ , that we shall indicate by  $J_m$  and  $Q_m$  (see e.g. Ref. [21])

$$J_m = \frac{x_m^2(2x_m - 3) + a^2(1 + 2x_m)}{a(1 - 2x_m)} \quad (8)$$

$$Q_m = \frac{x_m^3 [2a^2 - x_m(x_m - 3/2)^2]}{a^2(x_m - 1/2)^2}. \quad (9)$$

$x_m$  also represents the radius of the unstable circular photon orbit. This radius is fixed to  $3/2$  when  $a = 0$  (Schwarzschild black hole). In the case of Kerr black holes,  $x_m$  may vary between two limiting values  $x_{m+}$ ,  $x_{m-}$ , depending on the incoming direction of the photon. The two limiting values can be analytically obtained solving the equation  $Q_m = 0$ . To the third order in  $a$ , they read [16]

$$x_{m\pm} = \frac{3}{2} \mp \frac{2}{\sqrt{3}}a - \frac{4}{9}a^2 \mp \frac{20}{27\sqrt{3}}a^3 + O(a^4). \quad (10)$$

For example, photons whose orbit lies on the equatorial plane may turn either in the same sense of the black hole (prograde photons) or in the opposite sense (retrograde photons). Prograde photons are allowed to get closer to the black hole, with a minimum closest approach given by  $x_{m+}$ , while retrograde photons must stay farther than  $x_{m-}$ , in order to be deflected without falling into the black hole. Photons whose orbit does not lie

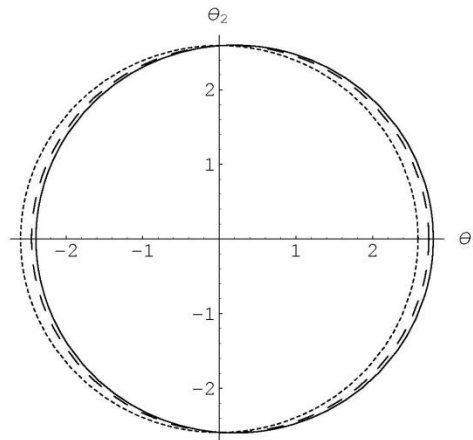


FIG. 2: The shadow of the black hole in the observer sky for  $a = 0.1$  and different values of the observer position  $\vartheta_o$ . The solid line is for  $\vartheta_o = \pi/2$  (equatorial observer), the dashed line is for  $\vartheta_o = \pi/4$  and the dotted line is for  $\vartheta_o = 0$  (polar observer).

on the equatorial plane are characterized by intermediate values of  $x_m$ , with  $Q_m > 0$ . Thus  $x_m$  can be used to parametrize the family of unstable photon orbits allowed in Kerr metric or, equivalently, the incoming direction of the photon. The corresponding values of the constants of motion are uniquely determined by Eqs. (8) and (9).

Although exact expressions for  $x_{m+}$  and  $x_{m-}$  are available, it is convenient to start with a perturbative expansion *ab initio* in order to be prepared to face more complicated quantities in the following [16]. Throughout our treatment, only for  $x_m$  we need to push the expansion to the third order, in order to obtain some quantities to the second order in  $a$ .

### III. THE SHADOW OF A KERR BLACK HOLE

The constants of motion  $J$  and  $Q$  have an immediate link to the position in the sky where the observer detects the photon. In fact, we can define angular coordinates  $(\theta_1, \theta_2)$  on the observer sky centered on the black hole position. We choose the orientation of these coordinates in such a way that the spin axis of the black hole is projected on the  $\theta_2$ -axis (see Fig.2).

As shown in Ref. [21], photons detected by the observer at angular coordinates  $(\theta_1, \theta_2)$  are characterized by constants of motion given by

$$J = -\theta_1 D_{OL} \sqrt{1 - \mu_o^2}, \quad (11)$$

$$Q = \theta_2^2 D_{OL}^2 + \mu_o^2 (\theta_1^2 D_{OL}^2 - a^2). \quad (12)$$

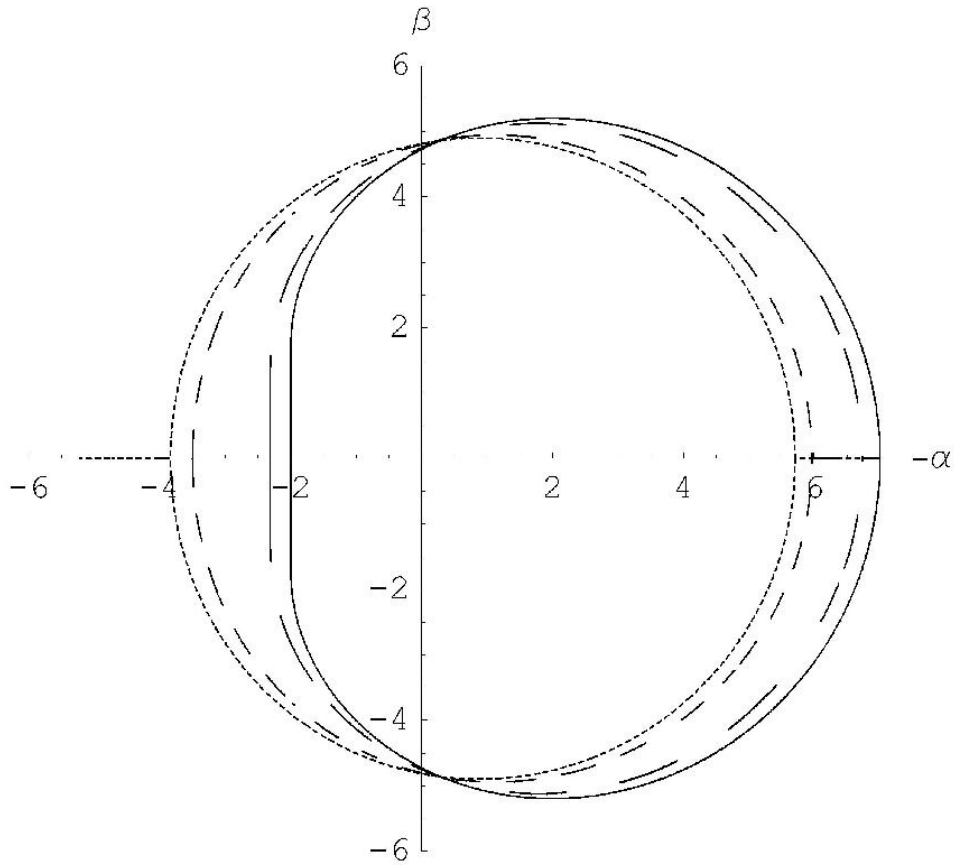


**Fig. 5.** Mirages around black hole for different angular positions of a distant observer and the spin  $a = 1$ . Solid, long dashed, short dashed and dotted lines correspond to  $\theta_0 = \pi/2, \pi/3, \pi/6$  and  $\pi/8$ , respectively.

# Direct Measurements of Black Hole Charge with Future Astrometrical Missions

A.F. Zakharov<sup>1,2,3</sup>, F. De Paolis<sup>4</sup>, G. Ingrosso<sup>4</sup>, A.A. Nucita<sup>4</sup>

<sup>1</sup> Institute of Theoretical and Experimental Physics, 25, B.Cheremushkinskaya st., Moscow, 117259, Russia,

<sup>2</sup> Astro Space Centre of Lebedev Physics Institute, 84/32, Profsoyuznaya st., Moscow, 117810, Russia,

<sup>3</sup> Joint Institute for Nuclear Research, Dubna, Russia

<sup>4</sup> Department of Physics, University of Lecce and INFN, Section of Lecce, Via Arnesano, I-73100 Lecce, Italy

Received / accepted

**Abstract.** Recently, Zakharov et al. (2005a) considered the possibility of evaluating the spin parameter and the inclination angle for Kerr black holes in nearby galactic centers by using future advanced astrometrical instruments. A similar approach which uses the characteristic properties of gravitational retro-lensing images can be followed to measure the charge of Reissner-Nordström black hole. Indeed, in spite of the fact that their formation might be problematic, charged black holes are objects of intensive investigations. From the theoretical point of view it is well-known that a black hole is described by only three parameters, namely, its mass  $M$ , angular momentum  $J$  and charge  $Q$ . Therefore, it would be important to have a method for measuring all these parameters, preferably by model independent way. In this paper, we propose a procedure to measure the black hole charge by using the size of the retro-lensing images that can be revealed by future astrometrical missions. A discussion of the Kerr-Newmann black hole case is also offered.

In this paper we focus on the possibility to measure the black hole charge as well and we present an analytical dependence of mirage size on the black hole charge. Indeed, future space missions like Radioastron in radio band or MAXIM in X-ray band have angular resolution close to the shadow size for massive black holes in the center of our and nearby galaxies.

## 2. Basic Definitions and Equations

The expression for the Reissner - Nordström metric in natural units ( $G = c = 1$ ) has the form

$$ds^2 = -(1 - 2M/r + Q^2/r^2)dt^2 + (1 - 2M/r + Q^2/r^2)^{-1}dr^2 + r^2(d\theta^2 + \sin^2\theta d\phi^2). \quad (1)$$

$$R(r_{max}) = 0, \quad \frac{\partial R}{\partial r}(r_{max}) = 0, \quad (6)$$

as it was done, for example, by Chandrasekhar (1983) to solve similar problems.

Introducing the notation  $\xi^2 = l$ ,  $Q^2 = q$ , we obtain

$$R(r) = r^4 - lr^2 + 2lr - qr. \quad (7)$$

The discriminant  $\Delta$  of the polynomial  $R(r)$  has the form (as it was shown by Zakharov (1991a,b, 1994a)):

$$\Delta = 16l^3[l^2(1 - q) + l(-8q^2 + 36q - 27) - 16q^3]. \quad (8)$$

The polynomial  $R(r)$  thus has a multiple root if and only if

$$l^3[l^2(1 - q) + l(-8q^2 + 36q - 27) - 16q^3] = 0. \quad (9)$$

Excluding the case  $l = 0$ , which corresponds to a multiple root at  $r = 0$ , we find that the polynomial  $R(r)$  has a multiple root for  $r \geq r_+$  if and only if

$$l^2(1 - q) + l(-8q^2 + 36q - 27) - 16q^3 = 0. \quad (10)$$

If  $q = 0$ , we obtain the well-known result for a Schwarzschild black hole (Misner, Thorne and Wheeler 1973; Wald 1984; Lightman et al. 1975),  $l = 27$ , or  $L_{cr} = 3\sqrt{3}$ . If  $q = 1$ , then  $l = 16$ , or  $L_{cr} = 4$ , which also corresponds to numerical results given by Young (1976).

The photon capture cross section for an extreme charged black hole turns out to be considerably smaller than the capture cross section of a Schwarzschild black hole. The critical value of the impact parameter, characterizing the capture cross section for a Reissner - Nordström black hole, is determined by the equation (Zakharov 1991a,b, 1994a)

$$l = \frac{(8q^2 - 36q + 27) + \sqrt{(8q^2 - 36q + 27)^2 + 64q^3(1 - q)}}{2(1 - q)}. \quad (11)$$



As it was explained by Zakharov et al. (2005a,b) this leads to the formation of shadows described by the critical value of  $L_{cr}$  or, in other words, in the spherically symmetric case, shadows are circles with radii  $L_{cr}$ . Therefore, measuring the shadow size, one could evaluate the black hole charge in black hole mass units  $M$ .

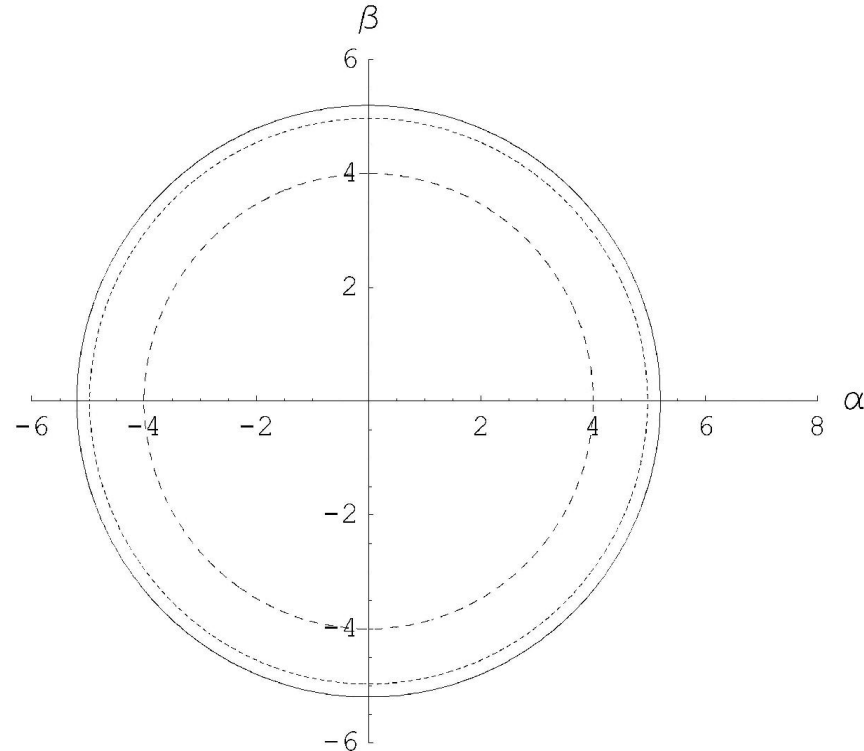
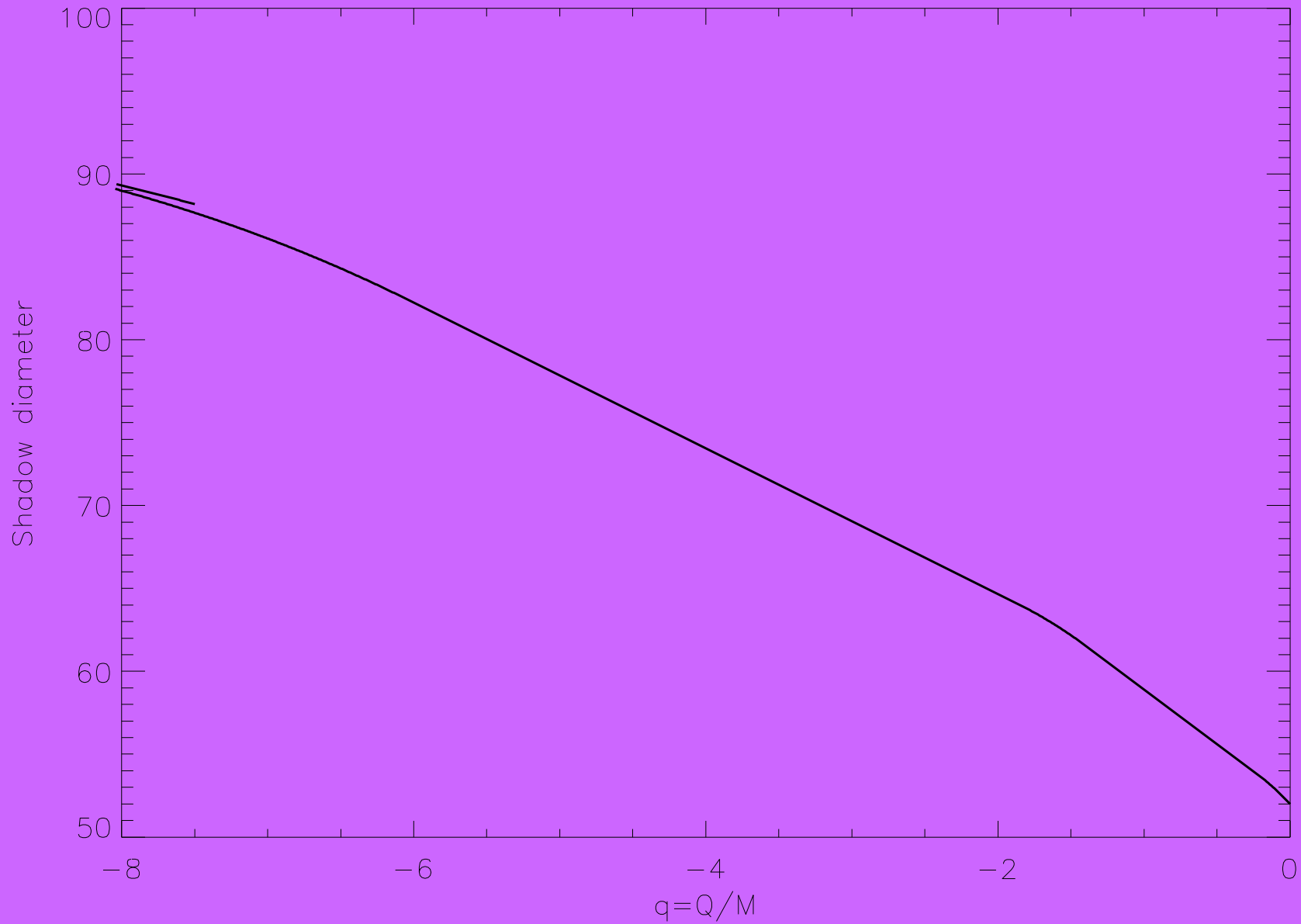


**Fig. 1.** Shadow (mirage) sizes are shown for selected charges of black holes  $Q = 0$  (solid line),  $Q = 0.5$  (short dashed line) and  $Q = 1$  (long dashed line).

Recently, Bin-Nun (2010) discussed an opportunity that the black hole at the Galactic Center is described by the tidal Reissner--Nordstrom metric which may be admitted by the Randall--Sundrum II braneworld scenario. Bin-Nun suggested an opportunity of evaluating the black hole metric analyzing (retro-)lensing of bright stars around the black hole in the Galactic Center. Doeleman et al. (2008) evaluated a shadow size for the black hole at the Galactic Center. Measurements of the shadow size around the black hole may help to evaluate parameters of black hole metric Zakharov et al (2005). We derive an analytic expression for the black hole shadow size as a function of charge for the tidal Reissner--Nordstrom metric. We conclude that observational data concerning shadow size measurements are not consistent with significant negative charges, in particular, the significant negative charge  $Q/(4M^2)=-1.6$  (discussed by Bin-Nun (2010) is practically ruled out with a very probability (the charge is roughly speaking is beyond  $9\sigma$  confidence level, but a negative charge is beyond  $3\sigma$  confidence level).



## LETTERS

## Event-horizon-scale structure in the supermassive black hole candidate at the Galactic Centre

Sheperd S. Doeleman<sup>1</sup>, Jonathan Weintroub<sup>2</sup>, Alan E. E. Rogers<sup>1</sup>, Richard Plambeck<sup>3</sup>, Robert Freund<sup>4</sup>, Remo P. J. Tilanus<sup>5,6</sup>, Per Friberg<sup>5</sup>, Lucy M. Ziurys<sup>4</sup>, James M. Moran<sup>2</sup>, Brian Corey<sup>1</sup>, Ken H. Young<sup>2</sup>, Daniel L. Smythe<sup>1</sup>, Michael Titus<sup>1</sup>, Daniel P. Marrone<sup>7,8</sup>, Roger J. Cappallo<sup>1</sup>, Douglas C.-J. Bock<sup>9</sup>, Geoffrey C. Bower<sup>3</sup>, Richard Chamberlin<sup>10</sup>, Gary R. Davis<sup>5</sup>, Thomas P. Krichbaum<sup>11</sup>, James Lamb<sup>12</sup>, Holly Maness<sup>3</sup>, Arthur E. Niell<sup>1</sup>, Alan Roy<sup>11</sup>, Peter Strittmatter<sup>4</sup>, Daniel Werthimer<sup>13</sup>, Alan R. Whitney<sup>1</sup> & David Woody<sup>12</sup>

The cores of most galaxies are thought to harbour supermassive black holes, which power galactic nuclei by converting the gravitational energy of accreting matter into radiation<sup>1</sup>. Sagittarius A\* (Sgr A\*), the compact source of radio, infrared and X-ray emission at the centre of the Milky Way, is the closest example of this phenomenon, with an estimated black hole mass that is 4,000,000 times that of the Sun<sup>2,3</sup>. A long-standing astronomical goal is to resolve structures in the innermost accretion flow surrounding Sgr A\*, where strong gravitational fields will distort the appearance of radiation emitted near the black hole. Radio observations at wavelengths of 3.5 mm and 7 mm have detected intrinsic structure in Sgr A\*, but the spatial resolution of observations at these wavelengths is limited by interstellar scattering<sup>4–7</sup>. Here we report observations at a wavelength of 1.3 mm that set a size of  $37^{+16}_{-10}$  microarcseconds on the intrinsic diameter of Sgr A\*. This is less than the expected apparent size of the event horizon of the presumed black hole, suggesting that the bulk of Sgr A\* emission may not be centred on the black hole, but arises in the surrounding accretion flow.

The proximity of Sgr A\* makes the characteristic angular size scale of the Schwarzschild radius ( $R_{\text{Sch}} = 2GM/c^2$ ) larger than for any other black hole candidate. At a distance of  $\sim 8$  kpc (ref. 8), the Sgr A\* Schwarzschild radius is  $10 \mu\text{as}$ , or 0.1 astronomical unit (AU). Multi-wavelength monitoring campaigns<sup>9–11</sup> indicate that activity on scales of a few  $R_{\text{Sch}}$  in Sgr A\* is responsible for observed short-term variability and flaring from radio to X-rays, but direct observations of structure on these scales by any astronomical technique has not been possible. Very-long-baseline interferometry (VLBI) at 7 mm and 3.5 mm wavelength shows the intrinsic size of Sgr A\* to have a wavelength dependence, which yields an extrapolated size at 1.3 mm of 20–40  $\mu\text{as}$  (refs 6, 7). VLBI images at wavelengths longer than 1.3 mm, however, are dominated by interstellar scattering effects that broaden images of Sgr A\*. Our group has been working to extend VLBI arrays to 1.3 mm wavelength, to reduce the effects of interstellar scattering, and to utilize long baselines to increase angular resolution with a goal of studying the structure of Sgr A\* on scales commensurate with the putative event horizon of the black hole. Previous pioneering VLBI work at 1.4 mm wavelength

uncertainties resulted in a range for the derived size of 50–170  $\mu\text{as}$  (ref. 12).

On 10 and 11 April 2007, we observed Sgr A\* at 1.3 mm wavelength with a three-station VLBI array consisting of the Arizona Radio Observatory 10-m Submillimetre Telescope (ARO/SMT) on Mount Graham in Arizona, one 10-m element of the Combined Array for Research in Millimeter-wave Astronomy (CARMA) in Eastern California, and the 15-m James Clerk Maxwell Telescope (JCMT) near the summit of Mauna Kea in Hawaii. A hydrogen maser time standard and high-speed VLBI recording system were installed at both the ARO/SMT and CARMA sites to support the observation. The JCMT partnered with the Submillimetre Array (SMA) on Mauna Kea, which housed the maser and the VLBI recording system and provided a maser-locked receiver reference to the JCMT. Two 480-MHz passbands sampled to two-bit precision were recorded at each site, an aggregate recording rate of  $3.84 \times 10^9$  bits per second ( $\text{Gbit s}^{-1}$ ). Standard VLBI practice is to search for detections over a range of interferometer delay and delay rate. Six bright quasars were detected with high signal to noise on all three baselines allowing array geometry, instrumental delays and frequency offsets to be accurately calibrated. This calibration greatly reduced the search space for detections of Sgr A\*. All data were processed on the Mark4 correlator at the MIT Haystack Observatory in Massachusetts.

On both 10 and 11 April 2007, Sgr A\* was robustly detected on the short ARO/SMT–CARMA baseline and the long ARO/SMT–JCMT baseline. On neither day was Sgr A\* detected on the CARMA–JCMT baseline, which is attributable to the sensitivity of the CARMA station being about a third that of the ARO/SMT (owing to weather, receiver temperature and aperture efficiency). Table 1 lists the Sgr A\* detections on the ARO/SMT–JCMT baseline. The high signal to noise ratio, coupled with the tight grouping of residual delays and delay rates, makes the detections robust and unambiguous.

There are too few visibility measurements to form an image by the usual Fourier transform techniques; hence, we fit models to the visibilities (shown in Fig. 1). We first modelled Sgr A\* as a circular Gaussian brightness distribution, for which one expects a Gaussian relationship between correlated flux density and projected baseline length. The weighted least-squares best-fit model (Fig. 1) corre-

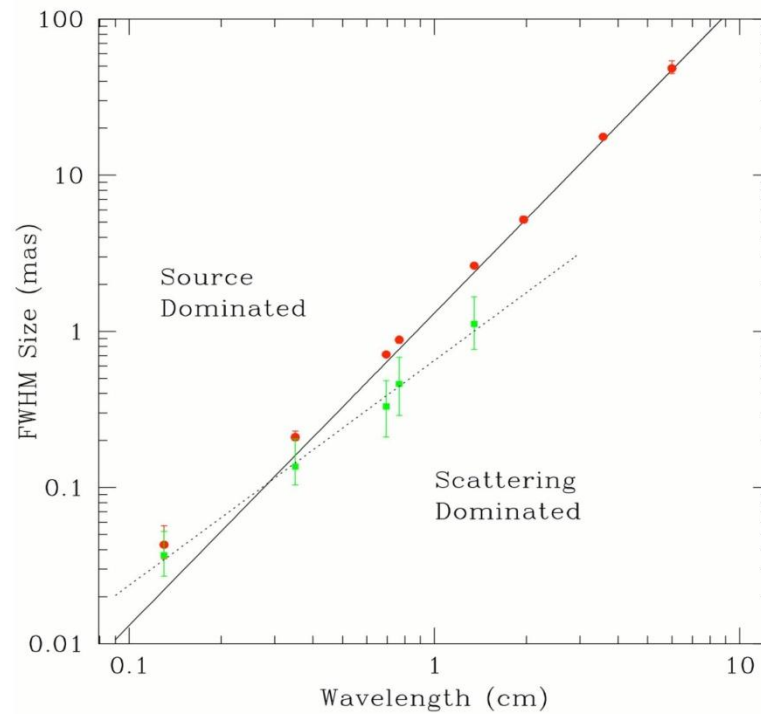


**Fig 2**

**Figure 2 Observed and intrinsic size of Sgr A\* as a function of wavelength.** Red circles show major-axis observed sizes of Sgr A\* from VLBI observations (all errors  $3\sigma$ ). Data from wavelengths of 6 cm to 7 mm are from ref. 13, data at 3.5 mm are from ref. 7, and data at 1.3 mm are from the observations reported here. The solid line is the best-fit  $\lambda^2$  scattering law from ref. 13, and is derived from measurements made at  $\lambda > 17$  cm. Below this line, measurements of the intrinsic size of Sgr A\* are dominated by scattering effects, while measurements that fall above the line indicate intrinsic structures that are larger than the scattering size (a ‘source-dominated’ regime). Green points show derived major-axis intrinsic sizes from  $2 \text{ cm} < \lambda < 1.3 \text{ mm}$  and are fitted with a  $\lambda^\alpha$  power law ( $\alpha = 1.44 \pm 0.07$ ,  $1\sigma$ ) shown as a dotted line. When the 1.3-mm point is removed from the fit, the power-law exponent becomes  $\alpha = 1.56 \pm 0.11$  ( $1\sigma$ ).



# RADIO INTERFEROMETER MUCH LARGER THE EARTH

## “SPECTR-R” (Mission “RadioAstron”)

### Main scientific tasks of the mission –

syntheses of high-precision images of various Universe objects, its coordinates measurements and search their variability with the time.  
A fringe width of the system is up to 7 micro arc seconds.

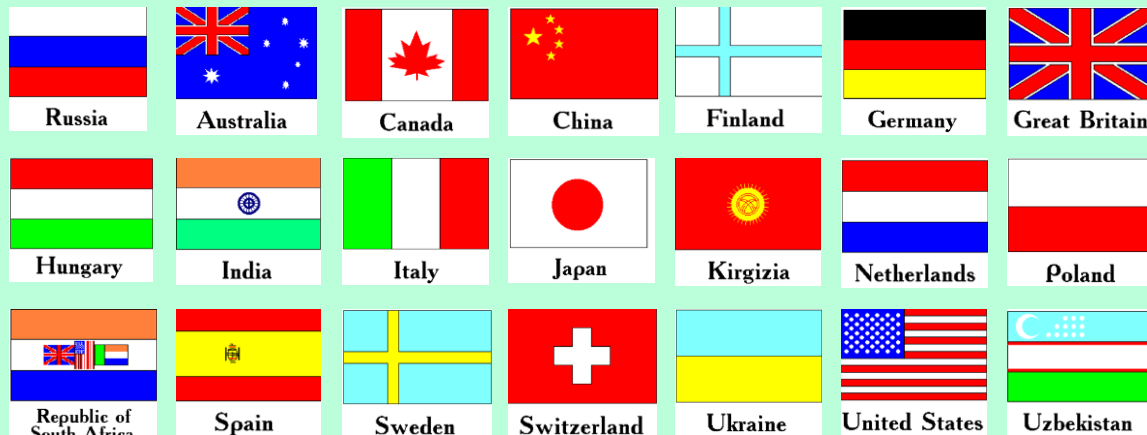
### Main characteristics of the space radio telescope

#### Spectral band:

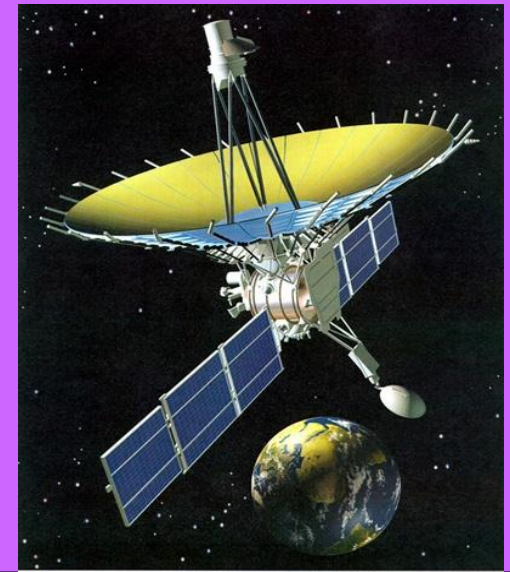
- wavelength (cm) - 92; 18; 6.2; 1.19-1.63
- frequency (GHz) - 0.327; 1.66; 4.83; 18-26

#### Main organizations:

**on scientific complex** - Astro Space Center of Lebedev Physical Institute of Russian Academy of Science;  
**of spacecraft** - Lavochkin Research Production Association of Russian Space Agency.

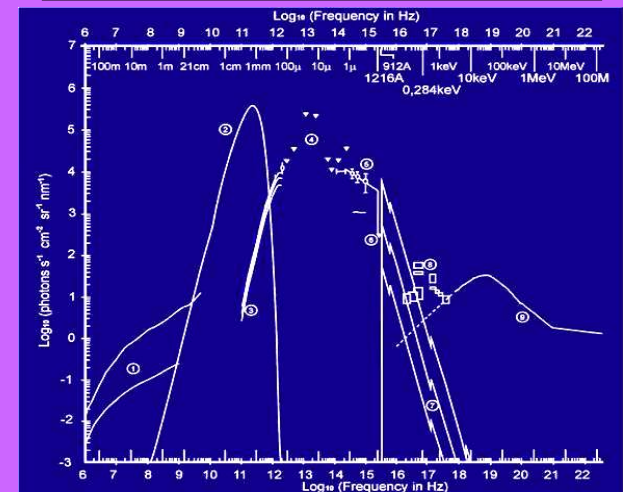


Planned launch date of the mission is 2007.



### The orbit of the mission :

apogee - 310 000 - 370 000 km  
perigee - 10 000 - 70 000 km  
declination - 51.6°  
period variation - 7 - 10 days  
Guaranteed time of activity - 5 years  
Scientific payload mass - 2100 kg  
Pointing accuracy of radio telescope - 35"





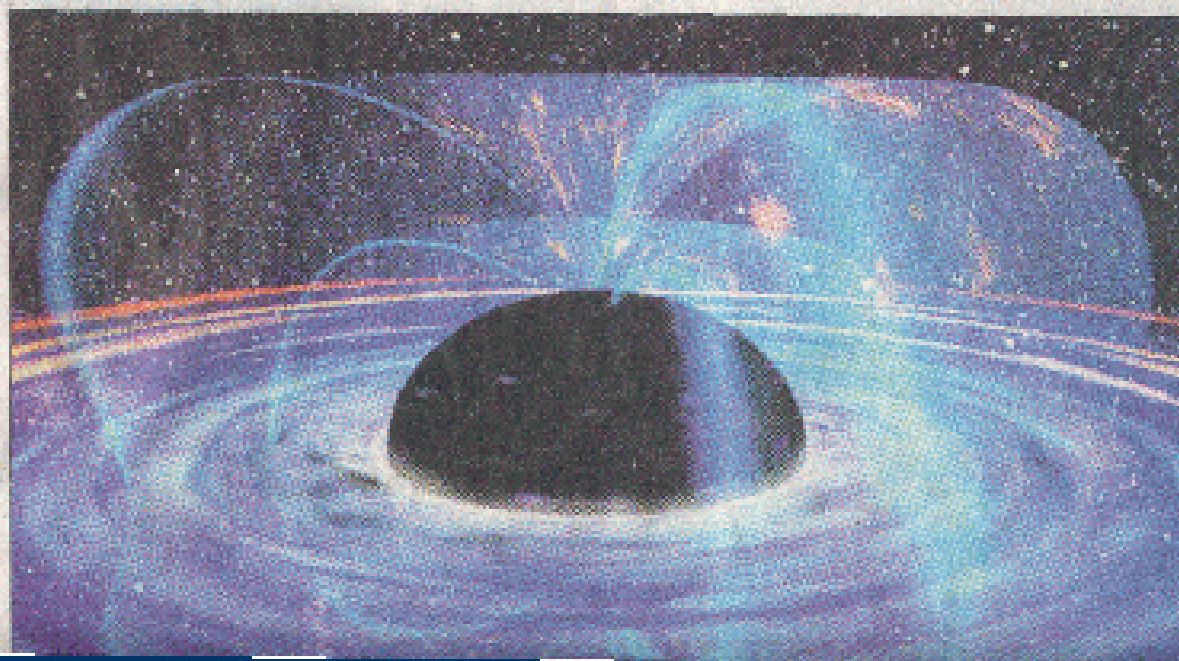
# What is a black hole?

Everyone already seems to know!

## NATIONAL POST

EDL'S NO 304 TUESDAY, OCTOBER 29, 2002 www.nationalpost.com

*Energy-sucking black hole puts on cosmic show for astronomers*



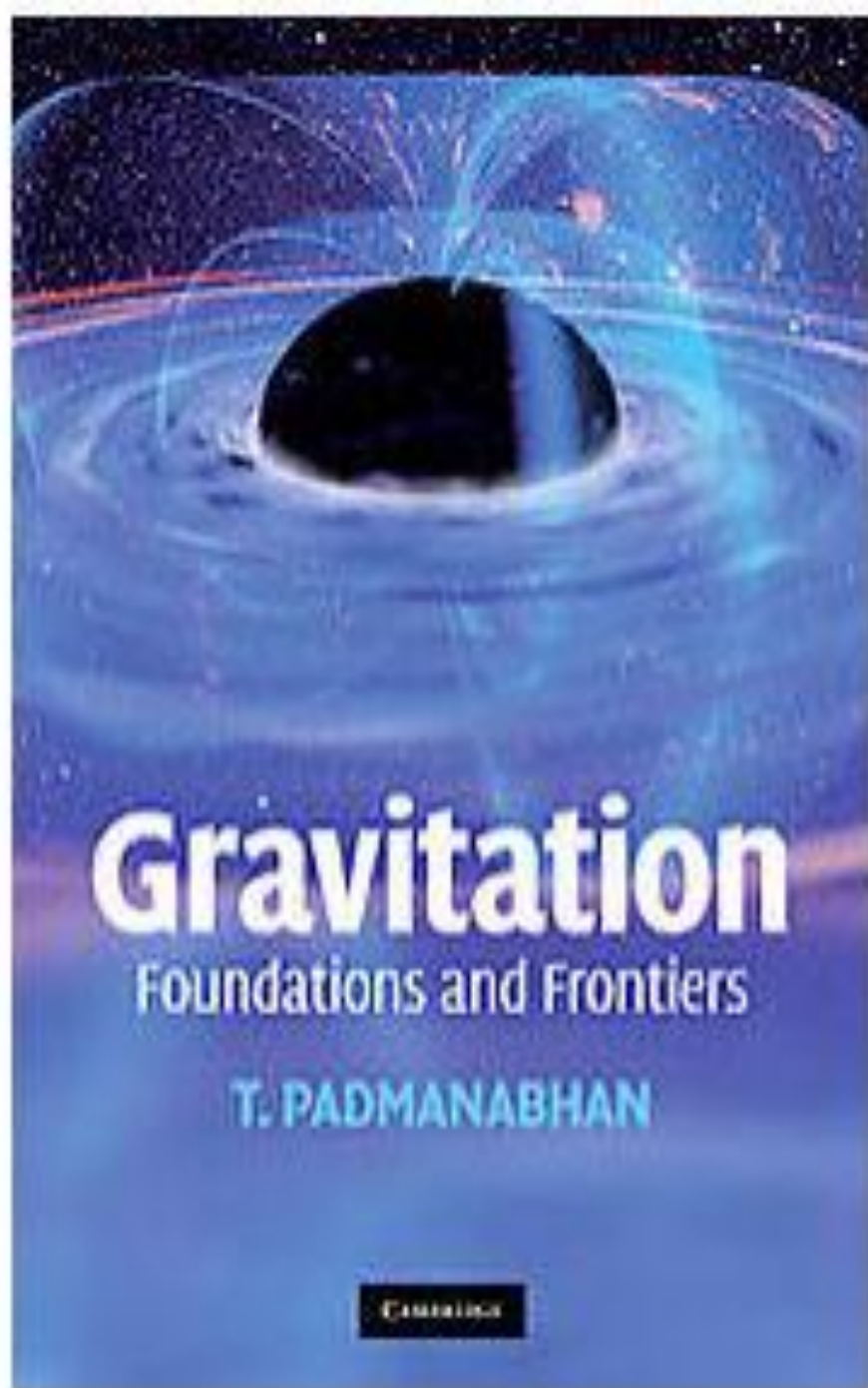
WILL GET CIPRO FROM BA

*Apoptosis and gene  
modification to begin  
in 'deep freeze'*

By Robert F. Kelly  
Special to the Post

ANN ARBOR, Mich. (AP) — A team of scientists from the University of Michigan has found that a gene that controls the rate at which cells die can be turned on or off in a way that allows them to survive in a state of suspended animation for long periods of time. The researchers reported their findings in the journal *Science* on Oct. 25. The team, led by Dr. Robert Kelly, found that the gene, called *p53*, is involved in a process called apoptosis, or programmed cell death. They found that the gene can be turned on or off in a way that allows cells to survive in a state of suspended animation for long periods of time. The researchers reported their findings in the journal *Science* on Oct. 25. The team, led by Dr. Robert Kelly, found that the gene, called *p53*, is involved in a process called apoptosis, or programmed cell death. They found that the gene can be turned on or off in a way that allows cells to survive in a state of suspended animation for long periods of time.





# Gravitation

Foundations and Frontiers

T. PADMANABHAN

Cambridge

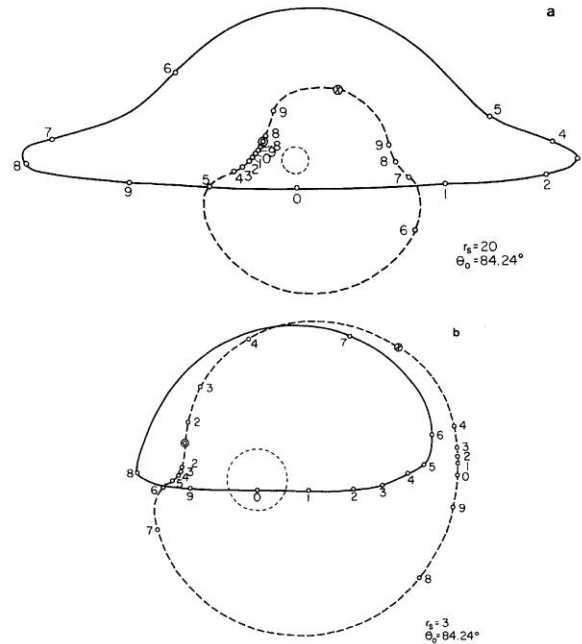


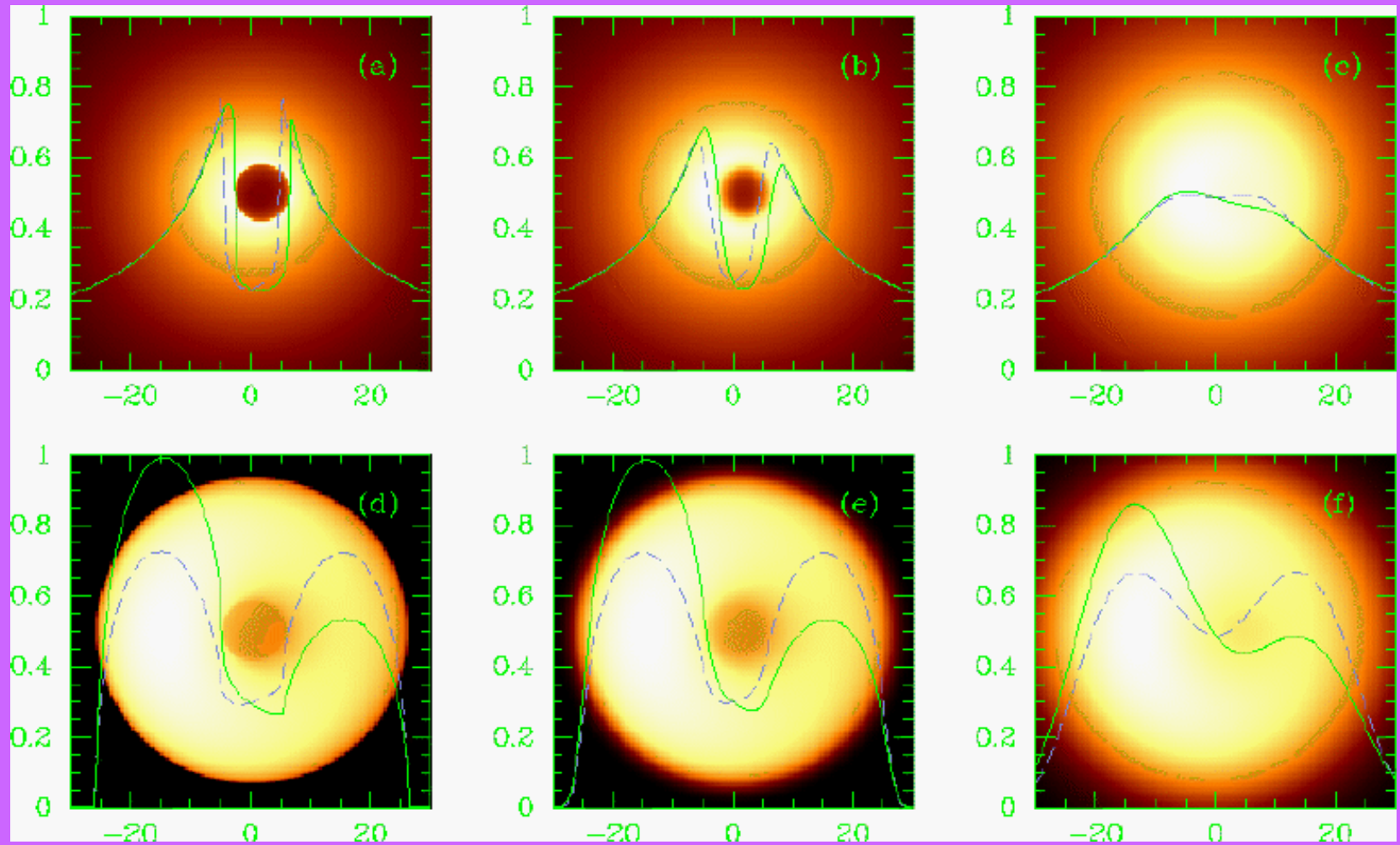
FIG. 8.—Apparent positions of the two brightest images as functions of time for two orbital radii and an observer at a polar angle  $\theta_0 = 84.24^\circ$ . The small, dashed circle in each plot is the locus  $\alpha^2 + \beta^2 = 1$  and gives the scale of the plot. The direct image moves along the solid line; the one-orbit image, along the dashed line. Ticks mark the positions of the images at 10 equally spaced times. A pair of one-orbit images appears to be created at the points  $\odot$  and annihilated at the points  $\otimes$ . See text.

fore of  $\alpha$ ) and the variation in surface brightness increase more rapidly for the one-orbit image than for the direct image as we consider stars of progressively smaller orbital radii.

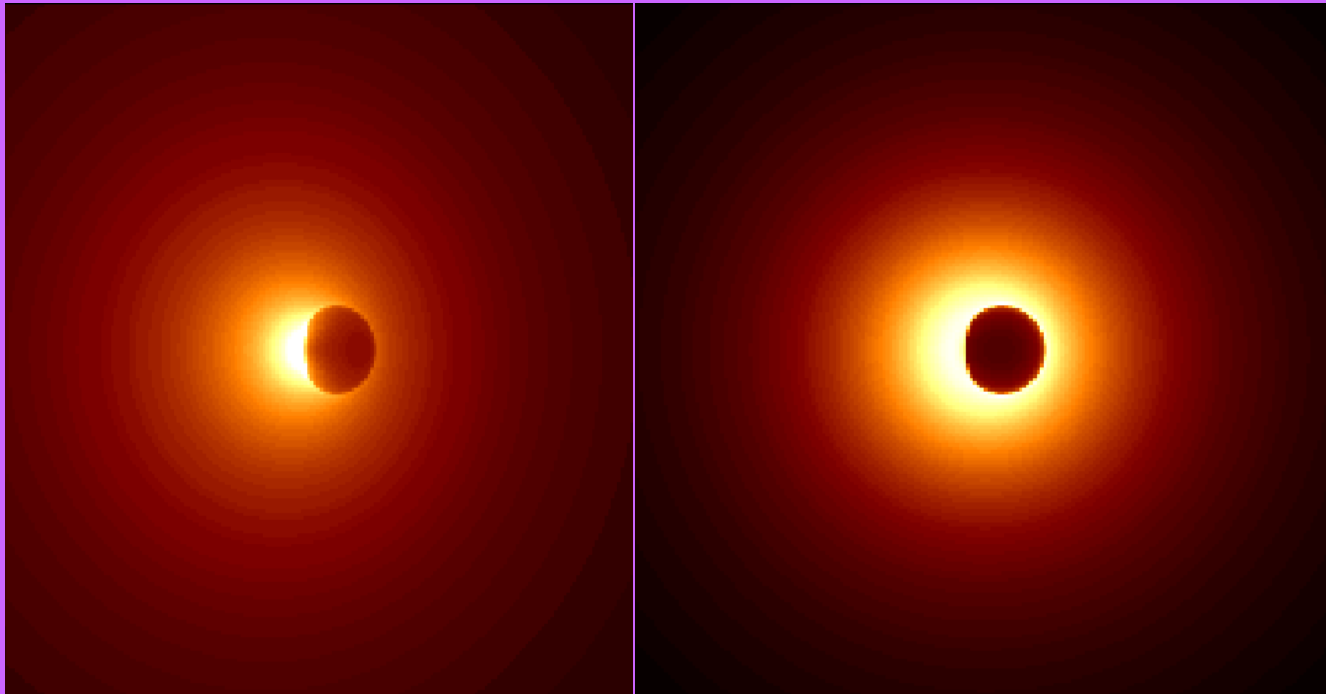
As the apparent position of the image seen by the distant observer changes, so does the corresponding direction of emission in the local rest frame of the star. If the instantaneous direction of emission of the beam of radiation which reaches the observer is represented by a point in figure 3 (for  $r_s = 1.5$ ), this point moves along the  $\cos \theta_0 = \text{const.}$  curve corresponding to the given type of image in the direction indicated by the arrows. Creation of pairs of images on the one-orbit curves is at the points marked  $\odot$ ; destruction, at points  $\otimes$ . For  $r_s = 1.5$  there is no retrograde image and, hence, no creation and destruction of images for observers with  $\theta_0 \lesssim 40^\circ$ .

When  $r_s$  is not much larger than unity, the images move very slowly on the parts of the curves nearest the backward  $\phi$ -direction and very rapidly on the remainder of the

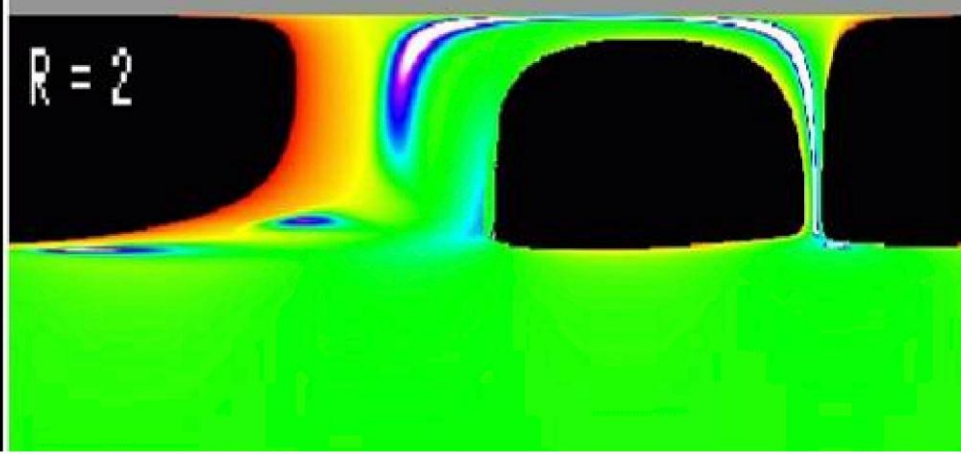
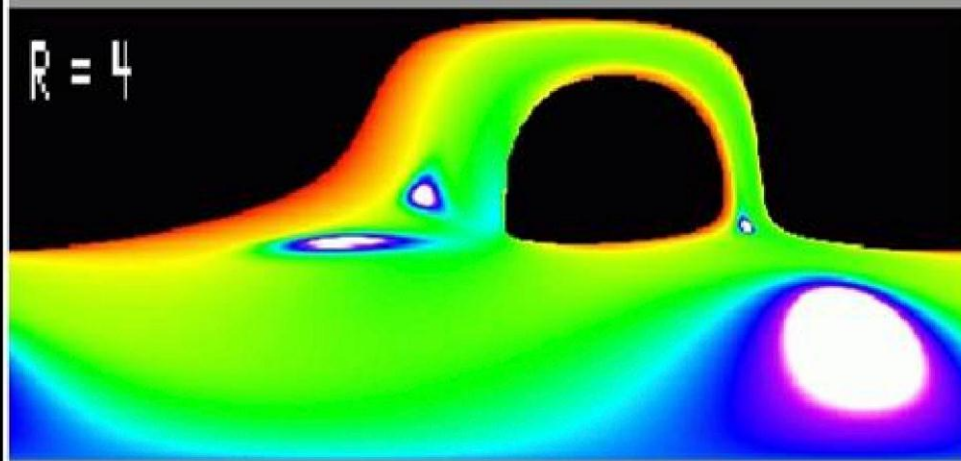
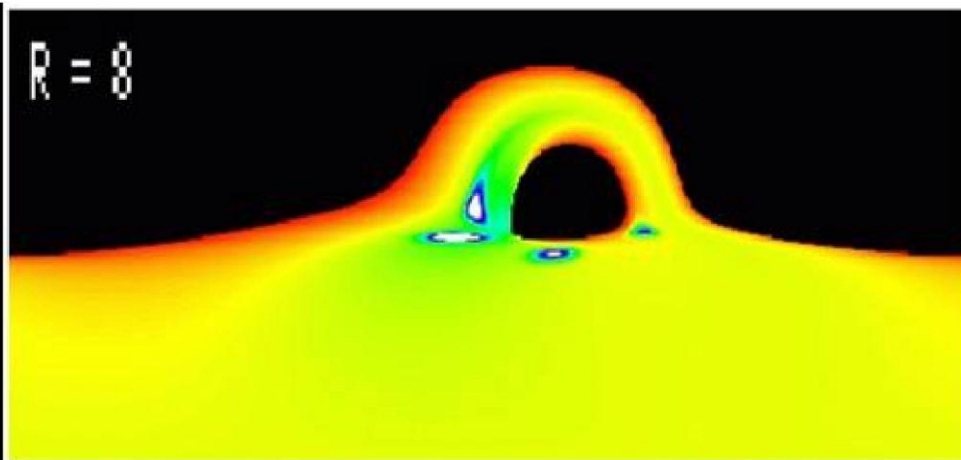
# Falcke, Melia, Agol



# Shadows from Melia



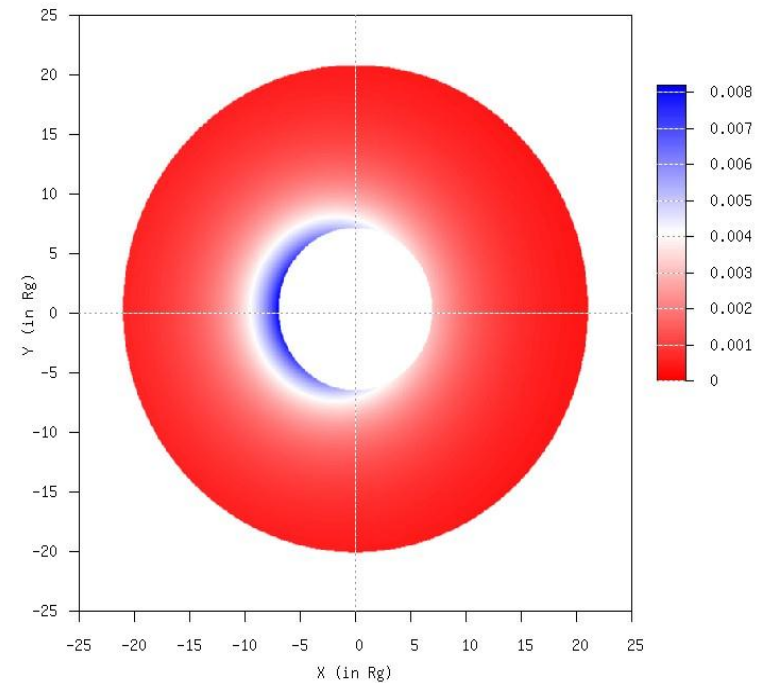
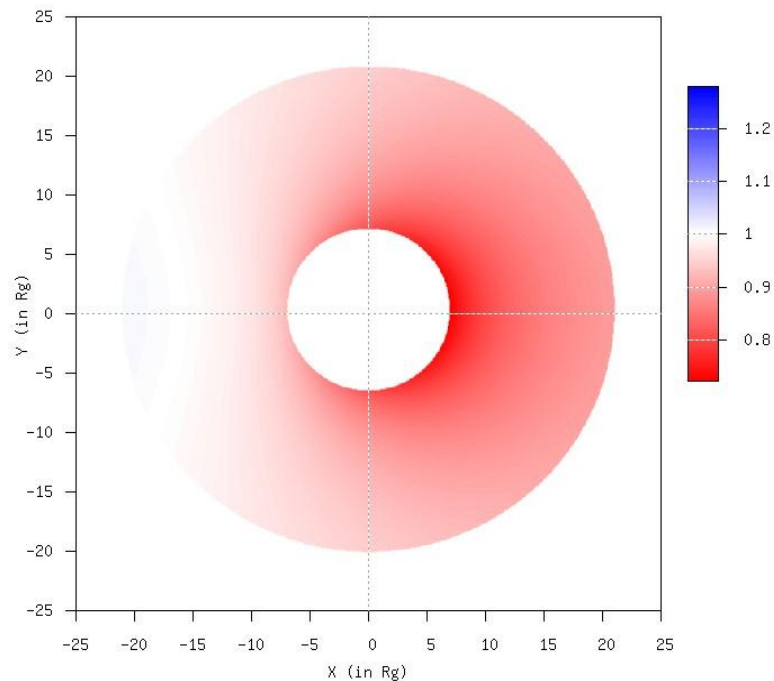
Kevin  
Rauch  
JHU



# Schwarzschild black hole images (P. Jovanovic , L.C. Popovic & A.F.Z. in preparation)

- $\theta=15$  deg
- Redshift map

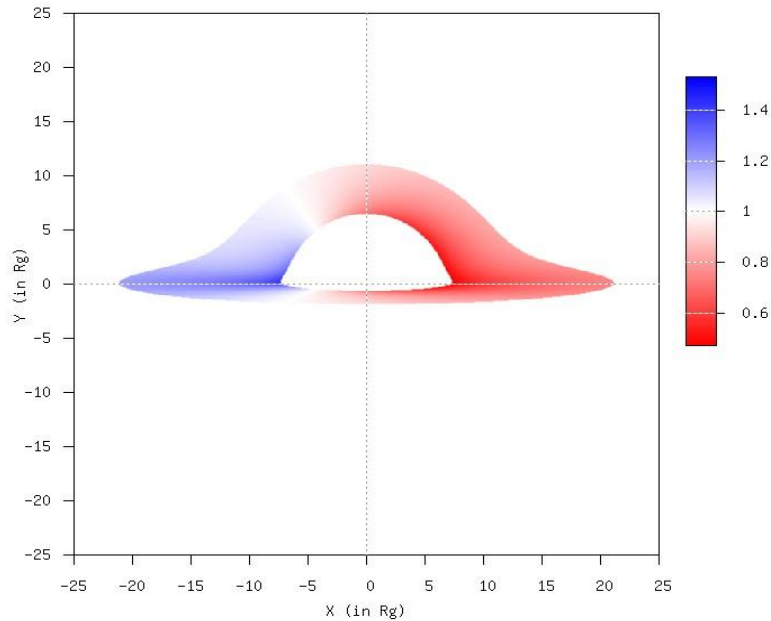
Intensity map





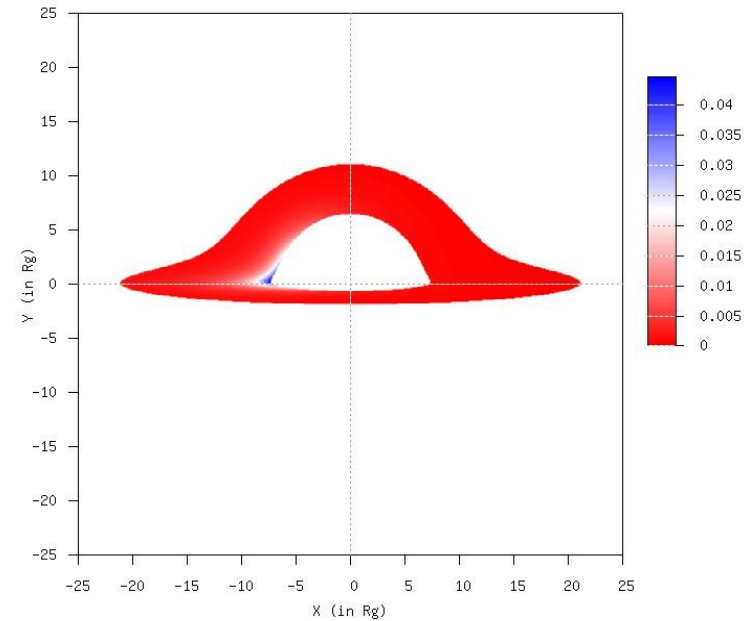
# Schwarzschild black hole images: $\theta=85$ deg

- Redshift map



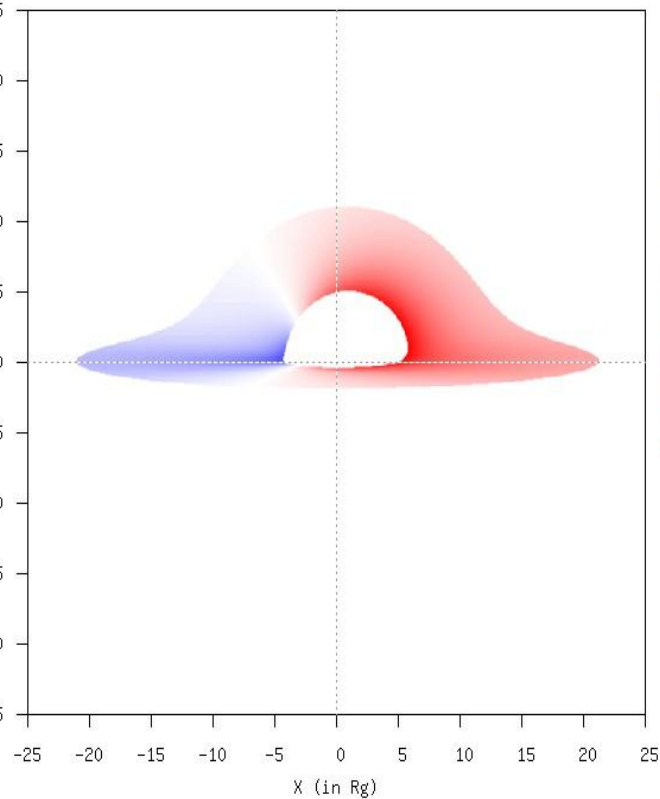
- 

Intensity map



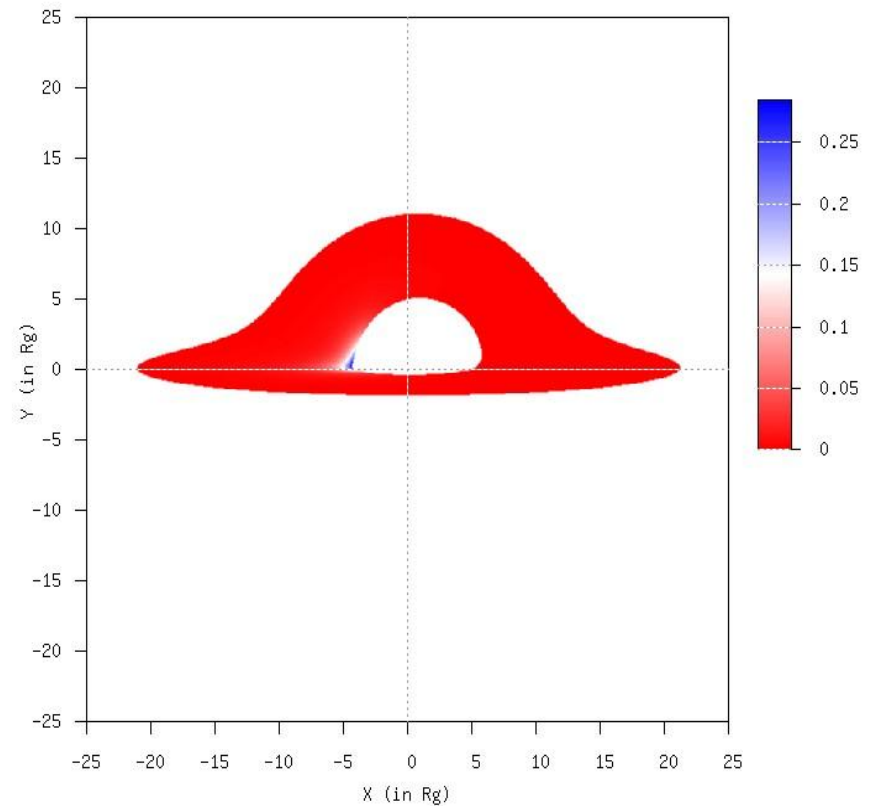
# Kerr black hole images ( $a=0.75$ ): $\theta=85$ deg

- Redshift map



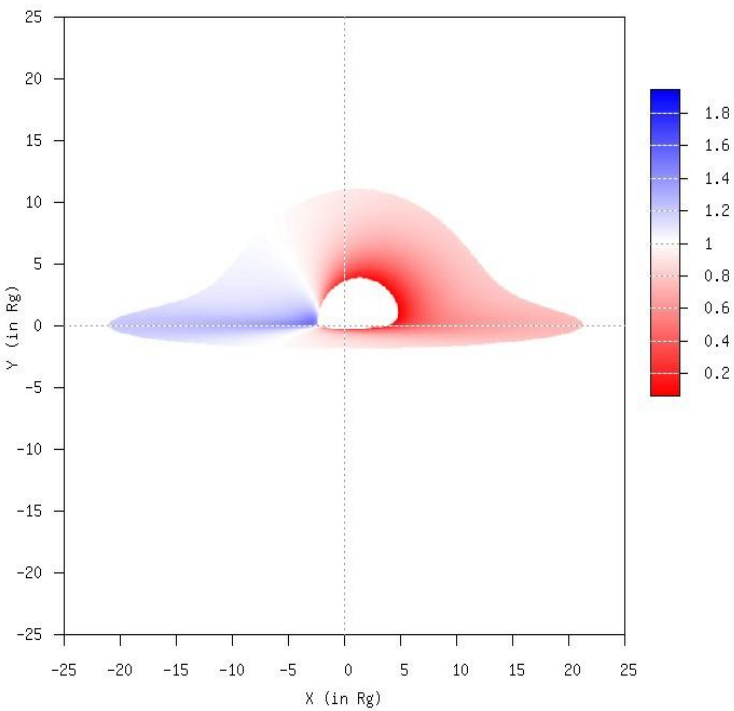
- 

Intensity map

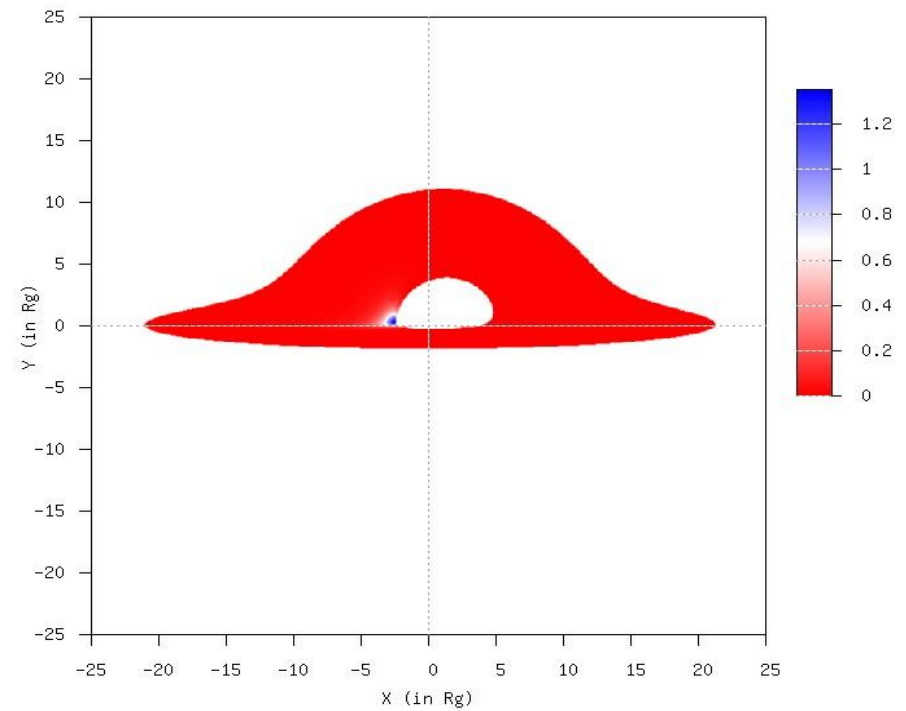


# Kerr black hole images ( $a=0.99$ ): $\theta=85$ deg

- Redshift map



- Intensity map



1995.50

S0-8

0".1

S0-26

S0-16

S0-2

S0-3

S0-1

S0-19

\*

S0-23

S0-4

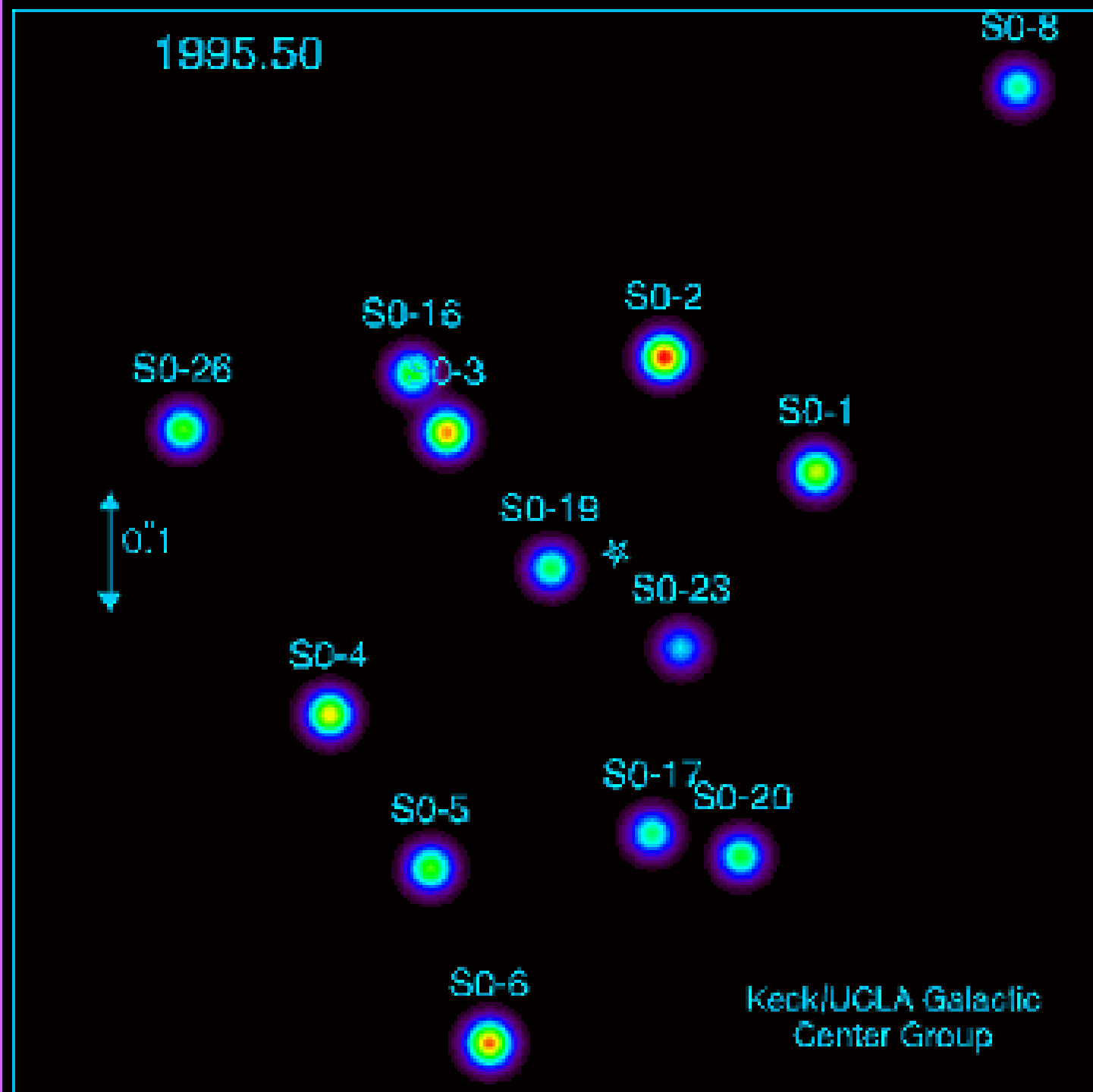
S0-17

S0-20

S0-5

S0-6

Keck/UCLA Galactic  
Center Group



## **2012 Crafoord Prize in Astronomy Goes to Genzel & Ghez**

The Royal Swedish Academy of Sciences has decided to award the Crafoord Prize in Astronomy 2012 to Reinhard Genzel, Max Planck Institute for Extraterrestrial Physics, Garching, Germany and Andrea Ghez, University of California, Los Angeles, USA, "for their observations of the stars orbiting the galactic centre, indicating the presence of a supermassive black hole".

### **The Dark Heart of the Milky Way**

This year's Crafoord Prize Laureates have found the most reliable evidence to date that supermassive black holes really exist. For decades Reinhard Genzel and Andrea Ghez, with their research teams, have tracked stars around the centre of the Milky Way galaxy. Separately, they both arrived at the same conclusion: in our home galaxy resides a giant black hole called Sagittarius A\*.

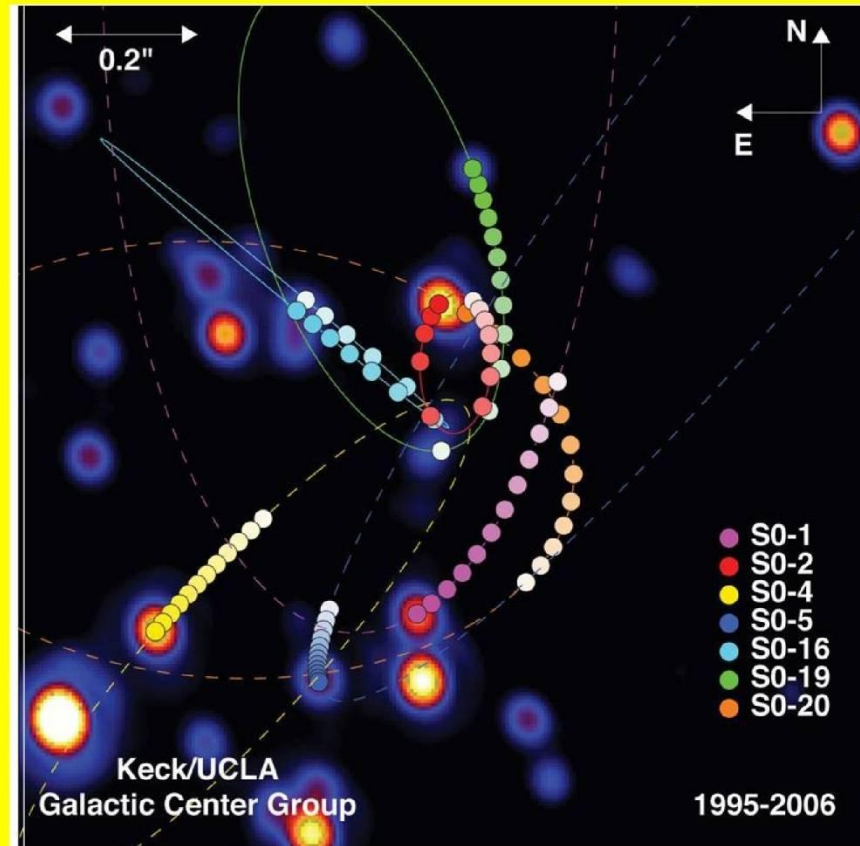


Figure 19: Bright stars near the Galactic Centre.



## MONITORING STELLAR ORBITS AROUND THE MASSIVE BLACK HOLE IN THE GALACTIC CENTER

S. GILLESSEN<sup>1</sup>, F. EISENHAEUER<sup>1</sup>, S. TRIPPE<sup>1</sup>, T. ALEXANDER<sup>3</sup>, R. GENZEL<sup>1,2</sup>, F. MARTINS<sup>4</sup>, T. OTT<sup>1</sup>*Draft version October 26, 2008*

## ABSTRACT

We present the results of 16 years of monitoring stellar orbits around the massive black hole in center of the Milky Way using high resolution near-infrared techniques. This work refines our previous analysis mainly by greatly improving the definition of the coordinate system, which reaches a long-term astrometric accuracy of  $\approx 300 \mu\text{as}$ , and by investigating in detail the individual systematic error contributions. The combination of a long time baseline and the excellent astrometric accuracy of adaptive optics data allow us to determine orbits of 28 stars, including the star S2, which has completed a full revolution since our monitoring began. Our main results are: all stellar orbits are fit extremely well by a single point mass potential to within the astrometric uncertainties, which are now  $\approx 6\times$  better than in previous studies. The central object mass is  $(4.31 \pm 0.06|_{\text{stat}} \pm 0.36|_{R_0}) \times 10^6 M_\odot$  where the fractional statistical error of 1.5% is nearly independent from  $R_0$  and the main uncertainty is due to the uncertainty in  $R_0$ . Our current best estimate for the distance to the Galactic Center is  $R_0 = 8.33 \pm 0.35$  kpc. The dominant errors in this value is systematic. The mass scales with distance as  $(3.95 \pm 0.06) \times 10^6 (R_0/8 \text{ kpc})^{2.19} M_\odot$ . The orientations of orbital angular momenta for stars in the central arcsecond are random. We identify six of the stars with orbital solutions as late type stars, and six early-type stars as members of the clockwise rotating disk system, as was previously proposed. We constrain the extended dark mass enclosed between the pericenter and apocenter of S2 at less than 0.066, at the 99% confidence level, of the mass of Sgr A\*. This is two orders of magnitudes larger than what one would expect from other theoretical and observational estimates.

*Subject headings:* blackhole physics — astrometry — Galaxy: center — infrared: stars

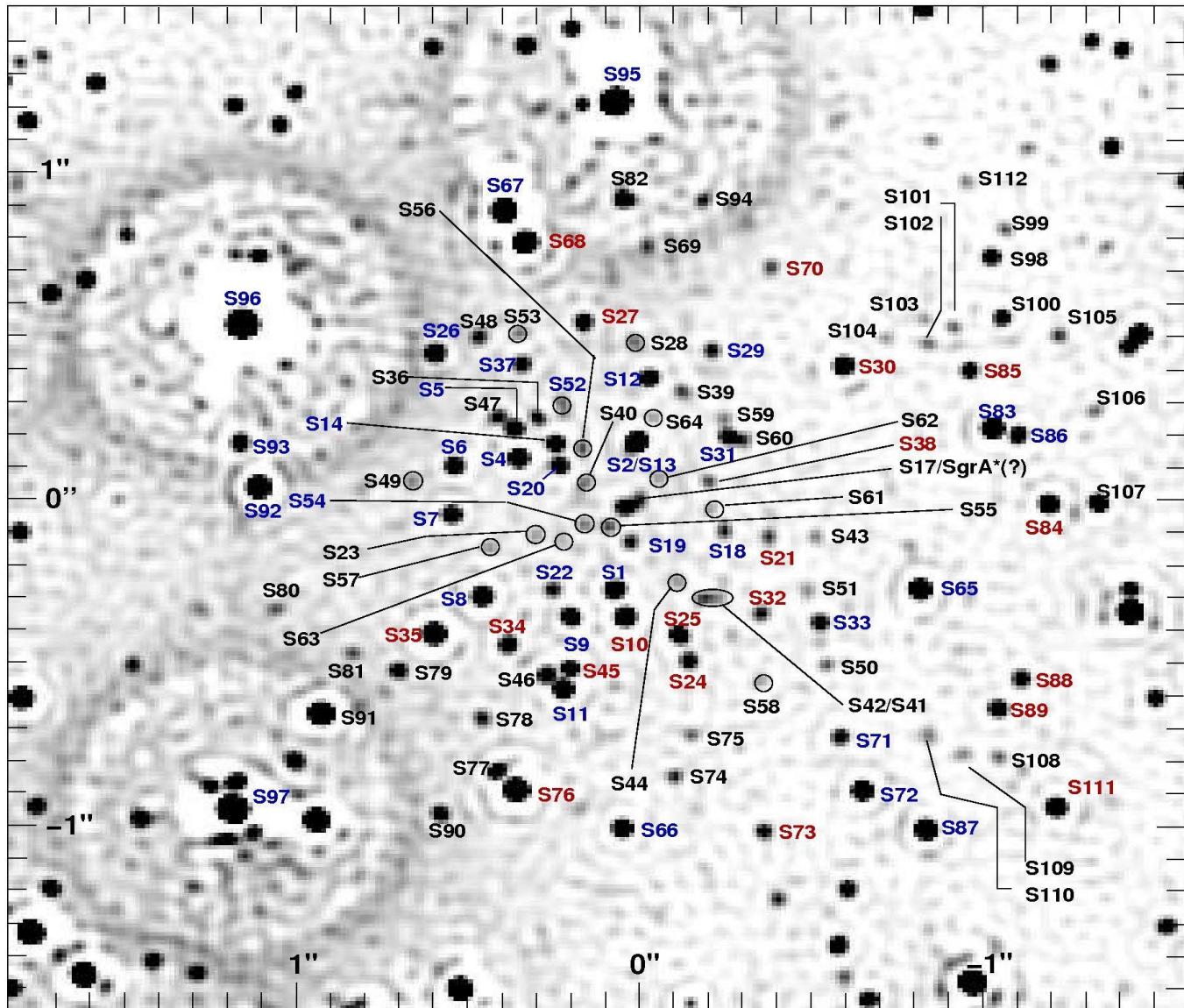


FIG. 1.— Finding chart of the S-star cluster. This figure is based on a natural guide star adaptive optics image obtained as part of this study, using NACO at UT4 (Yepun) of the VLT on July 20, 2007 in the H-band. The original image with a FWHM of  $\approx 75$  mas was deconvolved with the Lucy-Richardson algorithm and beam restored with a Gaussian beam with FWHM = 2 pix = 26.5 mas. Stars as faint as  $m_H = 19.2$  (corresponding roughly to  $m_K = 17.7$ ) are detected at the  $5\sigma$  level. Only stars that are unambiguously identified in several images have designated names, ranging from S1 to S112. Blue labels indicate early-type stars, red labels late-type stars. Stars with unknown spectral type are labelled in black. At the position of Sgr A\* some light is seen, which could be either due to Sgr A\* itself or due to a faint, so far unrecognized star being confused with Sgr A\*.



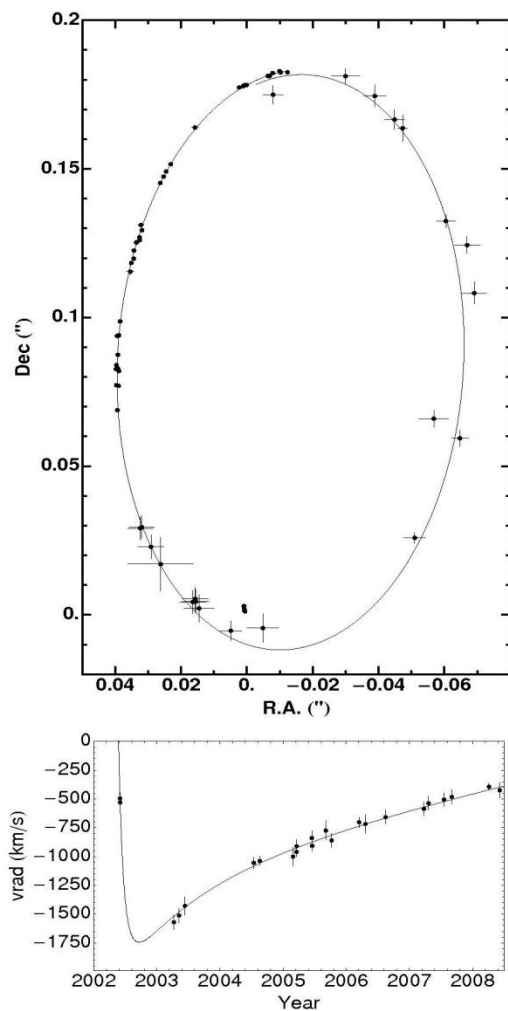


FIG. 13.— Top: The S2 orbital data plotted in the combined coordinate system and fitted with a Keplerian model in which the velocity of the central point mass and its position were free fit parameters. The non-zero velocity of the central point mass is the reason why the orbit figure does not close exactly in the overlap region 1992/2008 close to apocenter. The fitted position of the central point mass is indicated by the elongated dot inside the orbit near the origin; its shape is determined from the uncertainty in the position and the fitted velocity, which leads to the elongation. Bottom: The measured radial velocities of S2 and the radial velocity as calculated from the orbit fit.

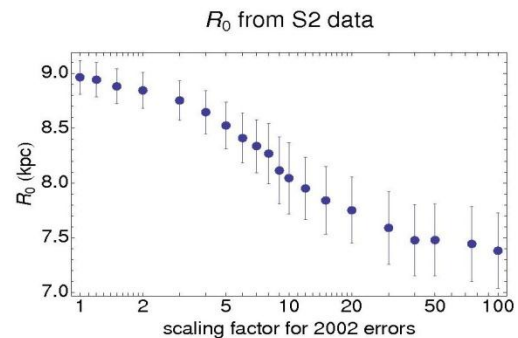


FIG. 14.— Fitted value of  $R_0$  for various scaling factors of the S2 2002 data, using a fit with the coordinate system priors. The factor by which the 2002 astrometric errors of the S2 data is scaled up strongly influences the distance. The mean factor determined in Figure 9 is  $\approx 7$ , corresponding to  $R_0 \approx 8.1$  kpc.

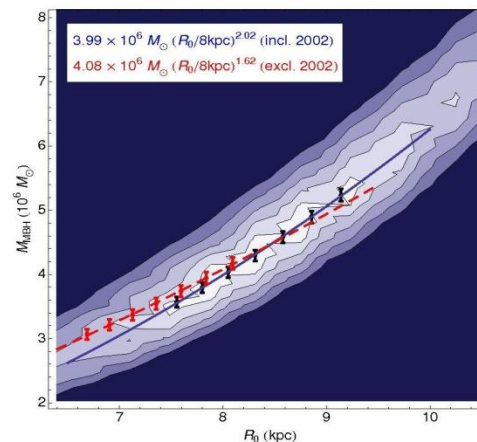
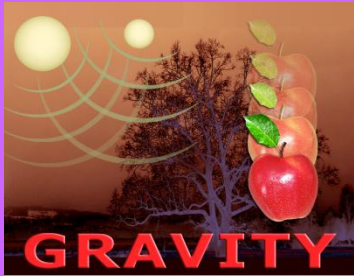


FIG. 15.— Contour plot of  $\chi^2$  as function of  $R_0$  and central point mass. The two parameters are strongly correlated. The contours are generated from the S2 data including the 2002 data; fitting at each point all other parameters both of the potential and the orbital elements. The black dots indicate the position and errors of the best fit values of the mass for the respective distance; the blue line is a power law fit to these points; the corresponding function is given in the upper row of the text box. The central point is chosen at the best fitting distance. The red points and the red dashed line are the respective data and fit for the S2 data excluding the 2002 data; the fit is reported in the lower row of the text box. The contour levels are drawn at confidence levels corresponding to  $1\sigma$ ,  $3\sigma$ ,  $5\sigma$ ,  $7\sigma$ ,  $9\sigma$ .

From the numbers it seems that the fit excluding the



# GRAVITY

## Studying the supermassive black hole at the center of the Galaxy

46<sup>th</sup> Rencontres de Moriond and GPHyS colloquium 2011  
*Gravitational Waves and Experimental Gravity*

Guy Perrin and the GRAVITY consortium



Thursday 25 March 2011

The VLT, *Very Large Telescope*  
4 european 8 m telescopes at Cerro Paranal in Chili

$\lambda/D @ 2 \mu\text{m} = 60 \text{ mas (600 a.u. or 0.003 pc)}$





GRAVITY – 4 giant telescope interferometer  
(General Relativity via VLTI Interferometry)  
 $\lambda/B @ 2 \mu\text{m} = 3 \text{ mas} (30 \text{ a.u. or } 0.00015 \text{ pc})$





# Going beyond boundaries thanks to accurate spatial information

- Bring the ultimate evidence that Sgr A\* is a black hole: the mass is contained in the Schwarzschild radius.
- Understand the nature of flares.
- Use the black hole as a tool to study general relativity in the strong field regime

Scale  $\sim 1 R_s$

10  $\mu$ as

- Study relativistic effects on nearby stars
- Understand the nature of S stars and their distribution

Scale  $\sim 100 R_s$

1 mas

# Where do we stand now ?

Concept Design Review: December  
2007

Preliminary Design Review:  
December 2009

Final Design Review: October  
2011

First tests at Paranal: 2014

Hopefully first results on Sgr A\* in 4 years.

In the last years intensive searches for dark matter (DM), especially its non-baryonic component, both in galactic halos and at galaxy centers have been undertaken (see for example Bertone et al. (2005,2005a) for recent results). It is generally accepted that the most promising candidate for the DM non-baryonic component is neutralino. In this case, the  $\gamma$ -flux from galactic halos (and from our Galactic halo in particular) could be explained by neutralino annihilation (Gurevich et al. 1997, Bergstrom et al. 1998, Tasitsiomi et al. 2002, Stoehr et al. 2003, Prada et al. 2004, Profumo et al. 2005, Mambrini et al. 2005). Since  $\gamma$ -rays are detected not only from high galactic latitude, but also from the Galactic Center, there is a wide spread hypothesis (see, Evans (2004) for a discussion) that a DM concentration might be present at the Galactic Center. In this case the Galactic Center could be a strong source of  $\gamma$ -rays and neutrinos (Bouquet 1989, Stecker 1988, Berezhinsky et al. 1994, Bergstrom et al. 1998, Bertone et al. 2004, Gnedin et al. 2004, Bergstrom et al. 2005, Horns 2005, Bertone et al. 2005) due to DM annihilation. Since it is also expected that DM forms spikes at



galaxy centers (Gondolo & Silk 1999, Ullio et al. 2001, Merritt et al. 2003) the  $\gamma$ -ray flux from the Galactic Center should increase significantly in that case.

At the same time, progress in monitoring bright stars near the Galactic Center have been reached recently (Genzel et al. 2003, Ghez et al. 2003, Ghez et al. 2005). The astrometric limit for bright stellar sources near the Galactic Center with 10 meter telescopes is today  $\delta\theta_{10} \sim 1$  mas and the Next Generation Large Telescope (NGLT) will be able to improve this number at least down to  $\delta\theta_{30} \sim 0.5$  mas (Weinberg et al. 2005) or even to  $\delta\theta_{30} \sim 0.1$  mas (Weinberg et al. 2005) in the K-band. Therefore, it will be possible to measure the proper motion for about  $\sim 100$  stars with astrometric errors several times smaller than errors in current observations.

The aim of this talk is to constrain the parameters of the DM distribution possible present around the Galactic Center by considering the induced apoastron shift due to the presence of this DM sphere and either available

data obtained with the present generation of telescopes (the so called *conservative* limit) and also expectations from future NGLT observations or with other advanced observational facilities.

**Celestial mechanics of S2 like stars for BH+cluster (A.A. Nucita, F. De Paolis, G. Ingrosso, A. Qadir, AFZ, PASP, v. 119, p. 349 (2007))**

GR predicts that orbits about a massive central body suffer periastron shifts yielding *rosette* shapes. However, the classical perturbing effects of other objects on inner orbits give an opposite shift. Since the periastron advance depends strongly on the compactness of the central body, the detection of such an effect may give information about the nature of the central body itself. This would apply for stars orbiting close to the GC, where there is a “dark object”, the black hole hypothesis being the most natural explanation of the observational data. A cluster of stars in the vicinity of the GC (at a distance  $< 1$  arcsec) has been monitored by ESO and Keck teams for several years.



For a test particle orbiting a Schwarzschild black hole of mass  $M_{\text{BH}}$ , the periastron shift is given by (see e.g. Weinberg, 1972)

$$\Delta\phi_S \simeq \frac{6\pi GM_{\text{BH}}}{d(1-e^2)c^2} + \frac{3(18+e^2)\pi G^2 M_{\text{BH}}^2}{2d^2(1-e^2)^2 c^4}, \quad (9)$$

$d$  and  $e$  being the semi-major axis and eccentricity of the test particle orbit, respectively. For a rotating black hole with spin parameter  $a = |\mathbf{a}| = J/GM_{\text{BH}}$ , the space-time is described by the Kerr metric and, in the most favorable case of equatorial plane motion ( $(\mathbf{a}, \mathbf{v}) = 0$ ), the shift is given by (Boyer and Price (1965))

$$\Delta\phi_K \simeq \Delta\phi_S + \frac{8a\pi M_{\text{BH}}^{1/2} G^{3/2}}{d^{3/2}(1-e^2)^{3/2} c^3} + \frac{3a^2\pi G^2}{d^2(1-e^2)^2 c^4}, \quad (10)$$

which reduces to eq. (9) for  $a \rightarrow 0$ . In the more general case,  $\mathbf{a} \cdot \mathbf{v} \neq 0$ , the

expected periastron shift has to be evaluated numerically.

The expected periastron shifts (mas/revolution),  $\Delta\phi$  (as seen from the center) and  $\Delta\phi_E$  (as seen from Earth at the distance  $R_0 \simeq 8$  kpc from the GC), for the Schwarzschild and the extreme Kerr black holes, for the S2 and S16 stars turn out to be  $\Delta\phi^{S2} = 6.3329 \times 10^5$  and  $6.4410 \times 10^5$  and  $\Delta\phi_E^{S2} = 0.661$  and  $0.672$  respectively, and  $\Delta\phi^{S16} = 1.6428 \times 10^6$  and  $1.6881 \times 10^6$  and  $\Delta\phi_E^{S16} = 3.307$  and  $3.399$  respectively. Recall that

$$\Delta\phi_E = \frac{d(1+e)}{R_0} \Delta\phi_{S,K} . \quad (11)$$

Notice that the differences between the periastron shifts for the Schwarzschild and the maximally rotating Kerr black hole is at most 0.01 mas for the S2 star and 0.009 mas for the S16 star. In order to make these measurements with the required accuracy, one needs to know the S2 orbit with a precision of at least  $10 \mu\text{as}$ .

The star cluster surrounding the central black hole in the GC could be sizable. At least 17 members have been observed within 15 mpc up to now (Ghez et al. (2005)). However, the cluster mass and density distribution, that is to say its mass and core radius, is still unknown. The presence of this cluster affects the periastron shift of stars orbiting the central black hole. The periastron advance depends strongly on the mass density profile and especially on the central density and typical length scale.

We model the stellar cluster by a Plummer model density profile (Binney & Tremaine (1987))

$$\rho_{CL}(r) = \rho_0 f(r) , \quad \text{with} \quad f(r) = \left[ 1 + \left( \frac{r}{r_c} \right)^2 \right]^{-\alpha/2} , \quad (12)$$



where the cluster central density  $\rho_0$  is given by

$$\rho_0 = \frac{M_{CL}}{\int_0^{R_{CL}} 4\pi r^2 f(r) dr}, \quad (13)$$

$R_{CL}$  and  $M_{CL}$  being the cluster radius and mass, respectively. According to dynamical observations towards the GC, we require that the total mass  $M(r) = M_{BH} + M_{CL}(r)$  contained within  $r \simeq 5 \times 10^{-3}$  pc is  $M \simeq 3.67 \times 10^6 M_\odot$ . Useful information is provided by the cluster mass fraction,  $\lambda_{CL} = M_{CL}/M$ , and its complement,  $\lambda_{BH} = 1 - \lambda_{CL}$ . As one can see, the requirement given in eq. (13) implies that  $M(r) \rightarrow M_{BH}$  for  $r \rightarrow 0$ . The total mass density profile  $\rho(r)$  is given by

$$\rho(r) = \lambda_{BH} M \delta^{(3)}(\vec{r}) + \rho_0 f(r) \quad (14)$$

and the mass contained within  $r$  is

$$M(r) = \lambda_{BH}M + \int_0^r 4\pi r'^2 \rho_0 f(r') dr' . \quad (15)$$

According to GR, the motion of a test particle can be fully described by solving the geodesic equations. Under the assumption that the matter distribution is static and pressureless, the equation of motion of the test particle becomes (see e.g. Weinberg 1972))

$$\frac{d\mathbf{v}}{dt} \simeq -\nabla(\Phi_N + 2\Phi_N^2) + 4\mathbf{v}(\mathbf{v} \cdot \nabla)\Phi_N - v^2\nabla\Phi_N . \quad (16)$$

For the S2 star,  $d$  and  $e$  given in the literature are 919 AU and 0.87 respectively. They yield the orbits of the S2 star for different values of the

black hole mass fraction  $\lambda_{BH}$  shown in Figure 20. The Plummer model parameters are  $\alpha = 5$ , core radius  $r_c \simeq 5.8$  mpc. Note that in the case of  $\lambda_{BH} = 1$ , the expected (prograde) periastron shift is that given by eq. (9), while the presence of the stellar cluster leads to a retrograde periastron shift. For comparison, the expected periastron shift for the S16 star is given in Figure 31. In the latter case, the binary system orbital parameters were taken from Schödel et al. (2003) assuming also for the S16 mass a conservative value of  $\simeq 10 M_{\odot}$ .



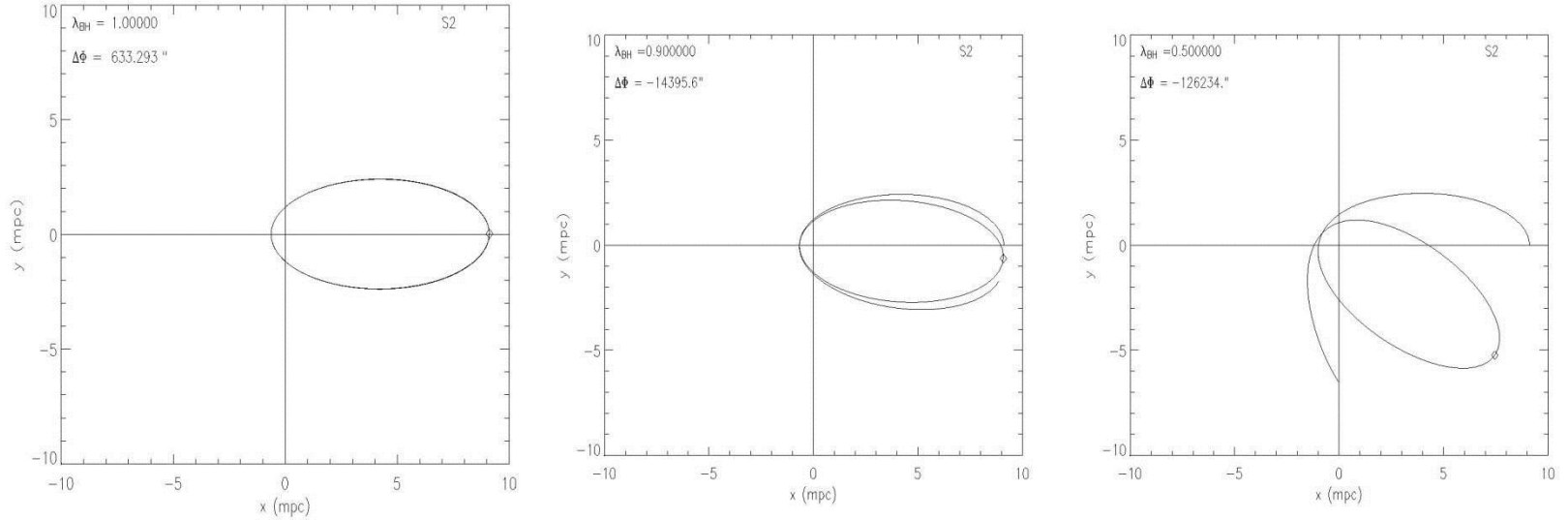


Figure 20: Post Newtonian orbits for different values of the black hole mass fraction  $\lambda_{BH}$  are shown for the S2 star (upper panels). Here, we have assumed that the Galactic central black hole is surrounded by a stellar cluster whose density profile follows a Plummer model with  $\alpha = 5$  and a core radius  $r_c \simeq 5.8$  mpc. The periastron shift values in each panel is given in arcseconds.

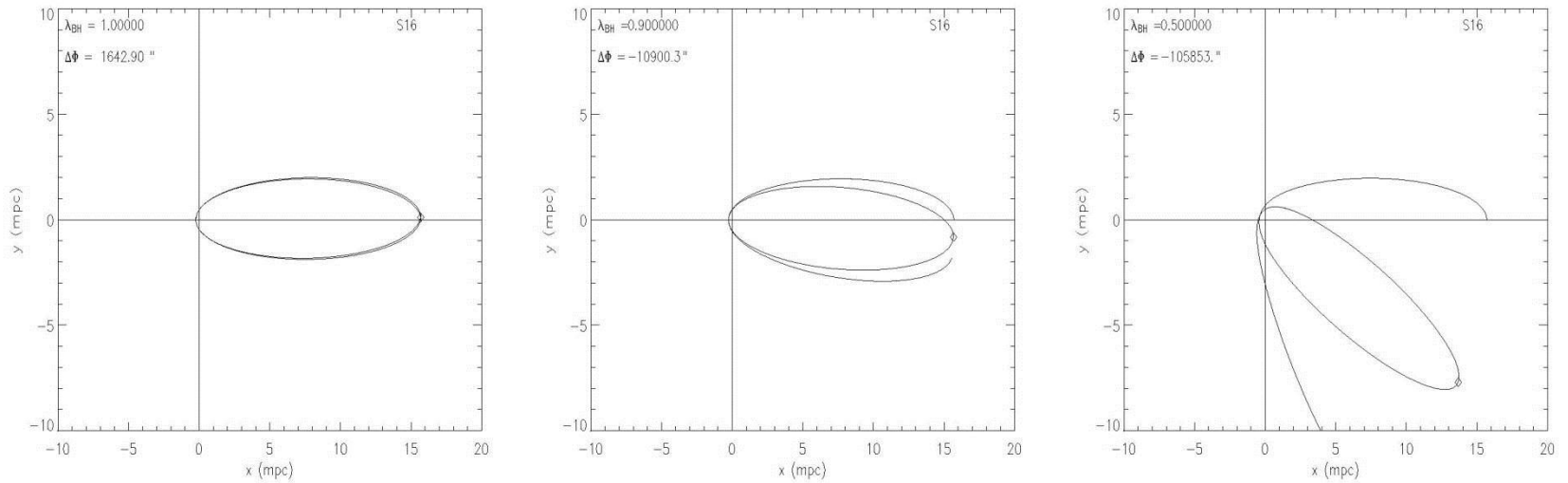


Figure 21: The same as in Figure 20 but for the S16–Sgr A\* binary system. In this case, the binary system orbital parameters were taken from Ghez et al. (2005) assuming for the S16 mass a conservative value of  $\simeq 10 M_{\odot}$ .

**AFZ, A.A. Nucita, F. De Paolis, G. Ingrosso, PRD 76,  
062001 (2007)**

## **The mass concentration at the Galactic Center**

Recent advancements in infrared astronomy are allowing to test the scale of the mass profile at the center of our galaxy down to tens of AU. With the Keck 10 m telescope, the proper motion of several stars orbiting the Galactic Center black hole have been monitored and almost entire orbits, as for example that of the S2 star, have been measured allowing an unprecedented description of the Galactic Center region. Measurements of the amount of mass  $M(< r)$  contained within a distance  $r$  from the Galactic Center are continuously improved as more precise data are collected. Recent observations (Ghez et al. (2003)) extend down to the periastron distance ( $\simeq 3 \times 10^{-4}$  pc) of the S16 star and they correspond to a value of the enclosed mass within  $\simeq 3 \times 10^{-4}$  pc of  $\simeq 3.67 \times 10^6 M_{\odot}$ . Several authors have used these observations to model the Galactic Center mass concentration. Here and in the following, we use the three component

model for the central region of our galaxy based on estimates of enclosed mass given by Ghez et al (2003, 2005) recently proposed by Hall and Gondolo (2006). This model is constituted by the central black hole, the central stellar cluster and the DM sphere (made of WIMPs), i.e.

$$M(< r) = M_{BH} + M_*(< r) + M_{DM}(< r) , \quad (17)$$

where  $M_{BH}$  is the mass of the central black hole Sagittarius A\*. For the central stellar cluster, the empirical mass profile is

$$M_*(< r) = \begin{cases} M_* \left( \frac{r}{R_*} \right)^{1.6} , & r \leq R_* \\ M_* \left( \frac{r}{R_*} \right)^{1.0} , & r > R_* \end{cases} \quad (18)$$

with a total stellar mass  $M_* = 0.88 \times 10^6 M_\odot$  and a size  $R_* = 0.3878$  pc.



As far as the mass profile of the DM concentration is concerned, Hall & Gondolo (2006) have assumed a mass distribution of the form

$$M_{DM}(< r) = \begin{cases} M_{DM} \left( \frac{r}{R_{DM}} \right)^{3-\alpha}, & r \leq R_{DM} \\ M_{DM}, & r > R_{DM} \end{cases} \quad (19)$$

$M_{DM}$  and  $R_{DM}$  being the total amount of DM in the form of WIMPs and the radius of the spherical mass distribution, respectively.

Hall and Gondolo (2006) discussed limits on DM mass around the black hole at the Galactic Center. It is clear that present observations of stars around the Galactic Center do not exclude the existence of a DM sphere with mass  $\simeq 4 \times 10^6 M_{\odot}$ , well contained within the orbits of the known stars, if its radius  $R_{DM}$  is  $\lesssim 2 \times 10^{-4}$  pc (the periastron distance of the S16 star in the more recent analysis (Ghez et al. 2005)). However, if one



considers a DM sphere with larger radius, the corresponding upper value for  $M_{DM}$  decreases (although it tends again to increase for extremely extended DM configurations with  $R_{DM} \gg 10$  pc). In the following, we will assume for definiteness a DM mass  $M_{DM} \sim 2 \times 10^5 M_{\odot}$ , that is the upper value for the DM sphere (Hall & Gondolo (2006)) within an acceptable confidence level in the range  $10^{-3} - 10^{-2}$  pc for  $R_{DM}$ . As it will be clear in the following, we emphasize that even a such small value for the DM mass (that is about only 5% of the standard estimate  $3.67 \pm 0.19 \times 10^6 M_{\odot}$  for the dark mass at the Galactic Center (Ghez et al. 2005)) may give some observational signatures.

Evaluating the S2 apoastron shift <sup>1</sup> as a function of  $R_{DM}$ , one can further constrain the DM sphere radius since even now we can say that there is no evidence for negative apoastron shift for the S2 star orbit at the

---

<sup>1</sup>We want to note that the periastron and apoastron shifts  $\Delta\Phi$  as seen from the orbit center have the same value whereas they have different values as seen from Earth (see Eq. (23)). When we are comparing our results with orbit reconstruction from observations we refer to the apoastron shift as seen from Earth.

level of about 10 mas (Genzel et al. 2003). In addition, since at present the precision of the S2 orbit reconstruction is about 1 mas, we can say that even without future upgrades of the observational facilities and simply monitoring the S2 orbit, it will be possible within about 15 years to get much more severe constraints on  $R_{DM}$ .

Moreover, observational facilities will allow in the next future to monitor faint infrared objects at the astrometric precision of about 10  $\mu$ as (Eisenhauer et al. 2005) and, in this case, previous estimates will be sensibly improved since it is naturally expected to monitor eccentric orbits for faint infrared stars closer to the Galactic Center with respect to the S2 star.

In Fig. 30, the mass profile  $M(< r)$  (Ghez et al. 2003) obtained by using observations of stars nearby the Galactic Center is shown (solid line). The dotted line represents the stellar mass profile as given in Eq. (18), while the dashed lines are for DM spheres with mass  $M_{DM} \simeq 2 \times 10^5 M_{\odot}$  and

radii  $R_{DM} = 10^{-3}$  and  $10^{-2}$  pc, respectively.



## Apoastron Shift Constraints

According to GR, the motion of a test particle can be fully described by solving the geodesic equations. Under the assumption that the matter distribution is static and pressureless, the equations of motion at the first post-Newtonian (PN) approximation become (see e.g. (Fock 1961, Weinberg 1972, Rubilar & Eckart 2001))

$$\frac{d\mathbf{v}}{dt} \simeq -\nabla(\Phi_N + 2\Phi_N^2) + 4\mathbf{v}(\mathbf{v} \cdot \nabla)\Phi_N - v^2\nabla\Phi_N . \quad (21)$$

We note that the PN-approximation is the first relativistic correction from which the apoastron advance phenomenon arises. In the case of the S2 star, the apoastron shift as seen from Earth (from Eq. (23)) due to the presence of a central black hole is about 1 mas, therefore not directly

detectable at present since the available precision in the apoastron shift is about 10 mas (but it will become about 1 mas in 10–15 years even without considering possible technological improvements). It is also evident that higher order relativistic corrections to the S2 apoastron shift are even smaller and therefore may be neglected at present, although they may become important in the future.

As it will be discussed below, the Newtonian effect due to the existence of a sufficiently extended DM sphere around the black hole may cause a apoastron shift in the opposite direction with respect to the relativistic advance due to the black hole. Therefore, we have considered the two effects comparing only the leading terms.

For the DM distribution at the Galactic Center we follow Eq. (19) as done in Hall & Gondolo (2006). Clearly, if in the future faint infrared stars (or spots) closer to the black hole with respect to the S2 star will be monitored (Eisenhauer, (2005)), this simplified model might well not hold



and higher order relativistic corrections may become necessary.

For a spherically symmetric mass distribution (such as that described above) and for a gravitational potential given by Eq. (20), Eq. (21) may be rewritten in the form (see for details Rubilar & Eckart (2001))

$$\frac{d\mathbf{v}}{dt} \simeq -\frac{GM(r)}{r^3} \left[ \left( 1 + \frac{4\Phi_N}{c^2} + \frac{v^2}{c^2} \right) \mathbf{r} - \frac{4\mathbf{v}(\mathbf{v} \cdot \mathbf{r})}{c^2} \right], \quad (22)$$

$\mathbf{r}$  and  $\mathbf{v}$  being the vector radius of the test particle with respect to the center of the stellar cluster and the velocity vector, respectively. Once the initial conditions for the star distance and velocity are given, the rosetta shaped orbit followed by a test particle can be found by numerically solving the set of ordinary differential equations in eq. (22).

In Fig. 20, as an example, assuming that the test particle orbiting the Galactic Center region is the S2 star, we show the Post Newtonian orbits

detectable at present since the available precision in the apoastron shift is about 10 mas (but it will become about 1 mas in 10–15 years even without considering possible technological improvements). It is also evident that higher order relativistic corrections to the S2 apoastron shift are even smaller and therefore may be neglected at present, although they may become important in the future.

As it will be discussed below, the Newtonian effect due to the existence of a sufficiently extended DM sphere around the black hole may cause a apoastron shift in the opposite direction with respect to the relativistic advance due to the black hole. Therefore, we have considered the two effects comparing only the leading terms.

For the DM distribution at the Galactic Center we follow Eq. (19) as done in Hall & Gondolo (2006). Clearly, if in the future faint infrared stars (or spots) closer to the black hole with respect to the S2 star will be monitored (Eisenhauer, (2005)), this simplified model might well not hold



and higher order relativistic corrections may become necessary.

For a spherically symmetric mass distribution (such as that described above) and for a gravitational potential given by Eq. (20), Eq. (21) may be rewritten in the form (see for details Rubilar & Eckart (2001))

$$\frac{d\mathbf{v}}{dt} \simeq -\frac{GM(r)}{r^3} \left[ \left( 1 + \frac{4\Phi_N}{c^2} + \frac{v^2}{c^2} \right) \mathbf{r} - \frac{4\mathbf{v}(\mathbf{v} \cdot \mathbf{r})}{c^2} \right], \quad (22)$$

$\mathbf{r}$  and  $\mathbf{v}$  being the vector radius of the test particle with respect to the center of the stellar cluster and the velocity vector, respectively. Once the initial conditions for the star distance and velocity are given, the rosetta shaped orbit followed by a test particle can be found by numerically solving the set of ordinary differential equations in eq. (22).

In Fig. 20, as an example, assuming that the test particle orbiting the Galactic Center region is the S2 star, we show the Post Newtonian orbits

obtained by the black hole only, the black hole plus the stellar cluster and the contribution of two different DM mass density profiles. In each case the S2 orbit apoastron shift is given. As one can see, for selected parameters for DM and stellar cluster masses and radii the effect of the stellar cluster is almost negligible while the effect of the DM distribution is crucial since it enormously overcome the shift due to the relativistic precession. Moreover, as expected, its contribution is opposite in sign with respect to that of the black hole (Nucita et al. (2007)).

We note that the expected apoastron (or, equivalently, periastron) shifts (mas/revolution),  $\Delta\Phi$  (as seen from the center) and the corresponding values  $\Delta\phi_E^\pm$  as seen from Earth (at the distance  $R_0 \simeq 8$  kpc from the GC) are related by

$$\Delta\phi_E^\pm = \frac{d(1 \pm e)}{R_0} \Delta\Phi, \quad (23)$$

where with the sign  $\pm$  are indicated the shift angles of the apoastron (+)



and periastron (-), respectively. The S2 star semi-major axis and eccentricity are  $d = 919$  AU and  $e = 0.87$  (Ghez et al. 2005).

In Fig. 32, the S2 apoastron shift as a function of the DM distribution size  $R_{DM}$  is given for  $\alpha = 0$  and  $M_{DM} \simeq 2 \times 10^5 M_{\odot}$ . Taking into account that the present day precision for the apoastron shift measurements is of about 10 mas, one can say that the S2 apoastron shift cannot be larger than 10 mas. Therefore, any DM configuration that gives a total S2 apoastron shift larger than 10 mas (in the opposite direction due to the DM sphere) is excluded. The same analysis is shown in Figs. 33 and 34 for two different values of the DM mass distribution slope, i.e.  $\alpha = 1$  and  $\alpha = 2$ , respectively. In any case, we have calculated the apoastron shift for the S2 star orbit assuming a total DM mass  $M_{DM} \simeq 2 \times 10^5 M_{\odot}$ . As one can see by inspecting Figs. 32-34, the upper limit of about 10 mas on the S2 apoastron shift may allow to conclude that DM radii in the range about  $10^{-3} - 10^{-2}$  pc are excluded by present observations.



We notice that the results of the present analysis allows to further constrain the results (Hall and Gondolo 2006) who have concluded that if the DM sphere radius is in the range  $10^{-3} - 1$  pc, configurations with DM mass up to  $M_{DM} = 2 \times 10^5 M_{\odot}$  are acceptable. The present analysis shows that DM configurations of the same mass are acceptable only for  $R_{DM}$  out the range between  $10^{-3} - 10^{-2}$  pc, almost irrespectively of the  $\alpha$  value.

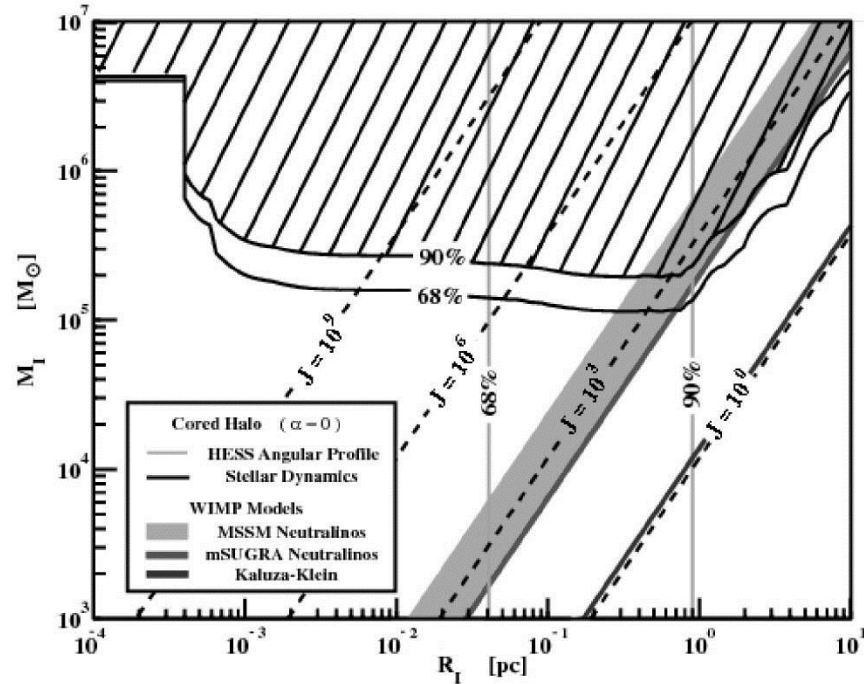


Figure 28: An allowed region for DM distribution from S2 like star trajectories near the Black Hole at the Galactic Center (Hall and Gondolo (2006)).

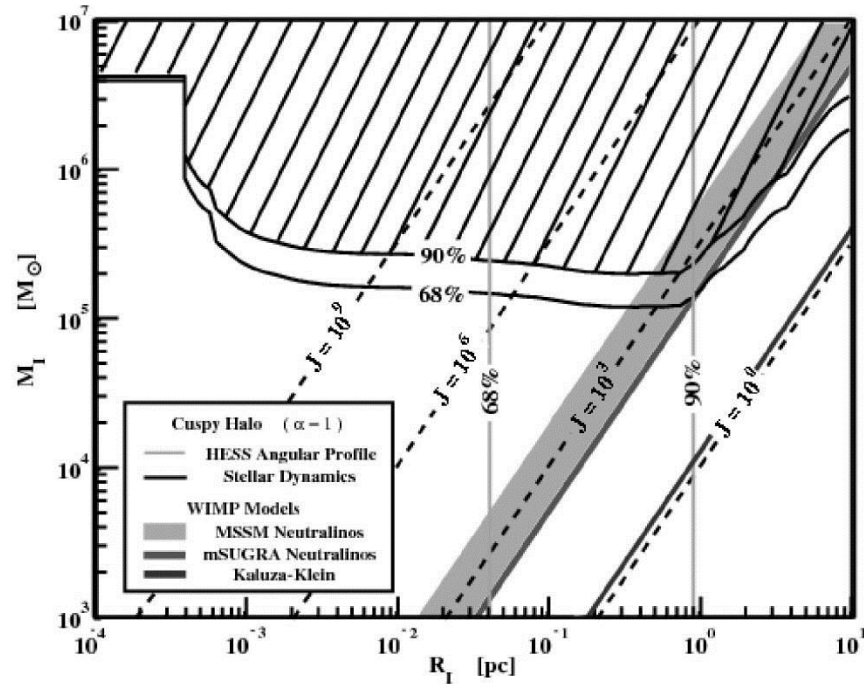


Figure 29: An allowed region for DM distribution from S2 like star trajectories near the Black Hole at the Galactic Center (Hall and Gondolo (2006)).

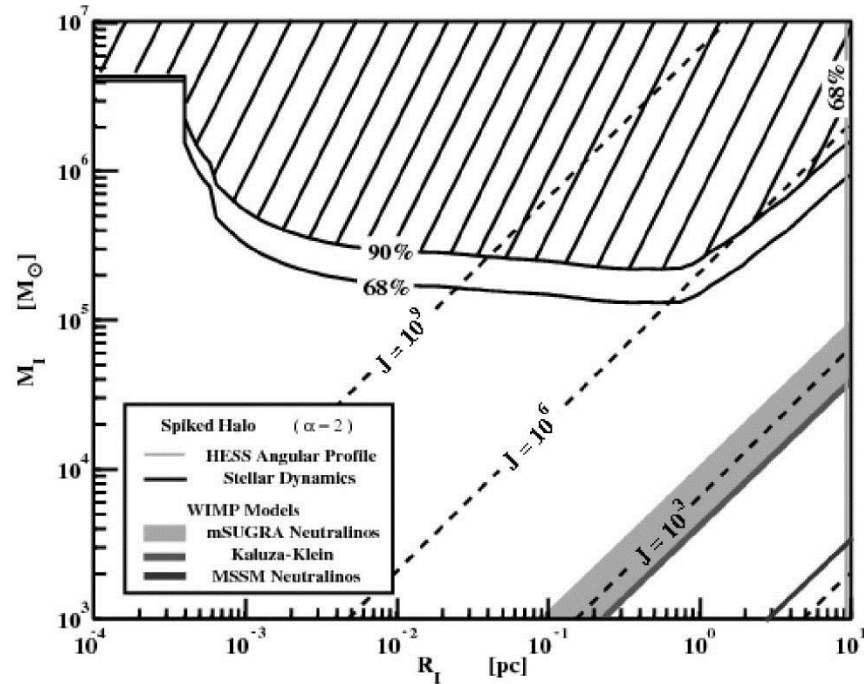


Figure 30: An allowed region for DM distribution from S2 like star trajectories near the Black Hole at the Galactic Center (Hall and Gondolo (2006)).

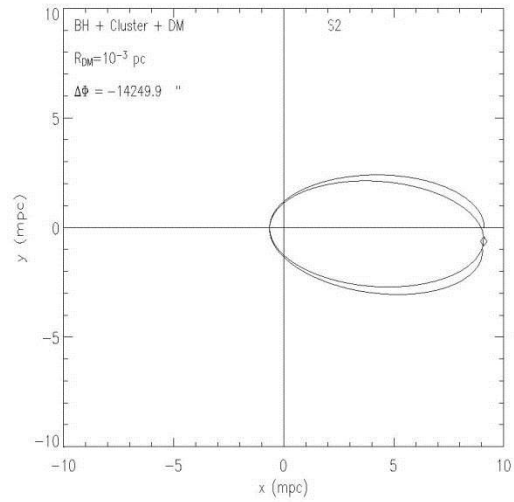
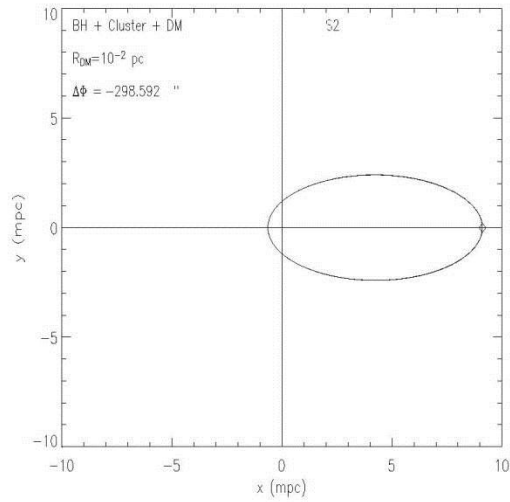
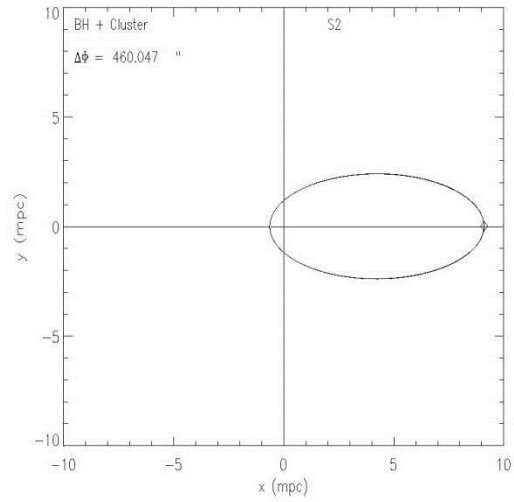
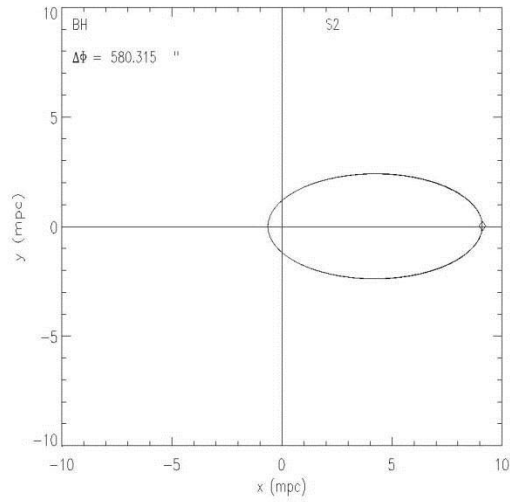




Figure 31: PN-orbits for different mass configurations at the Galactic Center. The S2 star has been considered as a test particle and its apoastron shift is indicated in each panel as  $\Delta\Phi$  (in arcsec). The top-left panel shows the central black hole contribution to the S2 shift that amounts to about 580 arcsec. The top-right panels shows the combined contribution of the black hole and the stellar cluster (taken following eq. 18) to the S2 apoastron shift. In the two bottom panels the contribution due to two different DM mass-density profiles is added (as derived in eq. 19). We assume that DM mass  $M_{DM} \simeq 2 \times 10^5 M_{\odot}$ .

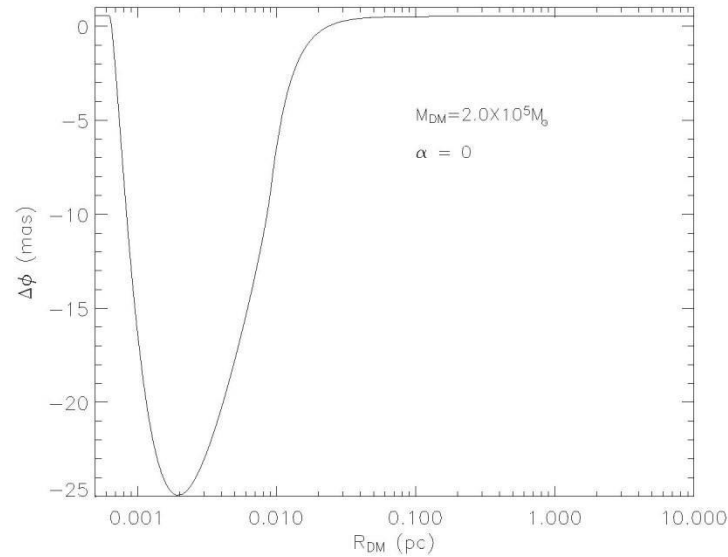


Figure 32: Apoastron shift as a function of the DM radius  $R_{DM}$  for  $\alpha = 0$  and  $M_{DM} \simeq 2 \times 10^5 M_{\odot}$ . Taking into account present day precision for the apoastron shift measurements (about 10 mas) one can say that DM radii  $R_{DM}$  in the range  $8 \times 10^{-4} - 10^{-2}$  pc are not acceptable.

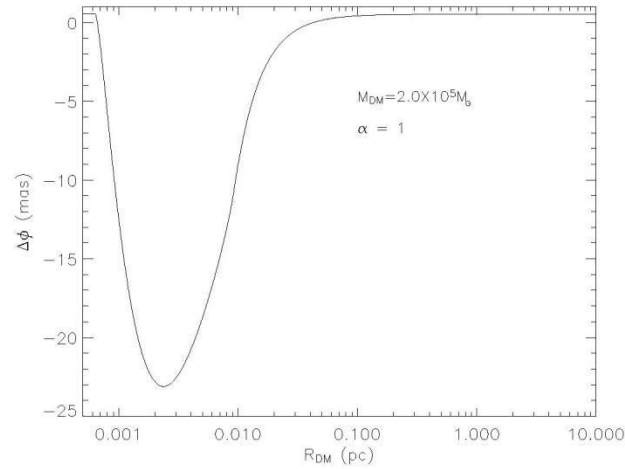


Figure 33: The same as in Fig. 32 for  $\alpha = 1$  and  $M_{DM} \simeq 2 \times 10^5 M_{\odot}$ . As in the previous case one can say that the S2 apoastron shift put severe limits on the DM mass radii that are not acceptable in the range  $9 \times 10^{-4} - 10^{-2}$  pc.

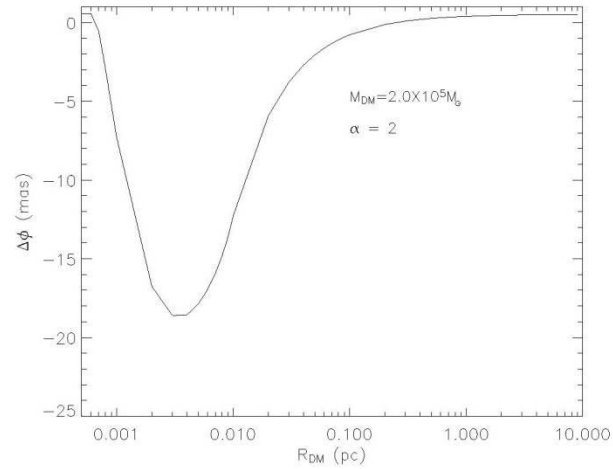


Figure 34: The same as in Fig. 32 for  $\alpha = 2$  and  $M_{DM} \simeq 2 \times 10^5 M_{\odot}$ . As in the previous case one can say that the upper limit to the S2 apoastron shift allows to constrain the DM radius to be out the range  $1.0 \times 10^{-3} - 1.1 \times 10^{-2}$  pc.

## MEASURING DISTANCE AND PROPERTIES OF THE MILKY WAY'S CENTRAL SUPERMASSIVE BLACK HOLE WITH STELLAR ORBITS

A. M. GHEZ<sup>1,2</sup>, S. SALIM<sup>1,4</sup>, N. N. WEINBERG<sup>3,5</sup>, J. R. LU<sup>1</sup>, T. DO<sup>1</sup>, J. K. DUNN<sup>1</sup>, K. MATTHEWS<sup>3</sup>, M. MORRIS<sup>3</sup>, S. YELDA<sup>1</sup>, E. E. BECKLIN<sup>1</sup>, T. KREMENEK<sup>1</sup>, M. MILOSAVLJEVIC<sup>6</sup>, J. NAIMAN<sup>1,7</sup>

*Draft version August 21, 2008*

### ABSTRACT

We report new precision measurements of the properties of our Galaxy's supermassive black hole. Based on astrometric (1995-2007) and radial velocity (2000-2007) measurements from the W. M. Keck 10-meter telescopes, a fully unconstrained Keplerian orbit for the short period star S0-2 provides values for the distance ( $R_0$ ) of  $8.0 \pm 0.6$  kpc, the enclosed mass ( $M_{bh}$ ) of  $4.1 \pm 0.6 \times 10^6 M_\odot$ , and the black hole's radial velocity, which is consistent with zero with 30 km/s uncertainty. If the black hole is assumed to be at rest with respect to the Galaxy (e.g., has no massive companion to induce motion), we can further constrain the fit and obtain  $R_0 = 8.4 \pm 0.4$  kpc and  $M_{bh} = 4.5 \pm 0.4 \times 10^6 M_\odot$ . More complex models constrain the extended dark mass distribution to be less than  $3.4 \times 10^5 M_\odot$  within 0.01 pc,  $\sim 100\times$  higher than predictions from stellar and stellar remnant models. For all models, we identify transient astrometric shifts from source confusion (up to 5x the astrometric error) and the assumptions regarding the black hole's radial motion as previously unrecognized limitations on orbital accuracy and the usefulness of fainter stars. Future astrometric and RV observations will remedy these effects. Our estimates of  $R_0$  and the Galaxy's local rotation speed, which it is derived from combining  $R_0$  with the apparent proper motion of Sgr A\* ( $\theta_0 = 229 \pm 18$  km s<sup>-1</sup>), are compatible with measurements made using other methods. The increased black hole mass found in this study, compared to that determined using projected mass estimators, implies a longer period for the innermost stable orbit, longer resonant relaxation timescales for stars in the vicinity of the black hole and a better agreement with the  $M_{bh}$ - $\sigma$  relation.

*Subject headings:* black hole physics – Galaxy:center — Galaxy:kinematics and dynamics — infrared:stars – techniques:high angular resolution

### 1. INTRODUCTION

Ever since the discovery of fast moving ( $v > 1000$  km s<sup>-1</sup>) stars within 0."3 (0.01 pc) of our Galaxy's central supermassive black hole (Eckart & Genzel 1997; Ghez et al. 1998), the prospect of using stellar orbits to make precision measurements of the black hole's mass ( $M_{bh}$ ) and kinematics, the distance to the Galactic center ( $R_0$ ) and, more ambitiously, to measure post-Newtonian effects has been anticipated (Jaroszynski 1998, 1999; Salim & Gould 1999; Fragile & Mathews 2000; Rubilar & Eckart 2001; Weinberg, Milosavljevic & Ghez 2005; Zucker & Alexander 2007; Kraniotis 2007; Will 2008). An accurate measurement of the Galaxy's central black hole mass is useful for putting the Milky Way in context with other galaxies through the apparent relationship between the mass of the central black hole and the velocity dispersion,  $\sigma$ , of the host galaxy (e.g., Ferrarese & Merrit 2000; Gebhardt et al. 2000; Tremaine et al. 2002). It can also

be used as a test of this scaling, as the Milky Way has the most convincing case for a supermassive black hole of any galaxy used to define this relationship. Accurate estimates of  $R_0$  impact a wide range of issues associated with the mass and structure of the Milky Way, including possible constraints on the shape of the dark matter halo and the possibility that the Milky Way is a lopsided spiral (e.g., Reid 1993; Olling & Merrifield 2000; Majewski et al. 2006). Furthermore, if measured with sufficient accuracy ( $\sim 1\%$ ), the distance to the Galactic center could influence the calibration of standard candles, such as RR Lyrae stars, Cepheid variables and giants, used in establishing the extragalactic distance scale. In addition to estimates of  $M_{bh}$  and  $R_0$ , precision measurements of stellar kinematics offer the exciting possibility of detecting deviations from a Keplerian orbit. This would allow an exploration of a possible cluster of stellar remnants surrounding the central black hole, suggested by Morris (1993), Miralda-Escudé & Gould(2000), and Freitag et al. (2006). Estimates for the mass of the remnant cluster range from  $10^4$ – $10^5 M_\odot$  within a few tenths of a parsec of the central black hole. Absence of such a remnant cluster would be interesting in view of the hypothesis that the inspiral of intermediate-mass black holes by dynamical friction could deplete any centrally concentrated cluster of remnants. Likewise, measurements of post-newtonian effects would provide a test of general relativity, and, ultimately, could probe the spin of the central black hole.

Tremendous observational progress has been made over the last decade towards obtaining accurate estimates of the orbital parameters of the fast moving stars at the

arXiv:0808.2870v1 [astro-ph] 21 Aug 2008

<sup>1</sup> UCLA Department of Physics and Astronomy, Los Angeles, CA 90095-1547; ghez, jlu, tdo, jkdunn, morris, syelda, becklin@astro.ucla.edu

<sup>2</sup> UCLA Institute of Geophysics and Planetary Physics, Los Angeles, CA 90095-1565

<sup>3</sup> California Institute of Technology, Division of Mathematics, Physics and Astronomy, Pasadena, CA 91125; kym@caltech.edu

<sup>4</sup> NOAO, 950 N Cherry Ave, Tucson, AZ 85719, samir@noao.edu

<sup>5</sup> University of California Berkeley, Department of Astronomy Berkeley, CA 94720-3411 nmw@astron.berkeley.edu

<sup>6</sup> University of Texas, Department of Astronomy, Austin, TX 78712 milos@astro.as.utexas.edu

<sup>7</sup> UCSC, Department of Astronomy & Astrophysics, Santa Cruz, CA 95064, jnaiman@astro.ucsc.edu



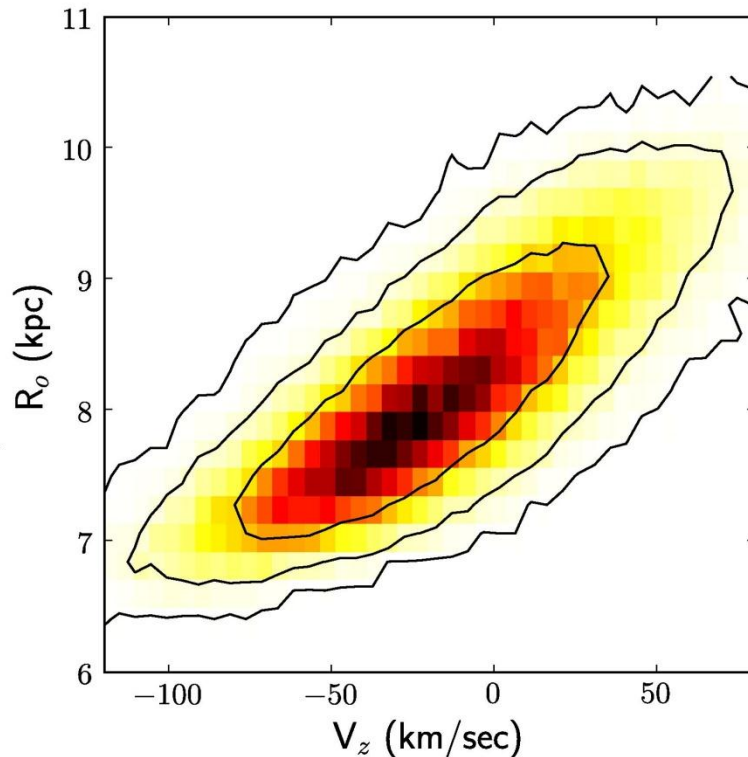


FIG. 12.— Correlation of the estimated black hole’s distance and line-of-sight velocity ( $V_z$ ) from our 13 parameter model fit.  $V_z$  dominates the uncertainties in  $R_0$  and consequently  $M_{bh}$ . Priors on  $V_z$  can reduce the uncertainties in  $R_0$  by a factor of two. All previous studies have set  $V_z$  to zero, which implicitly assumes that there are no massive companions to our Galaxy’s central supermassive black hole and that the local standard of rest is perfectly known.

#### 4.2. Point Mass Plus Extended Mass Distribution Analysis

Limits on an extended mass distribution within S0-2’s orbit are derived by assuming that the gravitational potential consists of a point mass and an extended mass distribution, and allowing for a Newtonian precession of the orbits (see, e.g., Rubilar & Eckart 2001). In order to do this, we use the orbit fitting procedure described in Weinberg et al. (2005), and adopt an extended mass distribution that has a power-law density profile  $\rho(r) = \rho_0(r/r_0)^{-\gamma}$ . This introduces two additional parameters to the model: the normalization of the profile and its slope  $\gamma$ . The total enclosed mass is then given by

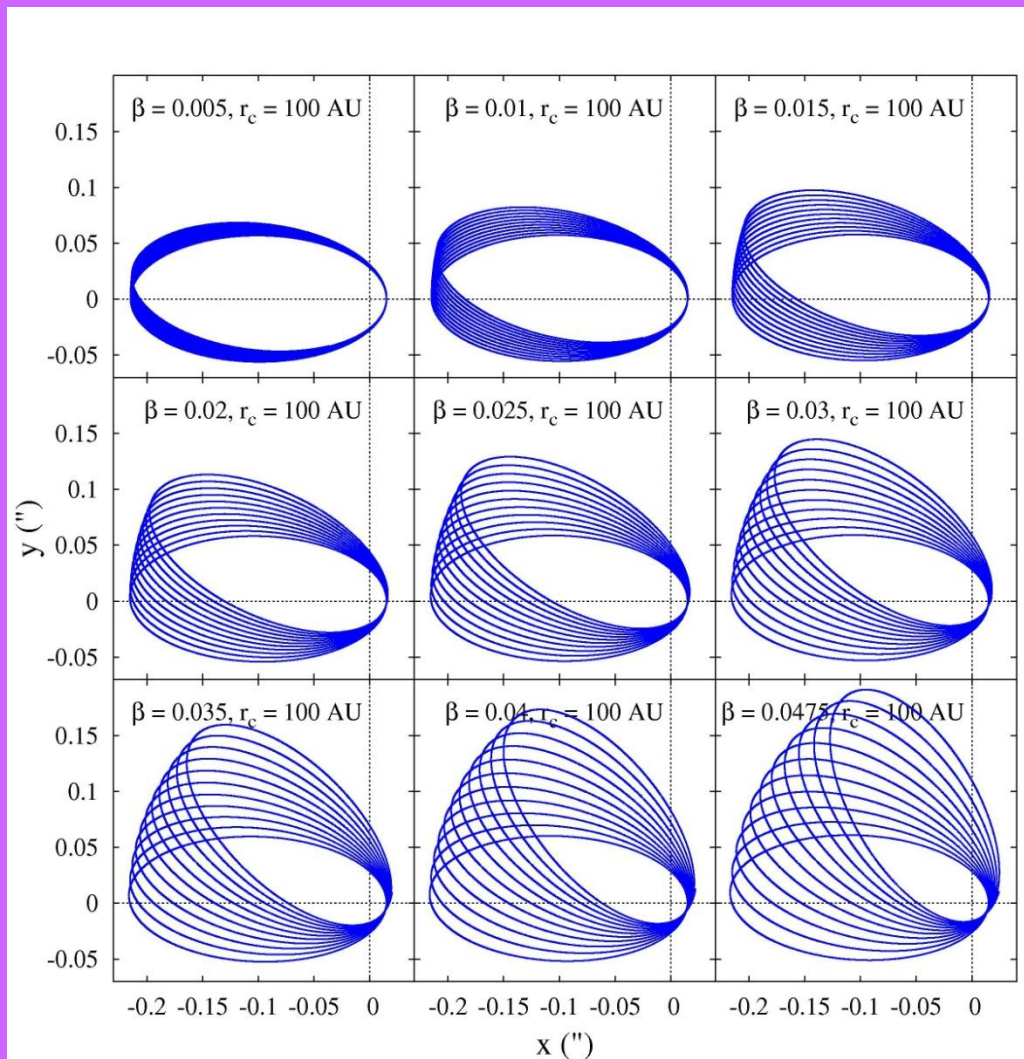
$$M(< r) = M_{\text{BH}} + M_{\text{ext}}(< r_0) \left( \frac{r}{r_0} \right)^{3-\gamma}, \quad (1)$$

where we quote values for the normalization  $M_{\text{ext}}(< r_0)$  at  $r_0 = 0.01$  pc, corresponding to the characteristic scale of the orbit. Figure 13 shows the constraint on  $M_{\text{ext}}(<$

0.01 pc) and  $\gamma$  from a fit to the astrometric and radial velocity measurements for S0-2. The 99.7% confidence upper-bound on the extended mass is  $M_{\text{ext}}(< 0.01 \text{ pc}) \simeq 3 - 4 \times 10^5 M_{\odot}$  and has only a weak dependence on  $\gamma$ .

Mouawad et al. (2005) report a similar upper-bound on the extended mass in fits to the orbit of S0-2. Their analysis differs only slightly from that presented here in that it forces the focus to be at the inferred radio position of Sgr A\*, assumes a Plummer model mass distribution, and is based on data presented in Eisenhauer et al. (2003). Similarly, Zakharov et al. (2007) use an order of magnitude analysis to show that if the total mass of the extended matter enclosed within the S0-2 orbit is  $\gtrsim 10^5 M_{\odot}$ , then it would produce a detectable apocenter shift  $\Delta\phi \gtrsim 10$  mas (see also § 3.2 in Weinberg et al. 2005). Hall & Gondolo (2006) fit the total measured mass concentration  $M(< r)$  given in Ghez et al. (2005) assuming a power-law density profile and obtain an upper bound of  $\approx 10^5 M_{\odot}$  between 0.001 – 1 pc.

D. Borka, P. Jovanovic, V. Borka Jovanovic and AFZ,  
PRD, **85**, 124004 (2012).



# • **Conclusions**

- VLBI systems in mm and sub-mm bands or MAXIM could detect mirages (“faces”) around black holes.
- Shapes of images give an important information about BH parameter
- Trajectories of bright stars or bright spots around massive BHs are very important tool for an evaluation of BH parameters
- Trajectories of bright stars or bright spots around massive BHs can be used to obtain constraints on alternative theories of gravity ( $f(R)$  theory, for instance)
- A significant tidal charge of the BH at GC is excluded by observations

- Thanks for your kind attention!





# BHs is a consequence of black failure in knowledge of mathematics

...шно продолжать заниматься важной и интересной научной работой, не остав-  
...своих прочих интересов.

*Коллеги по кафедре общей ядерной физики*

## «Черные дыры» — это следствие черного провала в знаниях математики

...общей теории относительности  
...рждается, что уравнения ОТО со-  
...крат решения, отвечающие «чер-  
...дырам». Это некие сферически-  
...метричные материальные объекты,  
...редоточенные в области, из которой  
...жду никакие сигналы выйти не мо-  
...Они проявляют себя лишь в грави-  
...онном взаимодействии с другими  
...ми. Их внутренняя структура ока-  
...ается недоступной для изучения. Т.е.  
...онные дыры» — непознаваемые объ-  
...ы!

...та непознаваемость уже сама по себе  
...жна была бы вызвать подозрение, так  
...объект создавался природой по за-  
...ам причинно-связанных процессов.  
...жна была бы возникнуть потреб-  
...ть более внимательно проанализиро-

...ход рассуждений, приведших к шварцшильдовскому решению для метриче-  
...х коэффициентов в галилеевых координатах, содержащему «черные дыры».

...Так в чем же там дело? А дело в следующем. При получении решения Шварц-  
...льда в галилеевых координатах в качестве внешнего решения некоего кусочно-  
...рерывного линейного дифференциального уравнения второго порядка бралось



В  
ме  
но  
ог  
до  
ре  
ос  
сл

тр  
го  
Рс  
не  
со  
м  
др  
ед  
ка  
фа  
«С  
ча  
ла  
но  
ге  
да  
ма  
зо  
на  
об  
ск  
ше  
пя  
СС  
нь  
уж  
ис  
ск  
нь

Rev. John Michell: *Phil. Trans. R. Soc. London*, 74, 35–57 (1784):

VII. *On the Means of discovering the Distance, Magnitude, &c. of the Fixed Stars, in consequence of the Diminution of the Velocity of their Light, in case such a Diminution should be found to take place in any of them, and such other Data should be procured from Observations, as would be farther necessary for that Purpose. By the Rev. John Michell, B. D. F. R. S. In a Letter to Henry Cavendish, Esq. F. R. S. and A. S.*

Read November 27, 1783.

Rev. John Michell: *Phil. Trans. R. Soc. London*, 74, 35–57 (1784):

42      *Mr. MICHELL on the Means of discovering the*

16. Hence, according to article 10, if the semi-diameter of a sphaere of the same density with the sun were to exceed that of the sun in the proportion of 500 to 1, a body falling from an infinite height towards it, would have acquired at its surface a greater velocity than that of light, and consequently, supposing light to be attracted by the same force in proportion to its vis inertiae, with other bodies, all light emitted from such a body would be made to return towards it, by its own proper gravity.

# Prizes awarded

The Crafoord Prize has been awarded:

**2010 WALTER MUNK**, Scripps Institution of Oceanography, University of California, San Diego, La Jolla, CA, USA, *“for his pioneering and fundamental contributions to our understanding of ocean circulation, tides and waves, and their role in the Earth’s dynamics”*.



PHOTO: MARKUS MARCETIC

WALTER MUNK



TOSHIO HIRANO

CHARLES DINARELLO

TADAMITSU KISHIMOTO

**2009 CHARLES DINARELLO**, University of Colorado School of Medicine, Denver, USA, **TADAMITSU KISHIMOTO**, Osaka University, Japan and **TOSHIO HIRANO**, Osaka University, Japan, *“for their pioneering work to isolate interleukins, determine their properties and explore their role in the onset of inflammatory diseases”*.

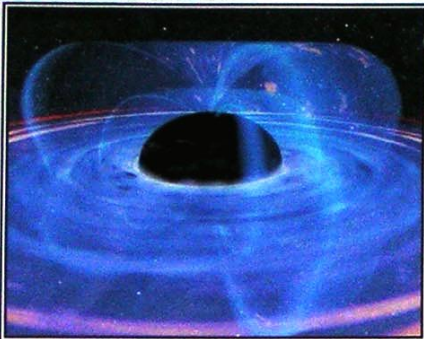
**2008 MAXIM KONTSEVICH**, IHÉS, France, and **EDWARD WITTEN**, Institute for Advanced Study, USA, *“for their important contributions to mathematics inspired by modern theoretical physics”*, and



MAXIM KONTSEVICH (LEFT) AND EDWARD WITTEN (RIGHT)

**RASHID ALIEVICH SUNYAEV**, Max Planck Institute for Astrophysics, Germany, *“for his decisive contributions to high-energy astrophysics and cosmology, in particular processes and dynamics around black holes and neutron stars and demonstration of the diagnostic power of structures in the background radiation”*.





# 学术报告

北京大学天文系  
北京天体物理中心

**Prof. Alexander Zakharov**

**Institute of Theoretical and Experimental Physics,  
Moscow, Russia**

## **Measuring Parameters of Supermassive Black Holes with Present and Future Space Missions**

**时间:** 2005年10月20日(星期四), 下午 3:30

**地点:** 北京大学理科二号楼 2907 (天文系会议室)

**欢迎参加**



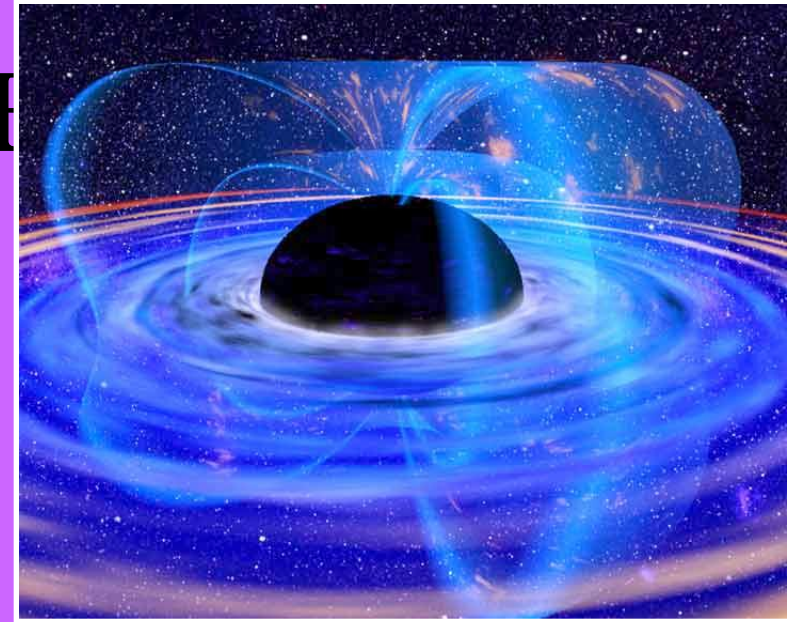
# XMM-Newton observations of MCG-6-30-15 in the 2-10 keV band



Wilms et al 2002; Fabian et al 2002;  
Vaughan et al 2002; Fabian & Vaughan  
2002; Ballantyne et al 2003; Reynolds et al  
2003; Vaughan & Fabian 2004

Understanding the spectral behaviour

# What Makes them H



Other than the classical Rees argument about **efficiency, size and luminosity** what observational properties make these objects black holes ?

- High mass in a small volume via direct measurements  
SGR A\*, NGC4258 etc
- Mass functions of stellar systems

*For the vast majority of objects thought to be black holes such information is not available*

- We must use indirect observational data
  - Spectra
  - Timing
  - Spectral/timing (reverberation mapping)
  - Imaging (micro-lensing)

Why are black hole interesting today

- Black Holes and Strong Gravity
  - Spectral and timing probes of strong gravity
  - Astrophysics in the strong gravity region
- AGN Winds & effect of BHs on cosmic structure
  - Outflows from AGN
  - Cooling flow and cluster entropy problems
  - Role of AGN in galaxy formation
- Evolution of AGN and SMBH growth
  - Paradigm shift in AGN evolution

1999 **JOHN MAYNARD SMITH**, University of Sussex, Great Britain, **ERNST MAYR**, Harvard University, Cambridge MA, USA, and **GEORGE C. WILLIAMS**, State University of New York, USA, *"for their fundamental contributions to the conceptual development of evolutionary biology"*.



ERNST MAYR

1998 **DON L. ANDERSON**, California Institute of Technology, Pasadena CA, USA, and **ADAM M. DZIEWONSKI**, Harvard University, Cambridge MA, USA, *"for their fundamental contributions to our knowledge of the structures and processes in the interior of the Earth"*.

1997 **FRED HOYLE**, UK and **EDWIN E. SALPETER**, Cornell University, Ithaca, NY, USA, *"for their pioneering contributions to the study of nuclear processes in stars and stellar evolution"*.

1996 **LORD ROBERT M. MAY**, University of Oxford, UK, *"for his pioneering ecological research concerning theoretical analysis of the dynamics of populations, communities and ecosystems"*.



LORD ROBERT M. MAY

1995 **WILLI DANSGAARD**, Københavns Universitet, Denmark, and **NICHOLAS SHACKLETON**, University of Cambridge, UK, *"for their fundamental work on developing and applying isotope geological analysis methods for the study of climatic variations during the Quaternary period"*.



WILLI DANSGAARD (LEFT) AND NICHOLAS SHACKLETON (RIGHT)

1994 **SIMON DONALDSON**, University of Oxford, UK, *"for his fundamental investigations in four-dimensional geometry through application of instantons, in particular his discovery of new differential invariants"*, and **SHING-TUNG YAU**, Harvard University, USA, *"for his development of non-linear techniques in differential geometry leading to the solution of several outstanding problems"*.

1993 **SEYMOUR BENZER**, California Institute of Technology, USA, *“for his pioneering genetical and neurophysiological studies on behavioural mutants in the fruit fly, *Drosophila melanogaster*”*, and **WILLIAM D. HAMILTON**, University of Oxford, UK, *“for his theories concerning kin selection and genetic relationship as a prerequisite for the evolution of altruistic behavior”*.



SEYMOUR BENZER

1992 **ADOLF SEILACHER**, Institut und Museum für Geologie und Paläontologie, Germany, *“for his innovative research concerning the evolution of life in interaction with the environment as documented in the geological record”*.

1991 **ALLAN R. SANDAGE**, The Observatories of the Carnegie Institution of Washington, USA, *“for his very important contributions to the study of galaxies, their populations of stars, clusters and nebulae, their evolution, the velocity-distance relation (or Hubble relation), and its evolution over time”*.



ALLAN R. SANDAGE

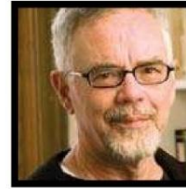
1990 **PAUL R. EHRLICH**, Stanford University, USA, *“for his research on the dynamics and genetics of fragmented populations and the importance of the distribution pattern for their survival probabilities”*, and **EDWARD O. WILSON**, Harvard University, USA, *“for the theory of island biogeography and other research on species diversity and community dynamics on islands and in other habitats with differing degrees of isolation”*.

1989 **JAMES VAN ALLEN**, University of Iowa, USA, *“for his pioneering exploration of space, in particular the discovery of the energetic particles trapped in the geomagnetic field which forms the radiation belts – the Van Allen belts – around our planet Earth”*.

1988 **PIERRE DELIGNE**, Institute for Advanced Study, USA, and **ALEXANDRE GROTHENDIECK**, Université des Sciences et Techniques du Languedoc, France, *“for their fundamental research in algebraic geometry”*. (Mr Grothendieck declined his prize.)



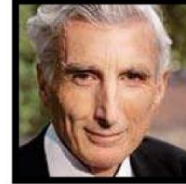
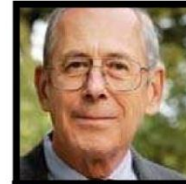
2007 **ROBERT L. TRIVERS**, Rutgers University, USA, for his fundamental analysis of social evolution, conflict and cooperation.



ROBERT L. TRIVERS

2006 **WALLACE S. BROECKER**, Lamont-Doherty Earth Observatory, Columbia University, USA, *“for his innovative and pioneering research on the operation of the global carbon cycle within the ocean atmosphere-biosphere system, and its interaction with climate”*.

2005 **JAMES E. GUNN** and **P. JAMES E. PEBBLES**, Princeton University, USA, and **SIR MARTIN J. REES**, Cambridge University, UK, *“for contributions towards understanding the large-scale structure of the Universe”*.



P. JAMES E. PEBBLES (ABOVE)  
AND LORD MARTIN J. REES

2004 **EUGENE C. BUTCHER**, Stanford University, USA, and **TIMOTHY A. SPRINGER**, Harvard Medical School, USA, *“for their studies on the molecular mechanisms involved in migration of white blood cells in health and disease”*.

2003 **CARL R. WOESE**, University of Illinois, USA, *“for his discovery of a third domain of life”*.

2002 **DAN P. MCKENZIE**, University of Cambridge, UK, *“for fundamental contributions to the understanding of the dynamics of the lithosphere, particularly plate tectonics, sedimentary basin formation and mantle melting”*.

2001 **ALAIN CONNES**, IHÉS and Collège de France, Paris, *“for his penetrating work on the theory of operator algebras and for having been a founder of the non-commutative geometry”*.

2000 **RAVINDER N. MAINI** and **MARC FELDMANN**, both of the Kennedy Institute of Rheumatology, London, UK, *“for their definition of TNF-alpha as a therapeutic target in rheumatoid arthritis”*.



- 1987 **EUGENE P. ODUM**, University of Georgia, USA, and **HOWARD T. ODUM**, University of Florida, USA, *“for their pioneering contributions within the field of ecosystem ecology”*.



EUGENE P. ODUM (LEFT) AND HOWARD T. ODUM (RIGHT)

- 1986 **CLAUDE J. ALLÈGRE**, Université de Paris, France, and **GERALD J. WASSERBURG**, California Institute of Technology, USA, *“for their pioneering studies of isotope geochemical relations and the geological interpretations that these results permit”*.

- 1985 **LYMAN SPITZER, Jr.**, Princeton University, USA, *“for his fundamental pioneering studies of practically every aspect of the interstellar medium, culminating in the results obtained using the Copernicus satellite”*.

- 1984 **DANIEL H. JANZEN**, University of Pennsylvania, USA, *“for his imaginative and stimulating studies on co-evolution which has inspired many researchers to further work in this field”*.

- 1983 **EDVARD N. LORENZ**, Massachusetts Institute of Technology, USA, and **HENRY STOMMEL**, Woods Hole Oceanographic Institution, USA, *“for their fundamental contributions to the field of geophysical hydrodynamics, which in a unique way have contributed to a deeper understanding of the large-scale motions of the atmosphere and the sea”*.



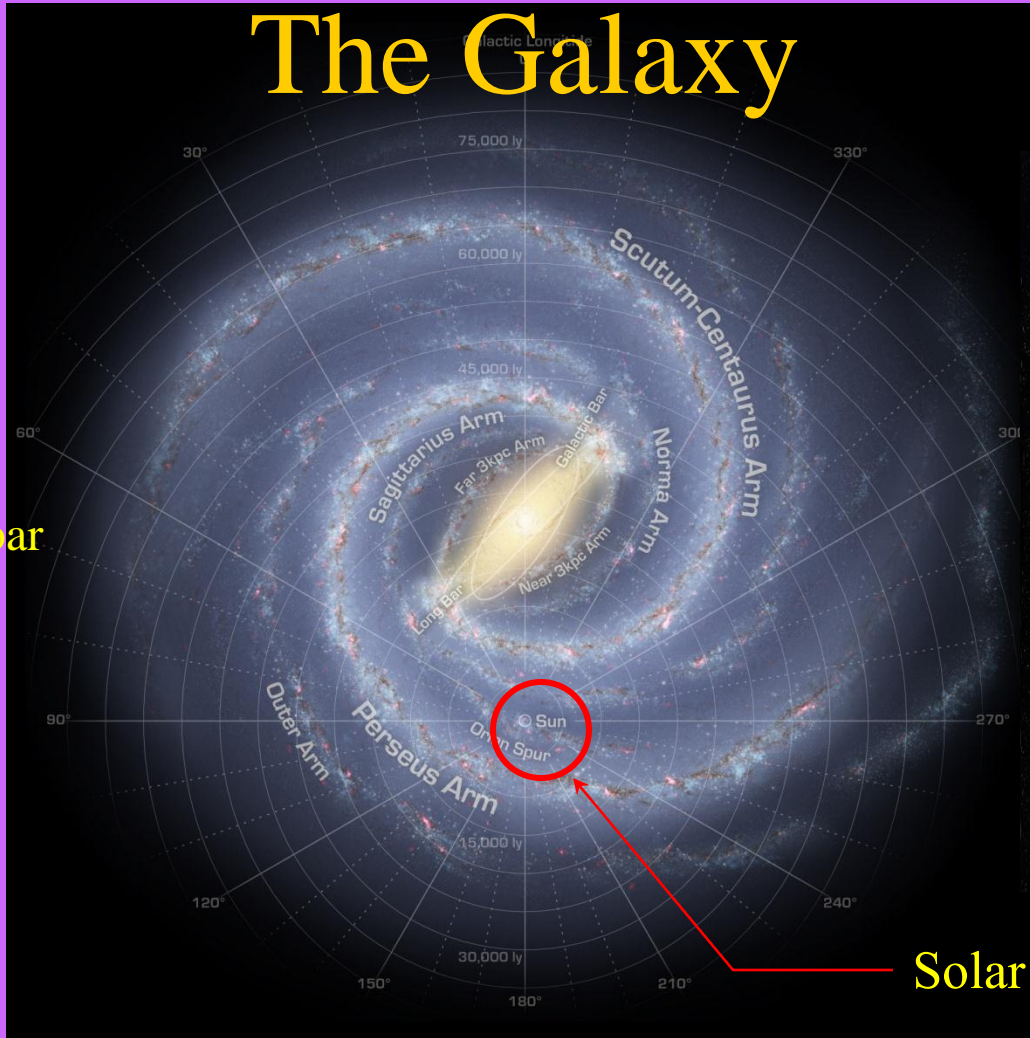
- 1982 **VLADIMIR I. ARNOLD**, Moscow State University, Soviet Union, and **LOUIS NIRENBERG**, Courant Institute, USA, *“for their outstanding achievements in the theory of non-linear differential equations”*.



VLADIMIR I. ARNOLD (ABOVE)  
AND LOUIS NIRENBERG

# The Galaxy

Diàmeter: 25 kpc  
Spiral galaxy with bar



Milky Way

Solar system

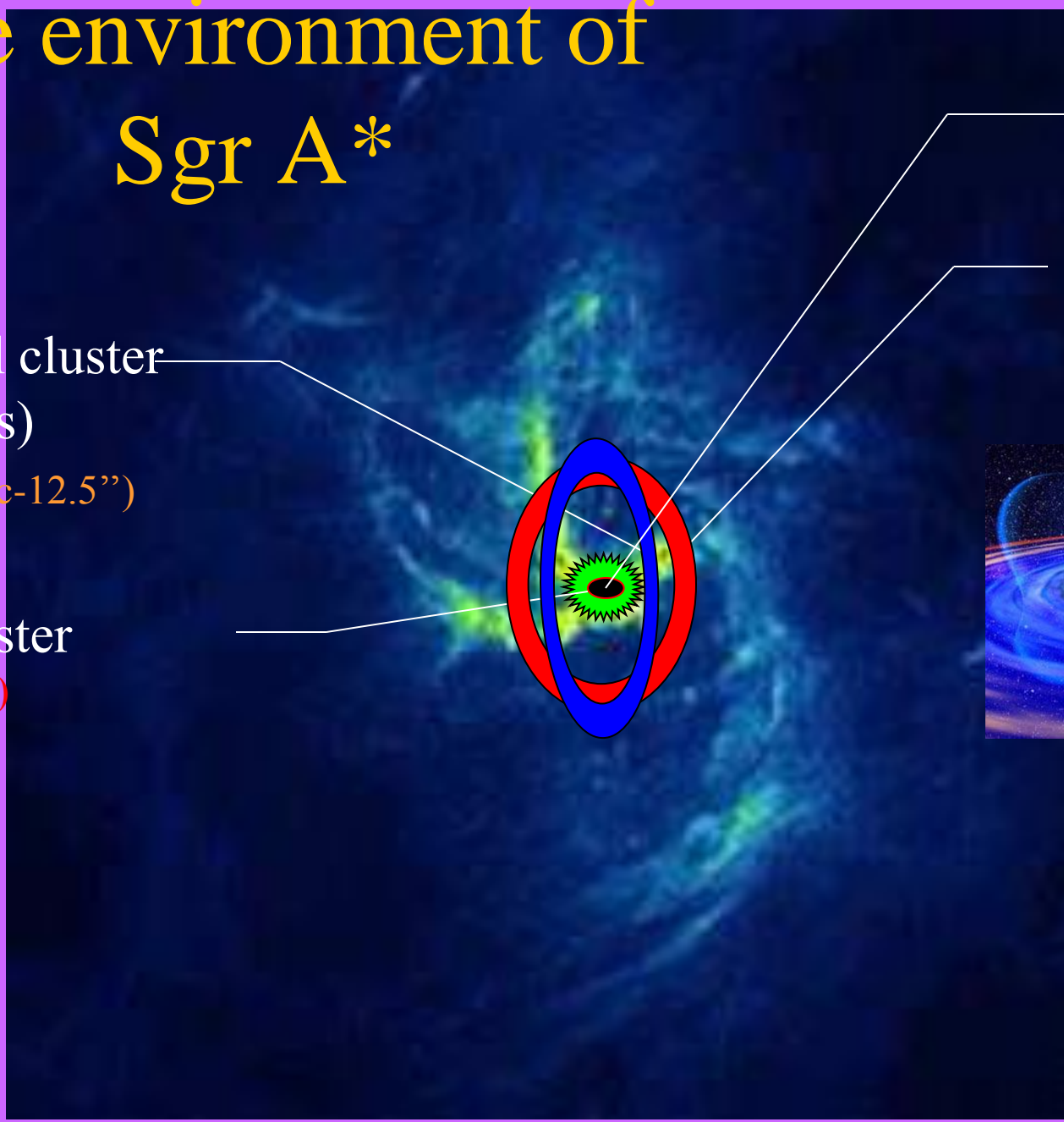
# The environment of Sgr A\*

Sgr A\*  
10  $\mu$ as

Mini spiral  
(50'')

Central cluster  
(2 disks)  
(0.5 pc-12.5'')

S star cluster  
(12-400 mas)



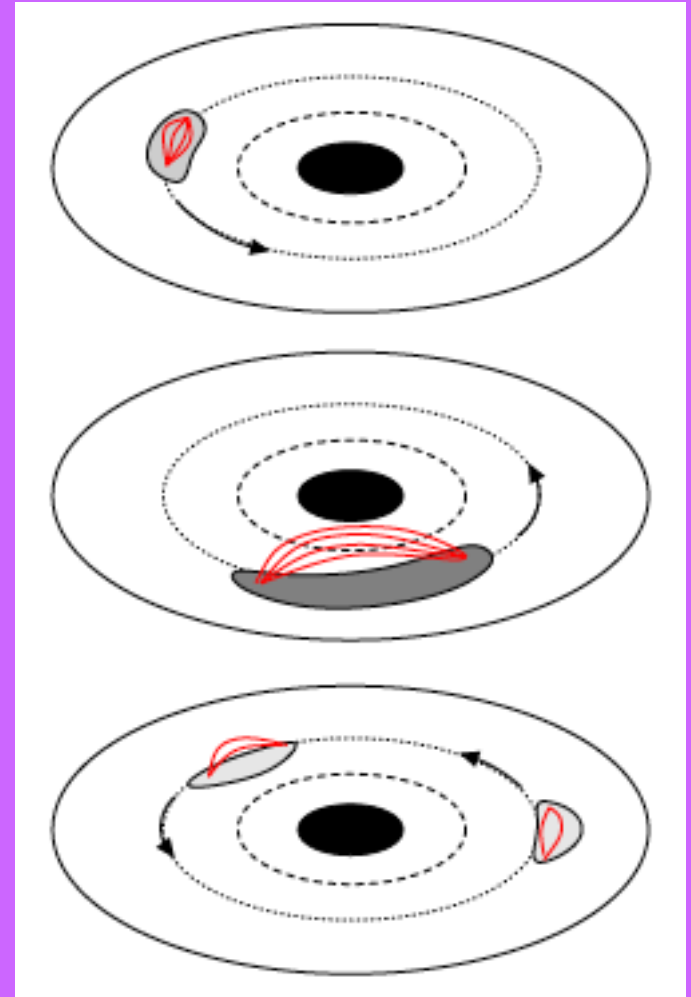
# Possible origin of flares

**Flare:** matter is heated on a (the innermost stable) circular orbit ( $30 \mu\text{as}$  if  $J=0$ )

**Flare period:** period of the orbit

*Fantastic* tool to study general relativity in the strong field regime.

The *hot spot* will be used as a test particle to measure the space time around Sgr A\*.



Eckart et al. A&A 500, 935 (2009)

# The Anna-Greta and Holger Crafoord Fund



PHOTO: MARKUS MARCETIC

BACK ROW: LENNART NILSSON, WALTER FISCHER, GUNNAR ÖQUIST, GEORGIA DESTOUNI, SVANTE LINDQVIST. FRONT ROW: MARGARETA NILSSON, WALTER MUNK, H.M. KING CARL XVI GUSTAF, H.M. QUEEN SILVIA, EBBA FISCHER.

The Fund was established in 1980 by a donation to the Royal Swedish Academy of Sciences from Anna-Greta and Holger Crafoord. The Crafoord Prize was awarded for the first time in 1982. The purpose of the Fund is to promote basic scientific research worldwide in the following disciplines:



ASTRONOMY AND  
MATHEMATICS



GEOSCIENCES



BIOSCIENCES  
WITH EMPHASIS ON ECOLOGY



POLYARTHRITIS

Support to research takes the form of an international prize awarded annually to outstanding scientists, and of research grants to individuals or institutions in Sweden. Both awards and grants are made according to the following order:

- year 1: Astronomy and Mathematics
- year 2: Geosciences
- year 3: Biosciences
- year 4: Astronomy and Mathematics
- year 5: Geosciences
- year 6: Biosciences
- etc.





# New Astronomy

## Top Cited Article 2005-2010

Awarded to:

*Zakharov, A.F., Nucita, A.A., Depaolis, F., Inghusso, G.*

For the paper entitled:

“Measuring the black hole parameters in the galactic center with  
RADIOASTRON”

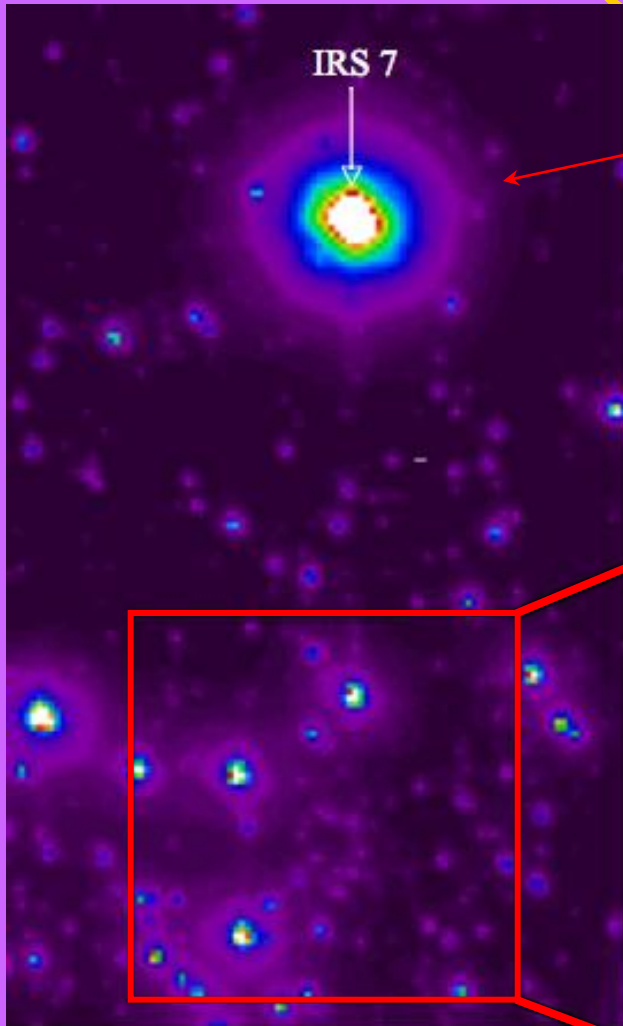
This paper was published in:  
New Astronomy, Volume 10, Issue 6, 2005

---

*David Clark*  
*Senior Vice President, Physical Sciences I*  
*Amsterdam, The Netherlands*

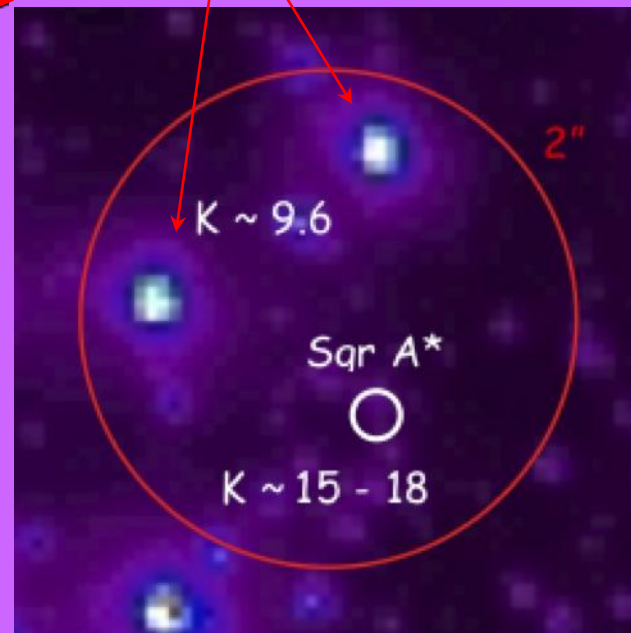
---

# Principle of the measurements with GRAVITY



Reference source for infrared  
adaptive optics

Reference sources for  $10 \mu\text{s}$   
astrometry and  $3 \text{ mas}$  phase  
reference imaging



## LETTERS

## A size of $\sim 1$ AU for the radio source Sgr A\* at the centre of the Milky Way

Zhi-Qiang Shen<sup>1</sup>, K. Y. Lo<sup>2</sup>, M.-C. Liang<sup>3</sup>, Paul T. P. Ho<sup>4,5</sup> & J.-H. Zhao<sup>4</sup>

Although it is widely accepted that most galaxies have super-massive black holes at their centres<sup>1–3</sup>, concrete proof has proved elusive. Sagittarius A\* (Sgr A\*)<sup>4</sup>, an extremely compact radio source at the centre of our Galaxy, is the best candidate for proof<sup>5–7</sup>, because it is the closest. Previous very-long-baseline interferometry observations (at 7 mm wavelength) reported that Sgr A\* is  $\sim 2$  astronomical units (AU) in size<sup>8</sup>, but this is still larger than the ‘shadow’ (a remarkably dim inner region encircled by a bright ring) that should arise from general relativistic effects near the event horizon of the black hole<sup>9</sup>. Moreover, the measured size is wavelength dependent<sup>10</sup>. Here we report a radio image of Sgr A\* at a wavelength of 3.5 mm, demonstrating that its size is  $\sim 1$  AU. When combined with the lower limit on its mass<sup>11</sup>, the lower limit on the mass density is  $6.5 \times 10^{21} M_{\odot} \text{pc}^{-3}$  (where  $M_{\odot}$  is the solar mass), which provides strong evidence that Sgr A\* is a super-massive black hole. The power-law relationship between wavelength and intrinsic size (size  $\propto$  wavelength<sup>1.09</sup>) explicitly rules out explanations other than those emission models with stratified structure, which predict a smaller emitting region observed at a shorter radio wavelength.

Past very-long-baseline interferometry (VLBI) observations<sup>12–16</sup> of Sgr A\* have revealed an east–west elongated structure whose apparent angular size at longer wavelengths is dominated by the interstellar scattering angle, that is,  $\theta_{\text{obs}} = \theta_{\text{obs}}^{\text{int}} \lambda^2$ , where  $\theta_{\text{obs}}$  is the observed size in milliarcseconds (mas) at wavelength  $\lambda$  in cm, and equals  $\theta_{\text{obs}}^{\text{int}}$  at 1 cm. Thus, VLBI observations at shorter millimetre wavelengths, where the intrinsic structure of Sgr A\* could become comparable to the pure scattering size, are expected to show deviations of the observed size from the scattering law. This has been demonstrated by the recent detection of the intrinsic size at 7 mm (ref. 8). On 20 November 2002, we successfully carried out an observation of Sgr A\* with the Very Long Baseline Array (VLBA) at its shortest wavelength of 3.5 mm (ref. 10). Our observation, with the steadily improved performance of the VLBA system, has produced the first (to our knowledge) high-resolution image of Sgr A\* made at 3.5 mm (Fig. 1), which exhibits an elongated structure too.

To yield a quantitative description of the observed structure, we tried a model fitting procedure<sup>17</sup> in which the amplitude closure relation is applied. Compared to the conventional VLBI

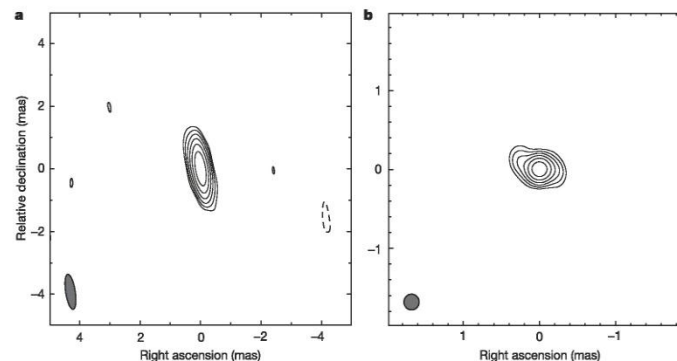


**Figure 1** High-resolution VLBI image of Sgr A\* at 3.5 mm obtained with the VLBA on 20 November 2002. The observations were flexibly scheduled to ensure good weather conditions at most sites, and the data were recorded at the highest possible recording rate of 512 Mbit s<sup>-1</sup>. Standard visibility amplitude calibration including the elevation-dependent opacity correction was done, and the final image was obtained after several iterations of the self-calibration and cleaning procedures. The calibrated total flux density is

about 1.2 Jy. **a**, A uniformly weighted image with the restoring beam (indicated at the lower left corner) of  $1.13 \text{ mas} \times 0.32 \text{ mas}$  at  $9^\circ$ . The peak flux density is  $1.08 \text{ Jy beam}^{-1}$ . Contour levels are drawn at  $3\sigma \times (-1, 1, 2, 4, 8, 16, 32)$ ;  $3\sigma = 17.5 \text{ mJy beam}^{-1}$ . **b**, A super-resolution image with a circular beam of  $0.20 \text{ mas}$  from which an east–west elongated structure can be seen (see Table 1). Note the different scales. The contour levels are the same as that in **a** with the corresponding peak flux density of  $1.01 \text{ Jy beam}^{-1}$ .

<sup>1</sup>Shanghai Astronomical Observatory, 80 Nandan Road, Shanghai 200030, China. <sup>2</sup>National Radio Astronomy Observatory, 520 Edgemont Road, Charlottesville, Virginia 22903, USA. <sup>3</sup>Division of Geological and Planetary Sciences, California Institute of Technology, Pasadena, California 91125, USA. <sup>4</sup>Harvard-Smithsonian CfA, 60 Garden Street, Cambridge, Massachusetts 02138, USA. <sup>5</sup>Institute of Astronomy & Astrophysics, Academia Sinica, PO Box 23-141, Taipei 106, Taiwan, China.





Reinhard Genzel, Prof. Dr.

Max Planck Institute for Extraterrestrial Physics, Garching

### **Curriculum Vitae**

Born on March 24, 1952 in Bad Homburg v.d.H. Study of physics Bonn Univ., doctorate Max Planck Institute for Radioastronomy Bonn (1978), Postdoctoral Fellow, Harvard-Smithsonian Center for Astrophysics (1978-1980), Cambridge, MA, Associate Professor of Physics and Associate Research Astronomer, Space Sciences Laboratory, University of California, Berkeley (1981- 1985), Full Professor of Physics, University of California, Berkeley (1985-1986), Director and Scientific Member at the Max Planck Institute for Extraterrestrial Physics (since 1986), Honorary Professor Munich Univ. (since 1988), Full Professor of Physics University of California Berkeley (since 1999).



American citizen. Born 1965 in  
New York City, NY, USA. Ph.D.  
1992 at California Institute of  
Technology, Pasadena, CA, USA.  
Professor at University of  
California, Los Angeles, CA, USA.



## Improving Galactic Center Astrometry by Reducing the Effects of Geometric Distortion

S. Yelda<sup>1</sup>, J. R. Lu<sup>2</sup>, A. M. Ghez<sup>1,3</sup>, W. Clarkson<sup>4</sup>, J. Anderson<sup>5</sup>, T. Do<sup>6</sup>, K. Matthews<sup>2</sup>

### ABSTRACT

We present significantly improved proper motion measurements of the Milky Way's central stellar cluster. These improvements are made possible by refining our astrometric reference frame with a new geometric optical distortion model for the W. M. Keck II 10 m telescope's Adaptive Optics camera (NIRC2) in its narrow field mode. For the first time, this distortion model is constructed from on-sky measurements, and is made available to the public in the form of FITS files. When applied to widely dithered images, it produces residuals in the separations of stars that are a factor of  $\sim 3$  smaller compared to the outcome using previous models. By applying this new model, along with corrections for differential atmospheric refraction, to widely dithered images of SiO masers at the Galactic center, we improve our ability to tie into the precisely measured radio Sgr A\*-rest frame. The resulting infrared reference frame is  $\sim 2$ - $3$  times more accurate and stable than earlier published efforts. In this reference frame, Sgr A\* is localized to within a position of 0.6 mas and a velocity of  $0.09 \text{ mas yr}^{-1}$ , or  $\sim 3.4 \text{ km s}^{-1}$  at 8 kpc ( $1\sigma$ ). Also, proper motions for members of the central stellar cluster are more accurate, although less precise, due to the limited number of these wide field measurements. These proper motion measurements show that, with respect to Sgr A\*, the central stellar cluster has no rotation in the plane of the sky to within  $0.3 \text{ mas yr}^{-1}$  arcsec<sup>-1</sup>, has no net translational motion with respect to Sgr A\* to within  $0.1 \text{ mas yr}^{-1}$ , and has net rotation perpendicular to the plane of the sky along the Galactic plane, as has previously been observed. While earlier proper motion studies defined a reference frame by assuming no net motion of the stellar cluster, this approach is fundamentally limited by the cluster's intrinsic dispersion and therefore will not improve with time. We define a reference frame with SiO masers and this reference frame's stability should improve steadily with future measurements of the SiO masers in this region ( $\propto t^{3/2}$ ). This is essential for achieving the necessary reference frame stability required to detect

---

<sup>1</sup>UCLA Department of Physics and Astronomy, Los Angeles, CA 90095-1547; syelda, ghez@astro.ucla.edu

<sup>2</sup>Astrophysics, California Institute of Technology, MC 249-17, Pasadena, CA 91125; jlu, kym@caltech.edu

<sup>3</sup>UCLA Institute of Geophysics and Planetary Physics, Los Angeles, CA 90095-1565

<sup>4</sup>Indiana University, Department of Astronomy, Bloomington, IN 47405; clarkson@astro.ucla.edu

<sup>5</sup>Space Telescope Science Institute, 3700 San Martin Drive, Baltimore, MD 21218; jayander@stsci.edu

<sup>6</sup>UC Irvine Department of Physics and Astronomy, Irvine, CA 92697; tdo@astro.ucla.edu

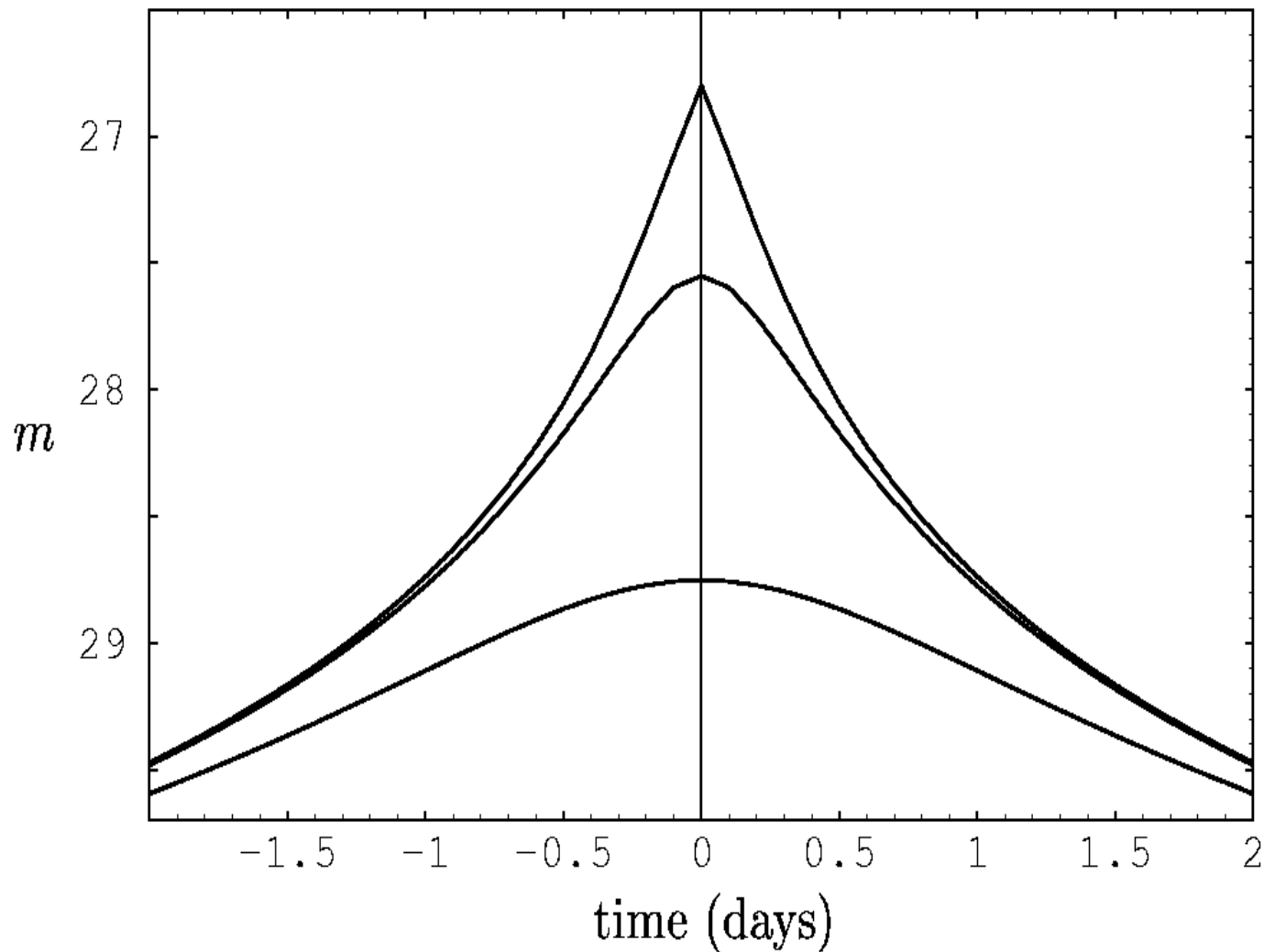


FIG. 3.— Solar retro-MACHO lightcurves: The apparent visual magnitude,  $m$ , of the Sun, imaged in a  $10 M_{\odot}$  black hole at a distance of 0.01 pc. The different curves are for the black hole at angular displacements from the ecliptic plane of 0,  $R_{\odot}/1 \text{ AU}$ , and  $1^{\circ}$  respectively (top to bottom).

TABLE 1  
RETRO-MACHO BRIGHTNESSES OF THE SUN

BH mass ( $M_{\odot}$ )	BH distance (pc)	$\beta = 0$ (perfect alignment)	$\beta = R_{\odot}/1 \text{ AU}$ (edge alignment)	$\beta = 1^{\circ}$	$\beta = \pi/4$	$\beta = \pi/2$ (max misalignment)
1	$10^{-2}$	31.0	32.6	34	38	38
1	$10^{-1}$	38.6	40.1	41	45	46
10	$10^{-2}$	26.1	27.6	29	33	33
10	$10^{-1}$	33.6	35.1	36	40	41
10	1	41.1	42.6	44	48	48

# GRAVITY Consortium



Amorim, Araujo-Hauck, Bartko, Baumeister, Berger, Brandner, Carvas, Cassaing, Chapron, Choquet, Clénet, Collin, Dodds-Eden, Eckart, Eisenhauer, Fédou, Fischer, Gendron, Genzel, Gillessen, Gräter, Hamaus, Haubois, Haug, Hippler, Hofmann, Hormuth, Houairi, Ihle, Jocu, Kellner, Kervella, Klein, Kolmeder, Lacour, Lapeyrère, Laun, Lenzen, Lima, Moratschke, Moulin, Naranjo, Neumann, Patru, Paumard, Perraut, Perrin, Pfuhl, Rabien, Ramos, Reess, Rohloff, Rousset, Sevin, Sturm, Straubmeier, Thiel, Vincent, Wiest, Zanker-Smith, Ziegleder, Ziegler